Copyright Undertaking

This thesis is protected by copyright, with all rights reserved.

By reading and using the thesis, the reader understands and agrees to the following terms:

1. The reader will abide by the rules and legal ordinances governing copyright regarding the use of the thesis.

2. The reader will use the thesis for the purpose of research or private study only and not for distribution or further reproduction or any other purpose.

3. The reader agrees to indemnify and hold the University harmless from and against any loss, damage, cost, liability or expenses arising from copyright infringement or unauthorized usage.

THREE-DIMENSIONAL INSOLE DESIGN FOR RELIEVING PLANTAR PRESSURES IN HIGH-HEELED SHOES

WAN KA WING FRANCES

PhD

The Hong Kong Polytechnic University

2019

The Hong Kong Polytechnic University

Institute of Textiles and Clothing

Three-Dimensional Insole Design for Relieving Plantar Pressures in High-Heeled Shoes

Wan Ka Wing Frances

A thesis submitted in partial fulfillment of the requirements for the

degree of Doctor of Philosophy

Mar 2018

CERTIFICATE OF ORIGINALITY

I hereby declare that this thesis is my own work and that, to the best of my knowledge and belief, it reproduces no material previously published or written, nor material that has been accepted for the award of any other degree or diploma, except where due acknowledgement has been made in the text.

_____ (Signed)

WAN Ka Wing Frances   (Name of Student)

ABSTRACT

High-heeled shoes (HHS) have long become part of the female attire in different contexts. Wearing HHSs, however, damages foot health in the long run. HHSs keep wearers' feet in plantar-flexed positions, change the morphology and weight bearing conditions of the feet, causing high forefoot plantar pressure and impact force during gait. These excessive plantar pressures over the forefoot regions could lead to foot problems such as forefoot pain, corns and calluses and deformities.

The primary goal of this research was to design, with reference to experimental and numerical analysis, an insole with different mechanical stress-strain properties in different foot regions that could lower peak plantar pressure whilst provide adequate foot support to maintain foot stability.

To achieve the project goal, a 3D foot and ankle imaging system was developed to study female foot anthropometry in heel-elevated postures. The high resolution scans acquired by the system allowed fine details to be recorded. The short capture time (within 1 second) minimized measurement errors introduced by unintentional body sways. After validating the accuracy and reliability of the system, foot anthropometric data of fifty young female subjects were collected by using the system. To the best of our knowledge, this foot anthropometric study was the first to focus on forefoot measurements while standing at different heel heights. The geometric characteristics of the forefoot, as illustrated by the various linear and angular measurements, were shown to change with different heel elevations. The most obvious observation is a wider toe spread in the horizontal plane, indicating that slight adjustments might be required in the toe box design when fabricating shoes of different heel heights, especially in the

metatarsal-phalangeal joint regions of the fourth and fifth toes and the distal interphalangeal region of the hallux and second toes. The anthropometric data depicted how the foot morphology changes with increasing heel elevations and provided a scientific basis for the geometric design parameters of the new insole.

To identify specific high plantar pressure regions and determine the functional requirements of the insole for different foot plantar regions, a thorough evaluation on plantar pressure distribution, foot stability, and activities of selected lower extremity muscles during the use of HHSs was carried out. Twenty young female subjects participated in the study. Four heel height conditions (1cm, 5cm, 8 cm and 10 cm) covering the most common heel range were tested. Muscles activities of rectus femoris (RF), vastus lateralis (VL), vastus medialis (VM), peroneous longus (PL), tibialis anterior (TA) and medial gastrocnemius (MG) were found to increase with heel height in both balanced stance and single-leg stance, suggesting that extra efforts were required to maintain body balance in HHS. From the pressure measurements taken from the Pedar®-X insole measuring system, the plantar pressure distribution during quiet standing and normal walking were found to change significantly in HHS in comparison to flat-heeled shoes. During quiet standing, the toes and metatarsal region was found to bear nearly 60% of the body weight at 10 cm heels, which was almost a double when compared to the flat-heeled condition. The peak and mean plantar pressures in the medial and centre metatarsal regions were found to increase significantly (>100% increase) in high-heeled conditions. When walking in 10 cm high-heeled shoes, the pressure contact area decreased significantly in the mid and rear-foot. These findings suggested that highly pressure relieving materials are necessary to cushion the forefoot area, while an arch cushion and a heel cup could help increasing the contact area in the rearfoot and thus maximize the pressure redistribution ability of the new insoles.

Through the examination of trajectories of centre of pressure (COP), the use of HHS was found to worsen foot stability in quiet standing as the variations of COP in both antero-posterior (AP) and medio-lateral (ML) directions increased with heel height. The adverse effects starts to accentuate when heel height reaches 8cm and become even worse at 10cm. High heel experience, however, appears to help maintaining one's postural control in high heeled conditions. The foot stability analysis also presented a method to quantify and analyse walking stability. By constructing a mean curve of the centre of pressure in ML direction (COPx) during the stance phase, the pattern of COPx progression, the intra-subject COPx variability among strides, and thus the walking stability could be determined.

Findings and observations in the experiments served as a reference to determine the appropriate range of geometric and functional design parameters of the new insole, including the form and shape, thickness, dimensions and locations of the cushions, and materials properties requirements. In order to evaluate the effects of these design parameters on peak plantar pressure reduction, eight insole design factors including insole thickness, arch cushion thickness, mid-foot cushion thickness, height of heel cup rim, insole stiffness, stiffness of pads for metatarsal and heel, stiffness of medial arch support, and stiffness of cushion underneath the proximal metatarsal head, were defined and three levels were assigned to each design factors. A set of 16 designs was generated with combinations of different levels of each design parameters through applying the techniques of D-Optimal design. FE simulations were then carried out for each of these 16 designs. Through assessing the magnitude of the peak plantar pressures of these simulations, the mean effect of each level of the design factor on pressure relief could be computed. An optimal design on plantar relief was then achieved through combining the "best" level (greatest effect on plantar relief) of each design factor.

Results of the study showed that insole thickness was the most critical design factor in forefoot pressure reduction, followed by the stiffness of materials to be used at the metatarsal region. In general, softer (Young's modulus < 2 MPa) and thicker materials (4 mm to 6 mm) could effectively reduce forefoot peak pressures. The result revealed that the design requirements for insoles to be used in HHS were different from those of insole to be used in flat-heeled condition.

The research enhanced our knowledge on female foot morphology in heel-elevated postures and provided useful information for the selection of suitable materials for insoles to be used in HHS. Having demonstrated satisfactory repeatability and accuracy, the newly developed 3D imaging system could be adopted in other anthropometric studies. The combined use of fractional factorial designs and FE simulation model provided efficient and reliable numerical solutions to evaluate the effects of different insole parameters on the pressure distribution in high-heeled condition, optimising the effectiveness of the new insole design. The output of the study could extend to the development of other customized insoles and inserts.

PUBLICATIONS ARISING FROM THE THESIS

Journal paper

Wan, F. K. W., Yick, K. L., and Yu, W. W. M. (2017). Validation of a 3D foot scanning system for evaluation of forefoot shape with elevated heels. *Measurement*, 99, 134-144.

Wan, F. K. W. and Yick, K. L. (2018). Effects of heel height and high-heel experience on foot stability during quiet standing. *Gait and posture*. Manuscript in submission

Book Chapter

Wan, F., Yeung, K. L., (2016). Chapter 3 Ladies High-heeled Shoes In Yick, K. (2016). *Footwear developments and innovations (pp. 20-26).* Saarbrücken, Germany: LAP Lambert Academic Publishing.

Conference Paper

Wan F. K. W. , Yick. K.L., Yeung K. L., Yu Winnie, Wong Kris (2014) *Limitations of Current 3D Foot Scanning Systems for Foot Geometry Evaluation in High-Heeled Postures*, TBIS, Hong Kong, paper ID 100, 6-8 August 2014

ACKNOWLEDGEMENTS

TABLE OF CONTENTS

LIST OF FIGURES

XII

LIST OF TABLES

Chapter 1 – Introduction

1.1.   Background of Research

As one of most popular types of female footwear, high-heeled shoes (HHS) not only add height to wearers, create the illusion of smaller feet and longer legs, but are believed to enhance sexuality, self-esteem, and attractiveness to the opposite sex (Smith and Helms, 1999; Yorkston et al., 2010; Branthwaite et al., 2013; Guéguen, 2015). Despite the fact that many physicians and surgeons have criticized HHS over the years for their deleterious effects on the health of women, the love affair with HHS has never ceased. According to the APMA Public Opinion Research on Foot Health and Care, a research study carried out by the American Podiatric Medical Association in 2014, 49% of women own at least one pair of HHS, among which 71% experience foot pain when wearing them. This percentage is the highest among the different types of shoes.

Many researchers, indeed, have reported on the adverse effects of wearing HHS. Walking in HHS greatly increases the dynamic load on the human musculoskeletal system (McBride et al., 1991; Voloshin and Loy, 1994). The increased impact forces, medial forefoot pressure and perceived discomfort during high-heeled (HH) gait and can lead to forefoot pain, muscular fatigue (Gefen et al., 2002), lower back pain (Lee et al., 2001; Mandato and Nester, 1999), knee osteoarthritis (Kerrigan et al., 1998) and many other health issues (Linder and Saltzman, 1998).

Research on footwear science has demonstrated that viscoelastic shock-absorbing insoles can effectively reduce impact forces on the foot (Cheung and Zhang, 2005; Hsu et al., 2008; Creaby et al., 2011). The effects of different parameters on insole design, such as shape and stiffness of insoles on plantar pressure and stress distribution in the

bony and soft tissue structures, have been studied for flat shoes. In general, the enhancement of comfort and redistribution of plantar pressure can be achieved by incorporating proper insoles that can be mechanically optimized to simultaneously support the body weight with minimal foot deviations and act as a reducer of contact-pressure in the precarious plantar zones (Hsu et al., 2008). Lee and Hong (2005) found that a total contact insert (TCI) can effectively reduce heel and medial forefoot pressure, and attenuate the impact force during HH gait.

Therefore, a more appropriately designed insole would create a better fit with the female foot and different components can be used to support different regions of the foot, and thus reduce and redistribute the peak plantar pressure in HHS.

To design an insole for optimal foot support when wearing HHS, a finite element analysis (FEA) along with an anatomically detailed 3D foot model can simulate the dynamic biomechanical interactions between the foot and insole, and systematically evaluate the effects of the insole design parameters from a biomechanical point of view. This approach allows the plantar pressure and internal stress and strain in the bony and soft tissue structures to be simulated under different loading conditions without the prerequisites of replicated subject trials and experimental and product testing.

Finite element method (FEM) has been widely used in foot biomechanics studies. For example, Cheung and Zhang (2005), Antunes et al. (2008) and Hsu et al. (2008) developed anatomically detailed ankle-foot models to carry out an FEA to study the biomechanics behavior of the human foot and performance of foot supports. However, they have only examined conditions with flat shoes. There are few studies that have used an FEA to simulate foot-insole interaction with elevated heels due to the complexities of doing so. Yu et al. (2008, 2013) developed a finite element model of a female foot and studied the effects of heel height, outsole stiffness and coefficient of

friction from a biomechanical perspective. Cheung and Zhang (2008) identified the sensitivity of five factors in the design of footwear (arch type, insole and mid-sole thicknesses, and insole and mid-sole stiffness) and their effects on the peak plantar pressure by combining FEM and the experimental techniques of the Taguchi method. They found that custom molded shape and insole stiffness are the most determinant design factors in reducing peak plantar pressure. Franciosa et al. (2013) investigated the sensitivity of geometric and material design factors of shoe soles on the comfort of the wearer by combining real experimental data and computer aided design-FEM (CAD-FEM) simulations. They found that softer materials and thicker soles can effectively enhance the degree of comfort.

Over the past decades, many studies and a large volume of research work have been carried out on foot anthropometry and footwear functionalities, not only driven by the need of the footwear industry and orthotics production, but because deformities of the foot could greatly affect posture and gait, which might result in long-term pain and cause other health problems. As the general public has become more aware of the health problems facilitated by improper footwear, people seek footwear products that are ergonomically designed to reduce health risks. To date and to the best of my knowledge, the parametric effects of different insole geometries and material properties on stability and stress on the foot-insole interface (such as plantar pressure and shear stress) for HHS remain unaddressed.

1.2.   Problem Statement

1.2.1.   Foot anthropometry in high-heeled postures

Unlike flat shoes, wearing HHS means that the feet are always plantar-flexed at a certain angle, subject to the height of the HHS. The elevated feet change how the weight of the body acts on the foot plantar surface. Different loading conditions such as sitting,

standing (half body load) or walking (full body load during the stance phase) further deform the feet, especially the forefoot and arch, to different extents. However, few research studies have been carried out to address the foot anthropometry in the heel-elevated position.

A variety of 3D foot scanners have emerged in the market driven by demand from the footwear market and facilitated by advanced computing and imaging technologies. These instruments, however, are designed to measure a foot that is resting flat on a horizontal plane surface. Therefore, when the heel is elevated and deviates from the designated scanning position, large measurement errors would occur. A new method, therefore, has to be developed to obtain the anthropometric measurements for feet in HH positions.

There are several basic criteria for such a measurement system:

(1) Fast scanning - the elevated heel position does not allow the wearer to avoid motion for a very long time. Therefore, a shorter scanning time would reduce measurement errors induced by body motion,

(2) Reasonable accuracy and repeatability, and

(3) Ability to acquire real colour and texture information.

With such a system, the recorded 3D measurements would be invaluable for foot deformity diagnoses and designing ergonomic footwear products and accessories.

1.2.2. Static and dynamic balance when wearing high-heeled shoes

The human body is an inherently unstable system as two-thirds of the body mass is found in two-thirds of the body height above the ground. A balance control system is therefore required to continuously maintain body balance due to the instability (Winter, 1995).

Whether at rest or during walking, wearing HHS causes a larger plantar flexion angle of the feet, and re-distributes the body weight over a smaller supporting base. This not only changes the anatomy, mechanics and neuromuscular control when compared to normal gait, but the standing posture becomes more unstable as the centre of mass (COM) is moved forward since the HHS cause the body to lean forward. The strategy of HHS wearers to maintain balance, therefore, would differ from that of wearers of low-heeled shoes. In order to understand how HHS wearers maintain their static and dynamic balance, a thorough study is necessary for an analysis of the plantar pressure distributions and muscle activity when wearing HHS. The findings would help to formulate the insole design parameters for HHS.

1.2.3. Insole design for high-heeled shoes

Due to lack of space in HHS, the structural design and the materials used for a shoe insole could be very challenging. There are several basic criteria in designing such an insole.

(1) The insole cannot be wide in order to fit into most HHS. This means that the peak plantar pressure has to be reduced by increasing the contact area across the foot plantar surface rather than simply providing a larger supporting base.

(2) The thickness of the insole is also limited due to the same reason. The selected materials need to provide the desired strength and elasticity to withstand the mechanical deformities produced by the body weight and extra forces generated during walking.

(3) Although softer materials can effectively reduce peak plantar pressure and thus enhance perceived comfort, they may not be able to provide adequate support to stabilize the foot, especially during heel strike and push off in the stance phase. Therefore, a balance needs to be maintained when selecting the insole materials.

(4) As the insole is to be used in a slanted position, the foot is always subjected to a sliding force that acts on the shoe base (the body weight) from the heel to the metatarsals, regardless whether the wearer is standing or sitting. The sliding effects of both the foot-insole and shoe-insole have to be minimized.

1.3. Project Objectives

The objectives of this study are as follows.

1. To establish a thorough evaluation of the foot biomechanics when wearing HHS of various heights in order to identify specific high plantar pressure regions and determine the functional requirements of the insole for different areas of the foot plantar surface.

2. To develop an efficient measurement system for foot anthropometry in HH positions and analyse the foot morphology in order to provide a scientific basis for the geometric design parameters of the new insole.

3. To evaluate the effects of different insole design parameters (insole geometry, material properties) on plantar pressure through FEM.

4. To design, with reference to the analysis of the experiment and FEM results, an insole with different mechanical stress-strain properties in different foot regions that could reduce peak plantar pressure whilst providing adequate foot support for foot stability.

5. To recommend design parameters for future insole designs for HHS.

1.4. Project Originality and Significance

In the extant literature, researchers have studied HH gait patterns by analyzing the plantar pressure distribution and muscle activity of the wearers, but few have critically

examined how static and dynamic stability can be improved in HH gait through the use of insoles.

Ladies who walk in HHS change their plantar pressure distribution pattern and significantly increase medial forefoot pressure and dynamic loading on their musculoskeletal system. In order to determine the design criteria for insoles exclusively used for HHS, thorough experiments have to be carried out to (1) evaluate the foot anthropometry in HH positions for various heel heights; (2) investigate static and dynamic stability when wearing HHS with various heel heights (high, medium and low heels); (3) evaluate the material properties for selected insole materials; and finally (4) obtain the optimal design parameters through FEM.

In view that few research studies have been done on insole design for HHS, this study aims to identify the key design factors that contribute to plantar pressure redistribution and comfort enhancement when designing HHS insoles. By evaluating the biomechanical foot-insole interactions in HHS through FE simulations, the parametric effects of different insole geometries and material properties on perceived comfort and stress on the foot-insole interface (such as plantar pressure and shear stress) can be investigated.

Style and fashion are often the first considerations in the designing of HHS. A better understanding of the HH gait and how the feet is deformed in HH positions would provide a better idea on shoe design parameters such as the dimensions of the toe box and heel counter, and longitudinal profile of the shoe sole. The results of this study will provide valuable information for designing ergonomically healthy insoles for HHS wearers.

1.5. Outline of the thesis

This thesis consists of eight chapters. Chapter 1 provides the background information, presents the key problems, and discusses the rationale and objectives of this study. A literature review will be given in Chapter 2, in which general concepts and previous research work on foot anthropometric measurements, general biomechanics, kinetics and kinematics of HH gait, and footwear analysis by using FEM will be discussed. The research plan and methodology will be elaborated in Chapter 3. In Chapter 4, the developmental work of a 3D foot scanning system and research findings of an anthropometric measurement study on the feet of female subjects in different HH positions will be presented. In Chapter 5, the experimental design, set up, and findings on plantar pressure distribution when wearing HHS will be presented. The experimental design, set up and findings of the evaluation of foot stability and muscle activity when wearing HHS will be provided in Chapter 6. The new insole design, rationale behind the selection of the design parameters, together with the FEA results to determine the optimal design will be discussed in Chapter 7. The last chapter, Chapter 8, provides the concluding remarks of this study in which the main findings and significance of the study will be highlighted and suggestions for future research directions will be provided.

Chapter 2 – Literature Review

2.1. Introduction

In order to identify the knowledge gap in current research on the insole design for HHS, a thorough review on previous research work will be carried out on (1) the types of foot pain and problems associated with wearing HHS; (2) current technologies in acquiring foot anthropometric measurements; (3) the general biomechanics of wearing HHS; (4) perceived comfort and design of HHS; (5) insole features for use in HHS; and (6) FEM and its application in footwear research. A summary will be given at the end of the chapter to discuss the knowledge gap of current works.

2.2. Types of foot pain and problems associated with wearing high-heeled shoes

Female foot anatomy

In comparison to the feet of males, women's feet are shorter in length and narrower. Manna et al. (2001) found that the feet of males are significantly larger in terms of the foot length, foot breadth, heel breadth, ankle height, foot height at joint, and foot volume. However, Hong et al. (2011) found that among young Chinese adults, women's feet are not merely a scaled down version of their male counterparts. They found that women's feet have narrower foot widths, smaller girths, and lower foot heights, but longer instep length when compared to men with the same foot length. Saghazadeh et al. (2015) also observed significantly smaller foot length, shorter instep length, lower navicular height, narrower width at the ball and heel, and smaller ball and instep girths in women as opposed to men among older Japanese adults.

Frey (2000) also stated that the female foot and ankle are structurally and biomechanically different from their male counterparts. Women tend to pronate more

and their Achilles tendons are thinner. Their feet are generally narrower than that of men with the same length.

Apart from the differences in foot morphology, women's feet might be more vulnerable to foot deformities. Hallux valgus (bunions) have been observed in women at a ratio of 9:1 compared to men (Frey, 2000), which might be directly related to the style of women's shoes.

Pains and problems related to high-heeled shoes

HHSs are shoes that raise the heels of the wearer significantly higher than the toes by means of platforms, wedges or heel structures. Nowadays, HHSs can be found in a wide variety of styles, which can be further categorized according to different shoe types, height of heels, shapes of heels. In the apparel industry, heeled shoes can be roughly categorized into low-heeled (1-2 inches), mid-heeled (2 inches up to 3 inches) and high-heeled (3 inches up) according the height of heels.

Although proving a direct relationship between HHS and foot problems had been difficult, the rate of foot problems was proven relatively high in shoe-wearing societies. Referring to a study involving barefoot natives of West Africa (Barnicot and Hardy, 1955), the hallux angles in either men or women are around a mean of approximately zero degree, which are significantly different from those of shoe-wearing European males (+6.9°) and females (+11°). In another study in mainland China by Lam and Hodgson (1958) also reported that shoe-wearing Chinese natives had a 33 % prevalence of bunions, while those who had never worn shoes had only a 2 % prevalence of bunions.

Several authors have reported on the harmful effects of footwear and ill-fitting shoes contribute the most to these effects. Women who suffer from foot pain and deformities

tend to wear shoes that are more than 1.3 cm (0.5 inch) less than the width of their forefoot (Frey et al., 1993). According to Menz and Morris (2005), wearing substantially narrower shoes is associated with the formation of corns on the toes, bunions and foot pain, whereas wearing shoes that are too short is associated with lesser toe deformities such as hammer toes and claw toes. The presence of bunions and plantar calluses in women are also strongly related to wearing shoes with a heel over 2.5 cm in height.

Despite the fact that narrow shoes could lead to different types of forefoot pain and deformities, the design of HHS often comes in a narrow, or even a pointed toe box and a narrow foot base in order to reshape the foot so as to create a "slim" appearance. These features interfere with the natural foot morphology and alter balancing and walking mechanisms.

The Society of Chiropodists and Podiatrists in the United Kingdom states that wearing HHS can cause long term foot problems such as blisters, corns and calluses, and the adverse effects are not limited to only the feet, but also affect the legs, knee joints and even the spine. The impacts of HHS on human feet include:

- Increasing the loading on the metatarsal heads, which may lead to corns, calluses, and bunions.
- Shifting the COM anteriorly, thus causing the wearer to bend the upper body backwards to maintain balance while standing, which could lead to lower back problems.
- Offering a narrow heel width which does not provide good support to the foot and destabilizes the ankle, thus resulting in ankle sprains.
- Shortening and tightening the calves with prolonged use.

Many research works have shown that an increase in heel height increases forefoot pressure. (Schwartz et al., 1964; Snow et al., 1992; Corrigan et al., 1993; Nyska et. al., 1996; Mandato and Nester, 1999; Speksnijder et al., 2005, Cong et al., 2011; Lam et al., 2014). Indeed, HHSs cause excessive body loading onto the metatarsal heads instead of distributing onto the heels where the loading normally should be distributed. Compensation has to be made through postural adjustments and extra energy is needed to maintain body balance during standing and walking. If these compensatory adjustments are maintained for a prolonged period of time without a sufficient recovery period, permanent damage which ranges from bodily pain to actual deformities could be actualized.

There is a strong established scientific link that shows back pain is related to the development of lower limb pathology in the use of HHS (Lee et al., 2001; Mandato and Nester, 1999). Cronin et al. (2012) found increased muscle moments and work carried out by the hip and knees in HH gait and suggested these would cause musculoskeletal pain in long-term HHS wearers. Cowley et al. (2009) also stated that the onset of pain and pathology is directly associated with increases in forefoot peak pressure and changes in spinal and pelvic movement over a prolonged period of time due to the use of HHS.

Prolonged wear of HHS could even alter the muscle-tendon architecture. According to a study by Csapo et al. (2010), the prolonged use of HHS could induce shortening of the medial gastrocnemius muscle fascicles and increase the stiffness of the Achilles tendon, hence reducing the active range of motion of the ankle joint. Cronin et al. (2012) also found that the muscle fascicles of habitual HHS wearers are shorter during standing, which suggests chronic adaptations in the muscle-tendon architecture due to prolonged use of HHS.

As greater plantar-flexion at the time of ground contact has been identified as the anatomic reason for increased risk of ankle sprain, the use of HHS could also lead to greater likelihood of ankle sprains. Foster et al. (2012) found that wearing HHS results in greater peak ankle plantar-flexion and inversion angles, thus indicating an increase in the risk of experiencing a lateral ankle sprain. A study by Liederbach (2014) on 30 female professional dancers found that they landed in significantly greater plantar flexion and inversion with significantly greater internal ankle eversion moment and longer time to reach stability when they wear HHS (3 inches) compared to flat shoes. Indeed, according to a survey conducted by Hotter Shoes in 2010 (PR Newswire Association, 2018) with 3000 women who wear HHS, almost half of the respondents indicated that they have experienced an ankle sprain because of their footwear.

2.3. Current technologies in acquiring foot anthropometric measurements

As the human foot plays an important role in weight bearing and locomotion, improper footwear could lead to health problems. The general public is being made more aware of the functional abilities and comfort when they purchase footwear. Driven by the need of the footwear industry to develop products with specific functional and/or ergonomic considerations, a reliable approach is necessary to quantify the dimensions and complex shape of the human foot.

Over the past decades, numerous studies have tried to establish a reliable and definitive foot anthropometric measurement framework that can best describe the shape, size, and proportions of the foot. The most comprehensive study on foot morphology reported in the literature was conducted by the Armored Medical Research Laboratory in Kentucky, US (Freedman et al. 1946) on American soldiers. A set of 27 dimensional characteristics were assessed for 6278 Caucasian and 1281 African American US Army

personnel. The measured variables included ten direct measurements - six heights and four girths, taken directly from the soldiers by using a sliding caliper and a cloth tape respectively. Seven lengths and five widths were derived from a photographic image of the foot. Four shape contours were extracted from cardboard templates.

Dahlberg and Lander (1950) described the human foot with 18 foot measurements derived from 8232 male military conscripts in Sweden. The measurements included two lengths, five breadths, five girths, and six angular measurements. No height measurements were taken.

White (1982) summarized the findings from 22 military and 4 civilian anthropometric surveys conducted between 1942 and 1977 and reported the mean values of 14 foot measurements including foot and instep lengths, foot, heel and bimalleolar breadths, the lateral malleolus, medial malleolus, calf and ankle heights, circumferences of the ball of the foot, instep, heel-ankle, ankle and calf.

Hawes and Sovak (1994) described the three-dimensional (3D) characteristics of the human foot with 22 essential foot measurements, including nine lengths and six heights taken with a Siber-Hegner anthropometer, three breadths taken with a small sliding caliper and four girths taken with a retractable steel tape. All linear measurements were recorded to the nearest 1 mm. A plantagram was also drawn for each subject by using a footprint pad.

Most of linear measurements in these studies were taken manually with the use of various measurement instruments such as flat rulers, sliding and spreading calipers (Figure 2-1), cloth tape, anthropometers, Brannock Device (Figure 2-2), etc. However, these traditional measurement methods are usually contact methods, which would

deform the skin surface and affect measurement accuracy. Inter-operator measurement errors might also be introduced in manual measurements.

Figure 2-1. Spreading caliper

Image source: http://www.seritex.com/gpm-large-spreading-caliper-rounded-ends-108/

Figure 2-2.

Image source: https://brannock.com/

In a study by Robinson et al. (1984) which aimed to determine if there is a correlation between the number of miles run per week and foot dimensions, eight linear foot measurements including foot length, foot width, heel width, length and height of the medial and lateral metatarsal phalangeal joints, and dorsum height were obtained solely through photographic images. Each subject was required to stand on a designated platform on which the anterior, posterior, medial and plantar views of the foot could be photographed on one slide. No direct measurements were taken.

Facilitated by rapidly growing digital imaging and computation technologies, 3D scanning technologies have become more popular and affordable. Many researchers have started to adopt 3D scanning technologies in studies related to foot anthropometry.

Three-dimensional scanning technologies enable digital representation of the human feet with an adequate level of detail. They have become imperative for a number of applications, including customized and ergonomic footwear and insole design,

production of foot orthotics (Payne, 2007; Hawke et al., 2008), and even assessment of foot deformities (Chen et al., 2003; Pfeiffer et al., 2006). Researchers have also adopted 3D foot scanning to establish data banks with foot anthropometric measurements for foot type classification (Mauch et al., 2009), evaluate shoe fit by comparing scans of the feet with those of shoe lasts (Witana et al., 2004), evaluate changes in foot shape with different weight bearing conditions (Cobey and Sella, 1981; Houston et al., 2006), and compare the foot geometry between males and females (Wunderlich et al., 2001; Krauss et al., 2008; Luo et al., 2009), and adults and children (Mauch et. al, 2009).

Mauch et al. (2009) adopted a 3D foot scanner developed by Human Solutions Inc. (Germany) to carry out the foot anthropometric measurements of 1450 boys and 1437 girls in their study. Five foot types were successfully identified through the scanned data. Carroll et al. (2011) proved that digital scanning is a reliable technique for capturing foot dimensions as measurement variability is reduced in all of the foot parameters in their study when compared to neutral suspension casting. Lee et al. (2014) also found 3D foot scanning to be an ideal measuring technique for collecting foot anthropometric measurements as it has relatively higher precision, accuracy and robustness as opposed to traditional methods such as the use of digital calipers, or inked or digital footprints.

Since reliable and automated foot measurement extraction algorithms are required by the footwear industry and researchers, many studies have also investigated ways to automatically collect foot anthropometric measurements. Witana et al. (2006) proposed an approach to automatically collect foot measurements from a scanned 3D foot model. Algorithms were developed to align the foot scans, and calculate the foot lengths, widths, heights and girths. The search algorithms and computation were well illustrated and explained in their work. Wang (2010) scanned a library of ten shoe lasts and

developed an algorithm for choosing the most suitable last for an individual from the library based on his or her ball, waist and instep girths of his/her foot.

Three-dimensional scanning, however, might be considered to be costly in terms of price and time. Luximon and Goonetilleke (2004) parameterized a "standard" foot model out of 25 foot scans by using sections of the scanned data obtained along the foot axis. They demonstrated that a prediction model could be generated by using foot length, width and height, and measured foot curvature. The prediction accuracy was found to be 2.1 mm for the left foot and 2.4 mm for the right foot.

While 3D body scanning technologies are gaining more attention in the academia, researchers have started to realize the limitations of some of the scanning systems. Corner and Hu (1997) noticed that body sway during the scanning process can affect image fidelity and thereby reduce accuracy. Jezeršek, and Možina (2009) also noticed the speed limitations of current laser scanning technologies and developed a fast scanning system by using a laser multiple-line triangulation technique, where each of several measurement modules uses a unique laser wavelength such that multiple scanning modules can be used at the same time without mutual pattern interference among multiple measurement modules. Schmeltzpfenning et al. (2009) also developed a 4D foot scanner called DynaScan4D, which comprises five scanner units that use full-field triangulation through structured light projection. The accuracy is up to 0.23 mm with a 640 x 480 resolution in static scans and 0.89 mm in a dynamic 4 x 4 binning mode at a velocity of 0.8 m/s. Barisch-Fritz et al. (2014) adopted a scanning system to study foot deformation in developing feet during walking.

Compared to traditional measurement methods such as 2D imaging, taping and 3D digitizing, 3D scanning is much faster and allows many more measurements to be taken. Whilst the taping method only allows 1D and 2D measurements (such as lengths and

girths), 3D scanning allows dense 3D point measurements to be recorded across the surface of interest. Two-dimensional imaging, such as plantar scanning, allows the outline of the footprint to be depicted but other information such as girth and arch shape cannot be retained. Three-dimensional digitizers allow discrete 3D point measurements to be taken at exact locations, but this is much more labour intensive and probing the soft skin surface might introduce measurement errors.

Scanning time is another critical issue in scanning that involves human subjects. All scanners designed for body scanning aim to acquire 3D data in the shortest time to avoid data inconsistencies due to unintended body movements. However, subjects in HHS cannot remain perfectly still for more than a few seconds. Longer scanning time means greater chances that there will be data inconsistencies due to body movement, especially in weight-bearing experiments in which subjects are required to stand still over the entire scanning process. Small body swings to maintain body balance might result in changes to the angle of the ankle and cause muscle contractions in the foot and ankle area. Participant fatigue might also lead to changes in the foot shape. The newly developed Imaging system in this study successfully limits the scanning time to within 1 second, thus rendering it an ideal instrument for taking foot measurements of feet with the heels elevated, especially in loaded conditions.

Although automated measurement extraction processes greatly reduce the processing time as the foot measurements contribute to a standard and reliable framework for further analyses in foot anthropometry, and are adequate for many applications such as footwear and insole design and foot orthotics production, to the best of my knowledge, there is no system that measures 3D foot anthropometry in HH positions. Since foot dimensions and foot geometry considerably change in response to increases in heel height, foot measurements obtained on a flat plane cannot be adopted to design the

shoe lasts of HHS. A suitable 3D foot scanning system which can integrate HH positions can facilitate the process of a high-quality HH footwear design with improved fit and comfort.

Although reliable fast scanners had been developed by other researchers, these are not yet available in the market. A fast and accurate 3D foot scanning system has to be tailor built to meet the needs of this project.

2.4. General biomechanics of wearing HHS

2.4.1. Normal gait cycle

The gait cycle is the fundamental unit that describes walking, and defined as the period between two successive occurrences of one of the repetitive events of walking. Generally, the instance at which the reference foot comes into contact with the ground (initial contact) is considered the start of a cycle.

A gait cycle has two major phases: stance and swing. During the stance phase, the reference foot is in contact with the ground, whilst the swing phase marks the period when the reference foot is off the ground. These two phases have been further subdivided into smaller functional phases by different researchers (Perry and Burnfield, 2010; Neumann, 2010; Whittle, 2012) to address the clinical examination aspects of gait. According to Whittle (2012) and Neumann (2010), seven events can be identified in a cycle (Figure 2-3): initial contact, opposite toe off, heel rise, opposite initial contact, toe off, feet adjacent, and tibia vertical.
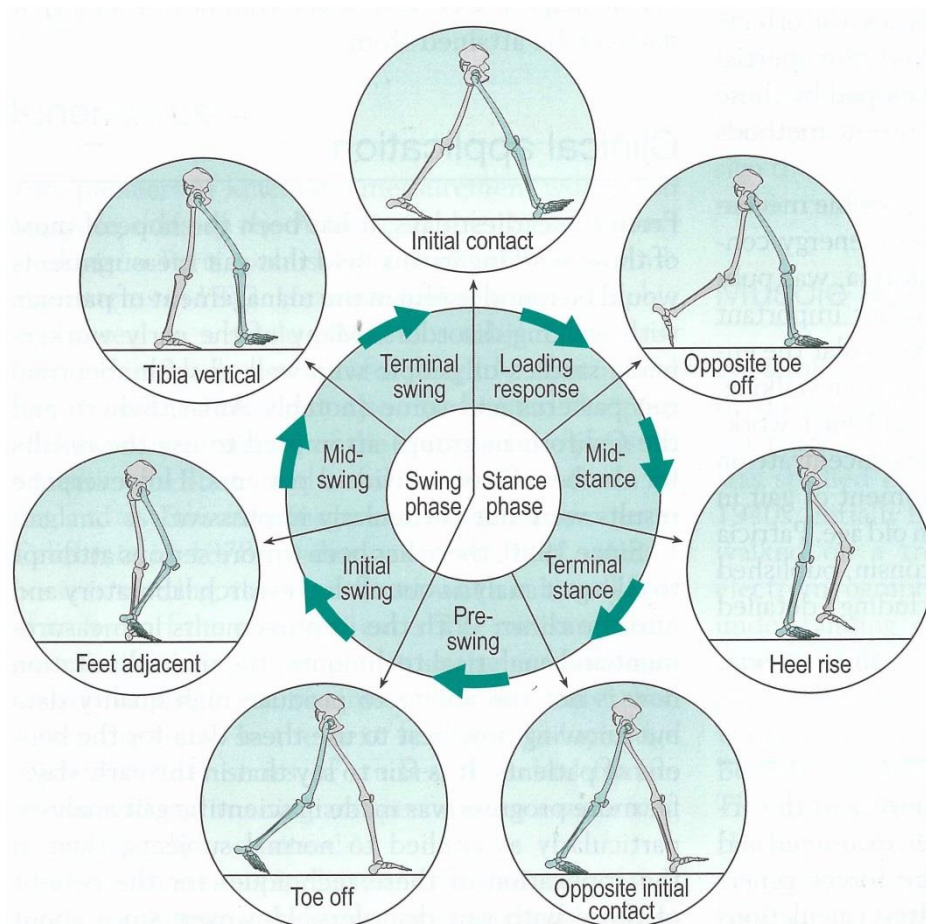
Figure 2-3. Gait events in a single gait cycle (green leg).
Adapted from *Whittle's Gait Analysis. 5th edition* (p. 32), by Levine et al. © 2012 by
Elsevier Ltd.

These seven events divide the gait cycle into seven phases, four in the stance phase
(loading response, mid-stance, terminal stance and pre-swing) and three in the swing
phase (initial swing, mid-swing and terminal swing).

In each gait cycle, there are two periods of double support (both legs on the ground)
and two periods of single support (Figure 2-4). In normal gait at a comfortable walking
speed, the stance phase usually lasts about 60 - 62% of the gait cycle and the remaining
38 - 40% comprises the swing phase. This percentage changes with walking speed. As a
person walks faster, the swing phase would become longer at the cost of a shorter
stance phase and double support phase. The elimination of the double support phase
marks the transition from walking to running.
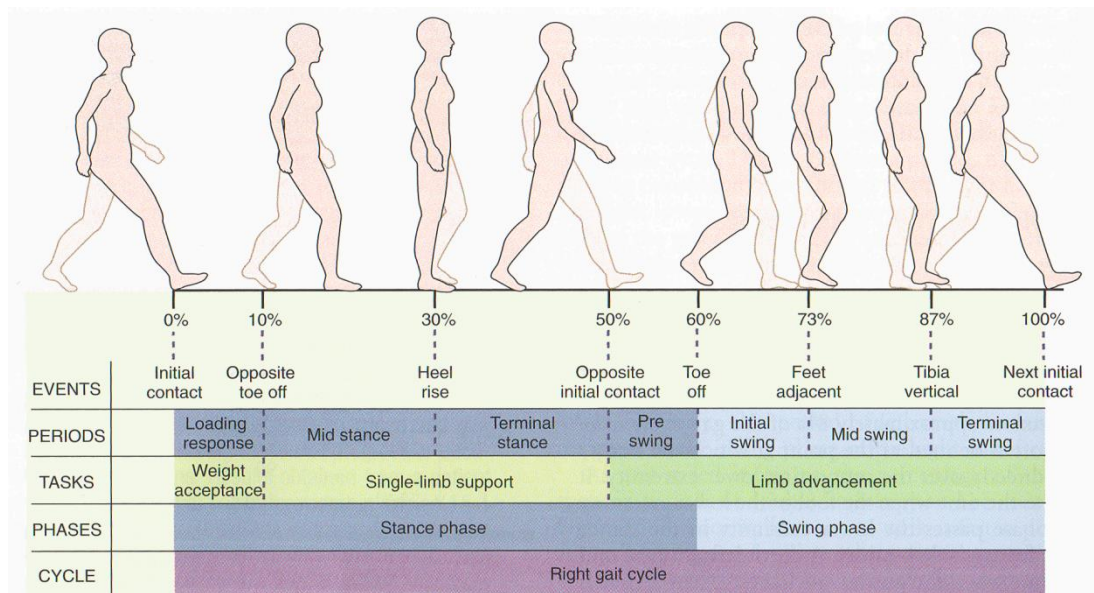
Figure 2-4. Terminology and phases of the gait Cycle (Neumann, 2010)

2.4.2. High-heeled gait pattern

Over the past decades, many studies have been carried out to evaluate HH gait and find that heel height has significant impacts on gait kinematics. In normal adult gait, the COM moves in a way that produces a sine wave pattern that is indicative of the efficiency of gait with correct timing of the gait phases (Braune and Fischer, 1987; Neumann, 2010). HH gait disrupts this ideal pattern (Cowley et al., 2009). Stefanyshyn et al. (2000) observed increases in the acceleratory and deceleratory forces when walking in high heels, thus indicating less fluent gait.

As heel height increases, more compensational adjustments would occur in the ankle, knee, hip, and vertebral column positions and movements, thus altering posture and gait pattern. Indeed, many studies have demonstrated that the use of HHS changes the lower-extremity joint kinetics and functions. Previous research work largely agrees that the use of HHS increases plantar and knee flexion, and reduces ankle eversion during stance (de Lateur et al., 1991; Ebbeling et al., 1994; Stefanyshyn et al., 2000; Esenyel et al.,2003; Mika et al., 2012a). Some have reported reduced flexion during the swing phase

(Oplia-Correia et al., 1990a; Snow and Williams, 1994). Some studies associate the increase in knee extensor moments and muscular activity to the increase of knee flexion. Stefanyshyn et al. (2000) regarded increased knee flexion as a counteractive measure to offset the forward displacement of the COM, hence leading to more active rectus femoris muscles to control the increased knee flexion.

Furthermore, whether the use of HHS increases lumbar lordosis is rather controversial. Many of the studies either observe a reduction (Bendix et al., 1984; Lee et al., 2001) or no significant difference (Snow and Williams, 1994). de Lateur et al. (1991) observed a reduced lumbar lordosis in males but no significant trend was observed in females. Oplia-Correia et al. (1988) measured the postures of 12 female and 7 males with anatomical landmarks and recorded lumber flattening rather than lumbar lordosis in HH (6.4 cm) stance in habitual wearers of HHS. De Oliveira Pezzan et al. (2011), however, reported an increase in lumbar lordosis in habitual wearers of HHS but a reduction in non-regular users when they wore HHS.

Studies have also shown that walking in HHS causes a significant decrease in walking speed and stride length but no difference in cadence (Adrian and Karpovich, 1966; Oplia-Corriea, 1990; de Lateur et al., 1991; Lee et al., 2001). The fact that people tend to adopt a slower self-selected walking speed in HHS might be explained by the increased use of energy due to greater friction demand. The freely chosen walking speed in flat shoes is generally considered the most efficient use of energy (Newmann et al., 2010). Walking at higher or lower speeds could increase energy cost (Cronin, 2014). Due to the smaller heel base of HHS, the contact area between the shoe and ground is reduced, thus leading to an increase in the friction demand. Esenyel et al. (2003) noticed the maximum anterior-posterior (AP) braking force increases with heel height. Blanchette et al. (2011) found that utilized friction increases with heel height, which indicates an

increase in friction demand when walking in HHS. A study by Luximon et al. (2015) found that a small heel base increases the center of pressure (COP) deviations during walking, which implies that the foot is less stable in HHS. Therefore, more muscular effort, hence higher energy cost, might be required to stabilize gait.

All these compensatory adjustments not only affect gait fluency, but the extra energy expended could lead to muscle fatigue and pain in the long run.

2.4.3.   Plantar pressure distribution in HHS

Previous research work has largely demonstrated that the use of HHS significantly increases forefoot peak pressure and the pressure time integral during gait, and shifts the COP in a forward and medial direction (Schwartz et al., 1964; Snow et al., 1992; Corrigan et al., 1993; Nyska et al., 1996; Mandato and Nester, 1999; Speksnigder et al., 2005; Cong et al., 2011; Lam et al., 2014).

While peak pressure records the highest pressure value over the stance phase, the pressure time integral denotes the total amount of pressure that has been applied over the period of foot contact. The peak pressure is one of the most important measurements in determining the performance of cushioned foot orthoses in pressure relief ability (Orlin and McPoil, 2000).

Speksnijder et al. (2005) found that walking in HHS (5.91 $\pm$ 1.03 cm) can cause a 34% and 30% increase in peak pressure (PP), and 47% and 48% increase in pressure time integral (PTI) in the medial forefoot (first metatarsal) and central forefoot (second to forth metatarsals) respectively when compared to walking in flat-heeled (1.95 $\pm$ 1.06 cm) shoes. They also found a positive correlation (>0.70) between heel height and PP and PTI in the medial forefoot and PP in the central forefoot. Mandato and Nester (1999) recorded a 63% and 110% increase in forefoot pressure when comparing 2-inch

and 3-inch HHS to sneakers. The use of HHS induces the body loads to the more sensitive and vulnerable metatarsal heads instead of resting on the heels where they should be. This could result in forefoot pain and deformities.

On top of the increased forefoot pressure, some studies (Speksnijder et al., 2005; Lam et al., 2014) have also noticed a significant decrease in the pressure contact area in the midfoot and heel regions when walking in HHS. Nyska et al. (1996) observed a reduced contact area on the lateral forefoot.

Although the findings in previous studies show good consistency, many have their own limitations. Some studies have only compared two heel conditions (Nyska et al., 1996; Speksnigder et al., 2005), that is, HH and low-heeled, which is inadequate for establishing a relationship between heel height and pressure measurements. Some studies have been performed by using the shoes of the participants themselves (Nyska et al., 1996; Speksnigder et al., 2005), which neglects control over the influence of shoe sole materials and toe box designs on the experimental results. Mandato and Nester (1999) compared 2-inch and 3-inch high-heels with sneakers. However, the effects of different shoe sole materials and footbed design of the sneakers on plantar pressure measurements are questionable. The highest heel height evaluated is 8.26 cm (Snow et al., 1992). However, it would be worthwhile to investigate shoes with a higher heel height which has been indicated as a topic for further study in some of latest literature (see for example, Mika et al., 2012; Blanchette et al., 2011; Hapsari and Xiong, 2016), as standing balance, muscular effort and utilized friction could be significantly different when the heel height is increased to around 10 cm. Moreover, most studies have evaluated pressure distribution for only walking. Cong et al. (2011) examined the effect of heel height on in-shoe triaxial stresses in both walking and balanced standing, but the

stress measurements were localized to only 5 spots due to the size limitation (2.3 cm^2) of the transducers used to carry out the measurements.

Standing and walking are two of the most frequent daily tasks in which the body weight is supported solely by the feet. Plantar pressure distribution during standing in HHS, however, is of little interest to researchers. This might be due to the relatively lower plantar pressure readings obtained from quiet standing. In considering the accumulative effects of persistent pressure, the PTI over the areas of peak pressure during standing might be comparable to that of walking for the same time span. Without switching the foot to different positions, leg muscles that are responsible for balance during standing would have to continuously exert higher muscular effort. This might more easily lead to pain and fatigue.

2.4.4. Foot stability in HHS

To stand upright is one of the most frequent daily tasks. The mechanism of maintaining balance in the standing posture, however, is rather complex. Maintaining balance involves inputs from the visual, vestibular and somatosensory sensory systems and their interactions to coordinate joints and muscle groups over the entire body, of which, ankle and hip strategies have been identified as most important for maintaining static balance.

The ankle strategy controls small body sways. Wearing HHS, however, puts the feet in a more plantar-flexed (Ebbeling et al., 1994; Stefanyshyn et al., 2005) and supinated position (Kouchi and Tsutsumi, 2000). This might affect the efficiency of the ankle strategy in postural control. On top of that, the use of HHS changes numerous variables that affect the stability of the body's equilibrium, such as the height of the COM (Ko et al., 2009) and position of the COP in relation to the support base, as well as the form

and size of the support base (Luximon et al., 2015; Chien et al., 2013). Studies have shown that wearing HHS indeed worsens balance (Gerber et al., 2012; Hapsari and Xiong, 2016), and reduces walking stability (Gefen et al., 2002) hence increasing the risks of falling (Blancchette et al., 2011) and ankle injuries (Mika et al., 2012, Ebbeling et al., 1994, Menz and Lord, 1999).

While most studies related to HHS have focused on the kinetics, kinematics, and muscle activity in gait (Luximon et al., 2015; Chien et al., 2013; Lee and Hong, 2005, Esenyel et al, 2003, Han et al., 1999, Snow and Williams, 1992), very few have evaluated the effect of heel height on static balance. Cho and Choi (2005) and Gerber et al. (2012) compared standing balance in bare feet versus HHS with a heel of 7 cm by analyzing the oscillation of COP and found that the standing balance is significantly worsened when wearing 7 cm HHS. Hapsari and Xiong (2016) extended the testing conditions to four heel heights (1 cm, 4 cm, 7 cm, and 10 cm) and conducted a comprehensive study with various balance tests and surface electromyography (sEMG) measurements to examine the effects of heel height and HHS wearing experience on standing balance, functional mobility and muscular effort. The results of a sensory organization test (which measured the AP postural sway) showed that standing balance is significantly worsened and significantly more hip strategy is applied with a 10 cm heel. However, the studies evaluated the standing balance in only the AP direction.

Apart from heel height, HHS experience might also be another intrinsic factor that affects postural control ability. Previous research suggest that the prolonged wear of high heels introduces biomechanical accommodations to HHS such as shortening of the calf muscles (Cronin et al., 2012) and gastrocnemius medialis muscle fascicles, and increase in Achilles tendon stiffness (Csapo et al., 2010), which may result in different balance strategies. Again, since most studies related to the HHS experience have

focused on gait (Chien et al., 2014; Cronin et al., 2012; Gefen et al., 2002; Stefanyshyn et al, 2000, Opila-Correia, 1990b), the effect of HHS experience on standing balance has remained rather unexplored. Although Hapsari and Xiong (2016) found that experienced HHS wearers do not show significantly better overall performance in standing balance nor exhibit significantly different amounts of ankle and hip movements, these findings are only valid for the AP direction.

Since the mechanisms that govern standing and walking are significantly different (Kang and Dingwell, 2006; Winter, 1995), the effects of heel height and HHS experience on standing balance must be addressed separately. Moreover, since the heel base of HHS is usually narrower than that of flat-heeled shoes, postural stability in the medial-lateral (ML) direction would very likely be reduced. More informative findings might result if postural stability is evaluated in both the ML and AP directions.

Foot stability during standing can be evaluated through COP-based measures (Ruhe et al., 2010; Winter, 1995; Prieto et al., 1996; Le Clair and Riach, 1996). COP is the point location of the vertical ground reaction force vector, which represents the weighted average of all the pressures over the base of support (Winter, 1995). It is informative for the underlying control strategies used in response to various footwear conditions. To assess one's static balance performance, postural sway, which can be quantified as the deviation from the mean COP of the foot (Guskiewicz and Perrin, 1996), as well the velocity of COP which describes the rate of change of COP movement, are the most common variables used to assess balance control.

2.4.5. Leg muscle activation in HHS

Functions of leg muscles

During weight bearing conditions, such as standing upright or during the stance phase of gait, leg muscles that control knee and ankle movements are activated to support the body weight and maintain balance. The dominant movements at the ankle joints are dorsiflexion and plantar flexion (Figure 2-5), which are controlled by the dorsi-flexors and plantar flexors that connect the tibia to the foot. The soleus and two heads of gastrocnemius (medial and lateral) (Figure 2-6) located at the posterior compartment of the tibia are the primary plantar flexors. Together they produce 93% of the plantar flexor torque (Perry and Burnfield, 2010).
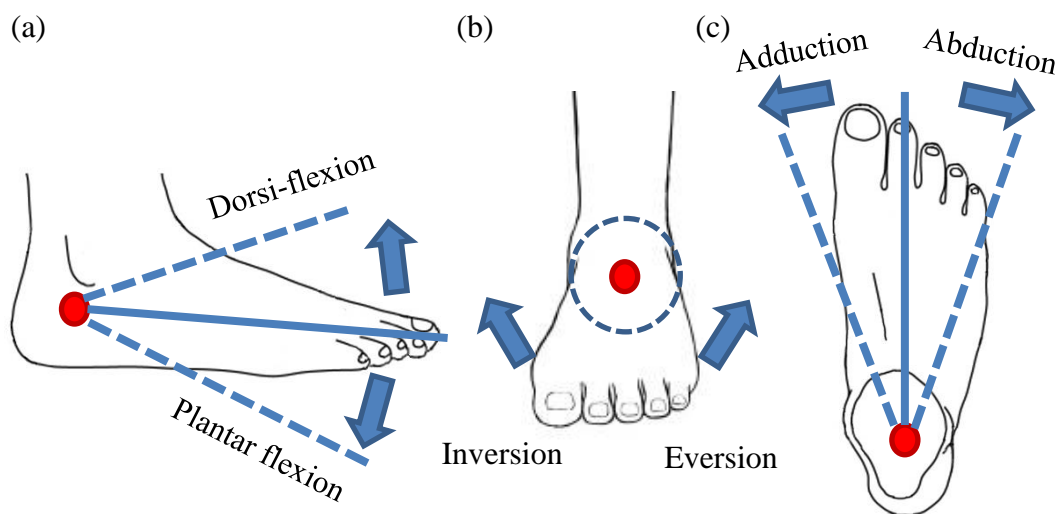
Figure 2-5 Foot movements

The tibialis anterior, extensor digitorum longus, extensor halluces longus and peroneus tertius muscles located at the anterior compartment of the tibia (Figure 2-4) are the primary dorsi-flexors. During quiet standing, the plantar flexors and dorsi-flexors together control anterior and posterior body movements in the sagittal plane. During locomotion, the dorsi-flexors are active during heel contact to decelerate passive plantar flexion caused by the ground reaction force acting on the heel, as well as during push

off to provide stability to the ankle through co-activation with the plantar flexors. The plantar flexors elongate during mid-stance to prevent excessive dorsiflexion and contract during push off to create plantar-flexion for the forward propulsion of the body.
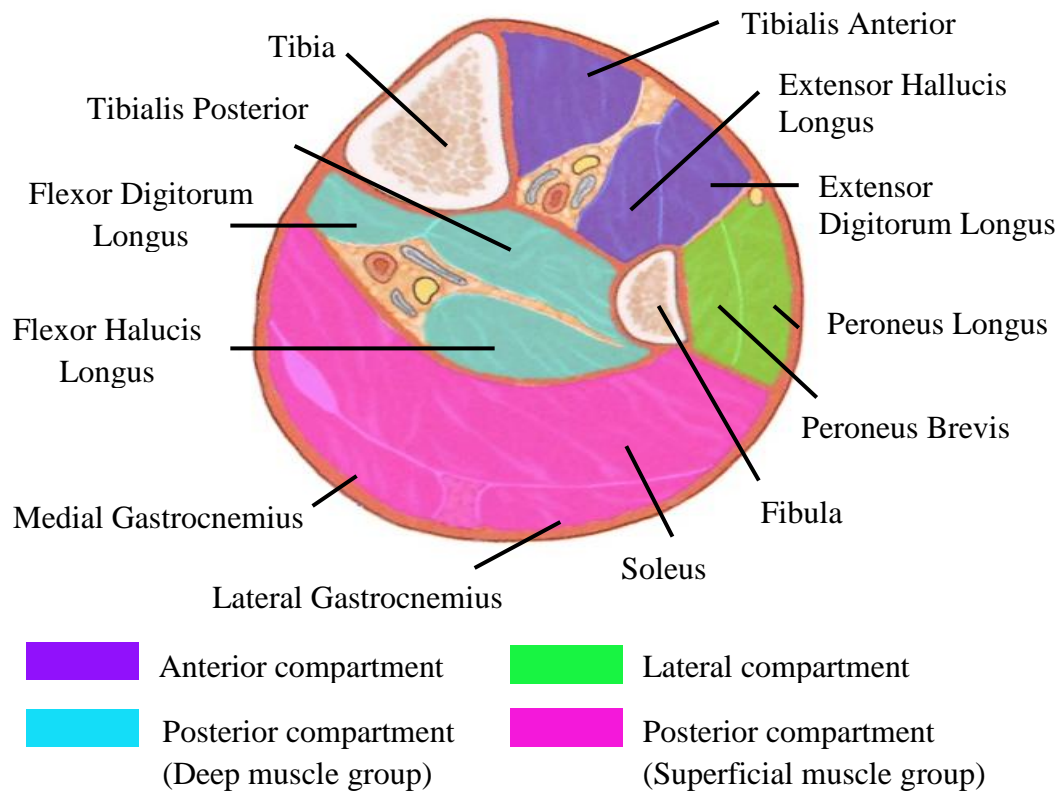
Figure 2-6. Muscles in calf compartments (cross-section of right leg) (Modified from Neumann, 2010)

Foot eversion and inversion (Figure 2-5(b)) are controlled by the evertors and invertors. The peroneus longus and peroneus brevis muscles located in the lateral compartment of the tibia (Figure 2-4) are the primary evertors of the foot. The primary invertor muscles are the tibialis posterior, tibialis anterior, flexor digitorum longus and flexor hallucis longus. Apart from the tibialis anterior, all the invertors are deep muscles which cannot be examined through sEMG. These evertors and invertors actively provide stability to the lateral side of the ankle.

The functional potential (relative strength) of the muscles to perform certain ankle movements is dependent on their size (cross-sectional area) and leverage (moment arms from the ankle joint). Table 2-1 summarizes the prime movers of ankle movement.

Table 2-1. Prime movers of ankle movement in terms of functional potential listed in descending order

Movement	Muscles of the ankle joint
Dorsiflexion	Tibialis anterior Extensor digitorum longus Extensor halluces longus Peroneus tertius
Plantar flexion	Soleus Gastrocnemius
Eversion	Peroneus longus Peroneus brevis
Inversion	Tibialis posterior* Tibialis anterior Flexor digitorum longus* Flexor hallucis longus*

*Deep muscles that cannot be assessed with sEMG

Muscles that control knee extension and flexion also play an important role during standing and local motion. The quadriceps, which cover the front and sides of the femur, are the knee extensors that help to prevent excessive knee flexion and serve to cushion impact forces at heel strike. The quadriceps include four prevailing muscles: rectus femoris, vastus intermedius, vastus medialis and vastus lateralis (Figure 2-7).

Rectus Femoris

Vastus Intermedius
(beneath Rectus Femoris)

Vastus Medials

Vastus Lateralis

Biceps Femoris

Semitendinosus

Semimembranosus

Anterior View   Posterior View
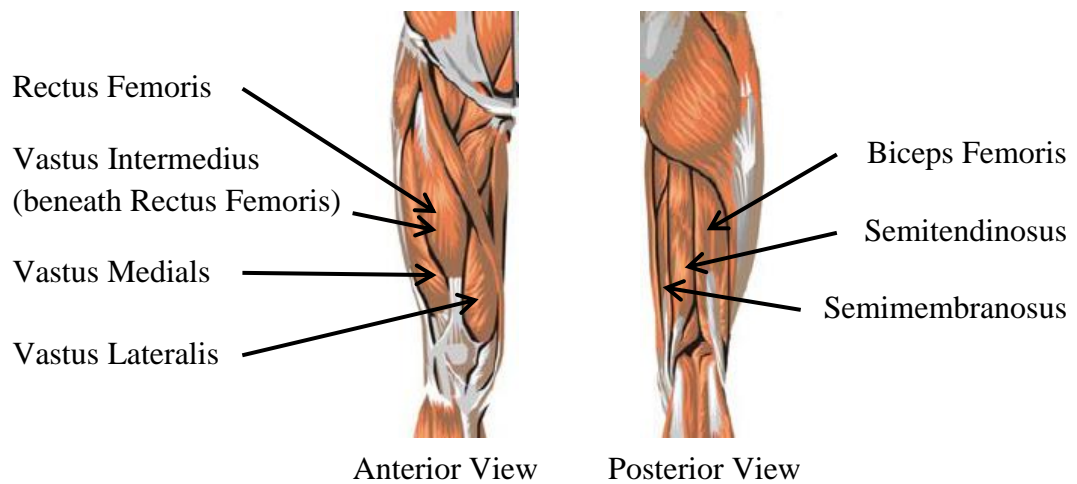
Figure 2-7. Thigh muscles that controls knee movements

At the back of the femur are the hamstrings, which are knee flexors as well as hip extensors. The hamstrings consist of three muscles: the bicep femoris, semitendinosus, and semimembranosus muscles (Figure 2-7). They help to decelerate knee extension at the moment just before heel contact, and assist with hip extension and stabilize the knee joint just after heel strike (Neumann et al., 2010; Perry and Burnfield, 2010).

Surface electromyography for evaluating foot muscles activity

Electromyography (EMG) is a recording technique that allows interpretation of the electrical activity that radiates from activated skeletal muscles (Newmann et al., 2010). EMG is an indirect means of identifying the timing and relative intensity of muscular functions (Perry and Burnfield, 2010). EMG signals can be expressed in magnitude and frequency. The former describes the amount of electrical activity during a contraction while the latter denotes the range of the firing rates of all motor units recorded. The EMG signals generated by a muscle can be recorded by using three types of electrodes: needle, surface and fine wire. As surface electrodes are non-invasive and easy to handle, sEMG has become the most common technique used in kinesiological studies, in which

the voluntary neuromuscular activation of muscles are examined during movement and postural tasks.

The typical arrangement of surface electrodes involves placing two surface electrodes 2 cm apart side by side along the axis of the muscle fibers, on the skin that overlies the muscle belly of interest. When a muscle contracts, electrical activity is generated as action potentials propagate along the muscle fibers. The electrode pair sums up these potentials of all innervated fibers detectable and electrically superposes these signals, giving the bipolar raw EMG signals with symmetric distribution of positive and negative amplitudes. The voltage of these raw EMG signals is only between a few microvolts and 2-3 millivolts when reading on the skin (Konrad, 2006). Therefore, they can be easily distorted by other electrical sources such as cable movement, adjacent or distant active muscles, and any background magnetic radiation. As such, extra care is required when placing the electrode pair. All cables have to be secured onto the skin surface with tape. Possible relative movement of the muscles next to the skin surface during muscle contraction has to be taken into consideration. Electrical artifacts can also be minimized by proper skin preparation such as hair removal and alcohol cleaning to ensure stable electrode contact and low skin impedance. The EMG signals can also be pre-amplified at the electrode site to reduce noise resultant of the movement of the electrode cables. Filtering of EMG signals during signal processing could also be done to retain only useful frequency ranges (10 to 500 Hz) from unwanted signals. A sampling frequency of at least 1000 Hz is required to avoid signal loss due to the filtering process.

Next, the filtered EMG signals have to be further processed to compute the amplitude, which indicates the intensity of muscle activation. One of the most common approaches is to compute the root mean squared (RMS) value of the EMG signals over a period of time, which correlates with the standard deviation of the voltage relative to

zero. This method involves squaring the signal, averaging a certain time window, and then calculating the square root. The time window is selected based on the nature of the task. For fast movements, a smaller time value such as 20 ms is needed, while a greater time value such as 500 ms can be used for slower and static activities. For most conditions, a time value between 50 and 100 ms works well (Konrad, 2006).

Since the absolute EMG amplitude is strongly influenced by given detection conditions which vary among electrode site, muscles, subjects, and sessions, it is therefore necessary to normalize the EMG signals to some common reference values when researchers wish to compare or average data across different subjects and muscles. This reference value is the maximum voluntary contraction (MVC) value, which is obtained prior to the test trials. MVC tests are performed separately for each investigated muscle. For the extremity muscles, isolated single-joint activities (statically held at middle positions within the range of motion) give the best results. To perform an MVC test, subjects are required to perform the MVC exercise with maximum effort and hold for 3 seconds. This is repeated at least once after a rest period of 30 to 60 seconds (Hermens, 1999). The MVC value is the mean amplitude of the highest signal portion obtained through a moving average computation with a time window of a duration of 500 ms (Konrad, 2006).

EMG normalization minimizes the artifacts of the detection condition, thus allowing direct quantitative comparison of EMG data between subjects and measurement sessions. The normalized data provide a better understanding on how much a muscle is activated to its maximal capacity level.

Although sEMG is easy to use, the technique also has its drawbacks. Since muscles function in synergy, signals from more than one muscle could arrive from the same surface area. Hence, the EMG signals recorded by a surface electrode pair generally

33

represent the action of more than those of the designated muscles. This is called muscle cross-talk (Perry and Burnfield, 2010; Konrad, 2006). Practically, it is difficult to isolate the signals of the designated muscle from those of the adjacent muscles. Moreover, the thickness of fat tissues affects sEMG signals. This reduces the applications of sEMG to superficial muscles without the presence of thick fat tissue layers. The activation of deeper muscles has to be examined by using fine wire electrodes.

EMG studies related to the use of HHS

In a biomechanical study carried out by Ebbeling et al. (1994), heart rate and oxygen consumption were found to increase with increasing heel height during HH gait. The higher metabolic consumption might be explained by the higher muscular effort exerted to compensate for the disrupted gait pattern and instability introduced by HHS. Indeed, many research studies have shown that walking in HHS could increase the muscular effort of the lower limbs.

Stefanyshyn et al. (2000) measured the EMG signals of the gastrocnemius, soleus, peroneus longus, tibialis anterior, rectus femoris, semitendinosus, bicep femoris, and vastus medialis muscles during the stance phase of gait on 13 healthy females. Four heel heights (1.4 cm, 3.7 cm, 5.4 cm and 8.5 cm) were tested. The results showed that the soleus and rectus femoris muscle activity demonstrated a graded response as the heel height is increased.

Lee et al. (2001) examined the biomechanical effects of shoes with three different heel heights (0 cm, 4.5 cm and 8 cm) on five female subjects during quiet standing and walking and found that the EMG signals of both the erector spinae and tibialis anterior increased with heel height but significance was identified only in the erector spinae

muscles. The effect of heel height on the EMG signals of the vastus lateralis muscles was not significant.

Mika et al. (2012b) found that walking in HHS (10 cm) significantly increases the muscle activation of the erector spinae, medial gastrocnemius, rectus femoris and tibialis anterior muscles (Mika et al., 2012a). do Nascimento et al. (2014) observed significantly higher muscle activity in the medial gastrocnemius, rectus femoris, tibialis anterior and rectus abdominis muscles when walking in HHS (7 cm) as opposed to walking barefoot. Foster et al. (2012) found that the activation of the peroneus longus muscle is significantly higher in HHS (9.5 cm) than low-heeled shoes (1.3 cm), while no difference was found in the activation of the tibialis anterior muscle.

Increased activity of muscles around the knee joint in HH gait indicates increased joint stiffness, which might be one of the strategies to deal with the instability induced by an increased heel height (Ebbeling et al., 1994). The increase in muscle activity not only means higher energy costs, but may lead to fatigue when HHS are worn for a prolonged period of time (Gefen et al., 2002; Hong et al., 2013).

The effect of HHS experience on gait biomechanics, balance control, and muscle activity is rather controversial. Some researchers (Csapo et al., 2010; Cronin et al., 2012) have reported chronic adaptations in the muscle-tendon architecture such as shorter gastrocnemius muscle fascicles, and a longer and stiffer Achilles tendon. Cronin et al. (2012) found that habitual HHS wearers have higher muscle activation in the medial gastrocnemius muscles than non-habitual HHS wearers during gait. Simonsen et al. (2012), however, reported no significant differences in lower limb joint moments and muscle activity between habitual and non-habitual HHS wearers. While the vast majority of research has focused on HH gait, Hapsari and Xiong (2016) examined the effects of HHS experience and heel height on standing balance and functional mobility.

Their results showed that experienced HHS wearers do not perform significantly better in terms of standing balance and functional mobility but have better directional control and larger maximum excursion. Experienced HHS wearers also exert less muscular effort in the tibialis anterior, vastus lateralis and erector spinae muscles but more effort from the medial gastrocnemius muscles to maintain postural balance.

2.5. Perceived comfort and design of HHS

In many footwear insole studies, plantar pressure distribution is found to be related to the perceived comfort of the wearers (Che et al., 1994; Jordan et al., 1997) and the shape of the insole and its resulting plantar pressure distribution have a pivotal impact on overall health. Perceived comfort increases with reduced peak pressure and contact area. Therefore, the footbed design has been one of the most discussed topics in footwear design. In other words, being able to design a footbed that could maximize the weight-bearing area means that the pressure could be distributed more evenly across the whole plantar surface and hence peak pressure can be reduced accordingly.

In a study by Witana et al. (2009) on the footbed design in HHS, a regression model was established between perceived feelings of comfort and peak pressure, contact area and percentage of force falling on the forefoot. The results revealed that perceived comfort is the highest with wedge angles of 4° - 5°, 10°- 11°, and 16° - 18° for heel heights of 2.5 cm, 5.0 cm and 7.5 cm respectively. The research team also proposed the necessary criteria for a comfortable footbed as follows.

(1) The contact area is greater than that when standing on a flat surface.
(2) The peak pressure is less than approximately 100 kPa during standing (this value can be considered as the discomfort threshold).

(3) The percentage of force on the forefoot is within approximately 15 – 22.5% of the total force on the foot.

Bae et al. (2015) revised a HHS design through the concept of tunnel technology for better shock absorption and a rearward decrease in the wedge angle in the hopes of attaining better static balance and a more balanced forefoot to rearfoot pressure distribution ratio during standing. The results were favourable with the revised design. Kim et al. (2017) demonstrated that pitting the fore-medial part of HHS could reduce the stress in the first metatarsal head and big toe area during standing and walking.

Some researchers (Speksnijder et al., 2005; Lam et al., 2014) noticed a reduction in the contact area in the mid-foot and heel region in HHS, and suggested that extra arch support in HHS designs could increase the pressure contact area between the insole and foot arch, hence improving the overall perceived comfort. Goonetilleke (2012) indicated that when the mid-foot area is poorly supported, this not only reduces the ride quality of the footwear, but the strain of the plantar fascia may even lead to plantar fasciitis.

Apart from the footbed shape, the size of the heel base has also drawn the attention of researchers. Luximon et al. (2015) found that a small heel base increases COP deviation and shifts the COP more medially at heel strike. The instability introduced by a small heel base indicates less stable plantar support, which might result in increased joint torque and muscle activity thus leading to lower limb problems (Lord and Bashford, 1996). In a study by Guo et al. (2012), the effects of the size of the heel base (1.2× 1.2 cm^2 and 2.2 × 3.5 cm^2) of HHS (7.8 cm) on plantar pressure were examined on thirteen healthy female subjects during walking and in nine healthy female subjects during slow running. The findings revealed that when wearing HHS with a narrow heel base, the plantar pressure of the hallux and toes is significantly greater during walking and significantly higher plantar pressure is observed in the forefoot and toe regions during

slow running when compared to HHS with wider heels. For both narrow and wide base heels, the plantar pressure in the medial forefoot during slow running (2.0 m/s) is significantly higher when compared with walking (1.0 m/s and 1.5 m/s).

2.6.　Insole features for use in high-heeled shoes

Shoe insoles are the interior liner of a shoe that is in contact with the plantar surface of the foot. In most footwear, the primary function of an insole is cushioning and moisture control. Due to different foot problems and abnormalities, insoles with a specific purpose such as arch support, pain relief, and foot realignment, are introduced. These functional insoles, or foot orthotics, can be prefabricated, customized (or modified), or custom-made. Prefabricated insoles are those off-the-shelf consumables available on the market. They are mass produced and are available in various shapes and sizes. Customized insoles are the modified versions of the prefabricated insole, where extra features, such as pads, wedges, fillers and heel cup, are added to existing insoles to satisfy different therapeutic needs. Custom-made insoles or foot orthotics are designed to alter the function and biomechanics of the foot for a specific individual and are usually fabricated from an impression of the individual's foot. They are regarded as a means of therapeutic treatment for various foot pathologies where accurate interventions are required.

Depending on the primary functions of the insole, an insole can also be classified as being "functional" or "accommodative". Functional insoles are therapeutic insoles that are designed and made based on the foot morphology of the user. They are used to provide mechanical control to correct and maintain the foot position and motion during gait (Owings and Botek, 2012; Guldemond et al., 2006; Crabtree et al., 2009). Rigid materials are used for the shell to provide adequate mechanical support to the heel and midfoot arch. Special features such as posting, wedges, heel cup, flange and cut-out can

be added to the insoles to treat various foot pathologies. Accommodative insoles are used to reduce plantar pressures at problematic foot regions (pain or deformities) by redistributing the high plantar pressures to other regions of the foot. Softer materials are usually adopted in these insoles to absorb shock during gait and provide cushioning to the foot (Owings and Botek, 2012; Crabtree et al., 2008).

Insoles for use in HHS are accommodative insoles. Their primary function is to accommodate the high plantar pressures at the metatarsal region. To redistribute the plantar pressure, a total contact insole would be ideal to maximise the pressure contact area. Lee and Hong (2005) investigated and compared the effects of custom-made metatarsal pad, arch support, heel cup and total contact inserts (TCI) on foot pressure, impact force and perceived comfort during HH gait. The result revealed that a heel cup insert reduces heel pressure and impact force and an arch support reduces the medial forefoot pressure. A TCI could even reduce heel pressure by 25% and medial forefoot pressure by 24%, and attenuate the impact force by 33.2%. However, considering the cost of fabricating custom-made inserts, using TCI might not be a popular choice for HHS users who are free from foot deformities.

Prefabricated insoles or inserts are therefore more popular for users of HHS. There are different types of insoles and inserts available on the market that are targeted to treat various problems introduced in HHS, such as blisters, heel slippage, forward sliding, and most importantly, pressure relief. Pressure relieving insoles are often in full length, or ¾ length (Figure 2-8). Inserts such as metatarsal pads, heel pads and arch cushions, are also available to relieve foot pain at specific plantar regions. Table 2-2 summarises the common insole features of prefabricated insoles for HHS.

Figure 2-8. 3/4 length insoles from ERGOFoot
(Source: www.amazon.com)

Table 2-2. Functions of common features of off-the-shelf insoles for HHS.

Insole features		Functions
Metatarsal pad		• Shift pressure away from metatarsal region • Relieve metatarsal pain • Cushioning calluses
Heel pad		• Shift pressure away from metatarsal region • Relieve heel pain • Shock absorption
Medial arch cushion		• Provide mechanical support and cushion to the medial arch • Prevent arch depression and flat foot
Mid-foot cushion (also referred to as metatarsal pads)		• Provide mechanical support and cushion to the latitudinal arch • Prevent arch depression • Relieve metatarsal pain • Relieve symptoms of splayed foot

(Source of images: www.amazon.com)

The most common materials of HHS insoles are silicone gel and memory foam. Gel insoles are excellent shock absorber. They can effectively redistribute plantar pressure and provide high level of comfort. Memory foam is viscoelastic polyurethane foam, which would soften in reaction to body heat. Hence, they can be shaped instantly to fit the shape of foot bed of a wide range of users. They are superior in shock absorbsion and cushioning. Luximon et al. (2014) investigated the effects of metatarsal pads that are made of different materials on pressure redistribution and perceived comfort in HHS. The tested materials include bio-gel, polyurethane (PU) and EVA. The results showed that the insertion of all the tested types of metatarsal pads could effectively reduce forefoot peak pressure and increase heel peak pressure during walking. While the bio-gel pad significantly improves subjective comfort ratings, polyurethane was identified as the most effective material to reduce forefoot peak pressure, which is 35.5% when compared to the controls.

2.7. Numerical analysis for optimal insole design

2.7.1. Finite element method (FEM)

Finite element method (FEM) is a numerical computational method widely used in mathematical physics and engineering. The method is usually used to solve physical problems where very complex mathematical models are involved.

To solve a problem by using the finite element method, the physical problem involved is idealised to a mathematical model with certain assumptions, which together lead to a set of differential equations. In other words, the complex physical problem is subdivided into smaller units and simpler geometry known as finite elements (Rao and Yip, 2014). The simple equations that model these finite elements are then assembled into a larger system of equations that models the entire problem. The method finally

yields approximate values of the unknowns at discrete number of points over the domain.

The finite element method is also known as an FEA when the method is adopted in practical applications as an integral part of CAD. FEA can simulate the mechanical interactions of a system under predefined loading and boundary conditions and predict resultant stresses and deformations. Through an FEA, the effects of any changes in the input parameters (such as material properties, loading conditions, model thickness) can be assessed with ease. With suitable optimization or iteration strategies, an "optimal" design can be generated through an FEA. These numerical simulations greatly reduce the number of prototypes and tests required in the design stage.

2.7.2. FEA in footwear research

Due to its capability to model structures with a complex geometry and material properties, the FEA has been adopted with great success in many biomechanical studies. Regarding the application of FEA on footwear research, most studies are related to the evaluation of therapeutic orthotics and shoe-insole in pressure reduction. Since the development of orthotics has been largely dependent on subjective views and measurements of interface pressure, researchers have used the FEA to obtain more quantitative information on the effects of orthotics thickness and materials on plantar tissue stress during the design stage.

Some researchers have evaluated the materials used and structure of the insoles without a foot model. For instance, Barani et al. (2005) performed linear and non-linear static analyses with a finite element model to analyse the effectiveness of four different types of materials: silicone gel, Plastozote, polyfoam, and EVA in plantar stress reduction. Loads were applied to 6 discrete locations (Figure 2-9) in accordance with the

experimental plantar pressure measurements obtained by Ziad et al. (1996). The results showed that silicone gel provides the best outcome.
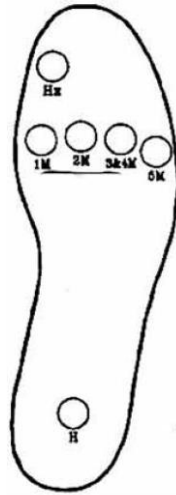
Figure 2-9. Six discrete locations: hallux (Hx), head of the first metatarsal (1 M), head of the second metatarsal (2 M), third and fourth metatarsal heads (3and4 M), head of the fifth metatarsal (5 M), and heel (H). (Barani et al., 2005)

Ghassemi et al. (2015) adopted finite elements to determine the number and order of insole layers in the manufacturing of a novel pressure reducing insole for diabetic neuropathic patients. Four materials, including silicone gel, EVA, polyfoam and Plastazote were tested in 22 order combinations (4 single-layered, 18 3-layered). Loads were applied at 10 locations (Figure 2-10) in accordance with those stipulated in the literature. The results showed that silicone gel outperforms the other insole materials. In considering its poor moisture absorption ability, a three-layer insole arrangement of Plastazote–silicone gel–EVA was deemed to be a better alternative to a single-layer silicone gel insole for diabetic patients in terms of stress concentration, weight and absorption of moisture.
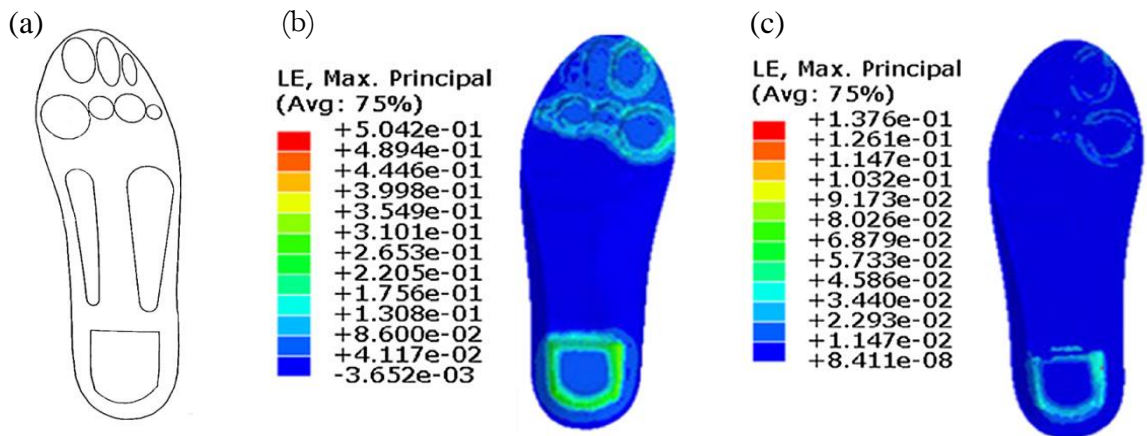
Figure 2-10. (a) 10 prescribed locations for loading and boundary condition. (b) Logarithmic strain contour for silicone monolayer insole in static mode (c) Logarithmic strain contour for poly foam monolayer insole, in static mode (Ghassemi et al., 2015)

These approaches which carry out simulation without a foot model simplify the process and evaluate the pressure absorption ability of the insole but the impact on the plantar surface is not assessed. Moreover, loads were only applied to discrete locations. This approximation might over-simplify the real situation where loads could be applied on the insoles across a continuous plantar surface.

In order to investigate the foot-insole interface stresses, other researchers have incorporated a foot model in their study, which has soft tissues and bone structure into their FE simulations. Lemmon et al. (1997) constructed a 2D plane strain FE model with a length of 90 mm length to represent the sagittal section through the second metatarsal bone with dorsal and plantar soft tissues. Chu et al. (1995) developed a linearly elastic model with a simplified geometrical structure of the foot and ankle for FE simulations on orthotics (Figure 2-11). Chen et al. (2003) developed a 3D foot and ankle model with bones and major plantar ligaments by using computed tomography (CT) to image orthotics (Figure 2-12). The model was used to evaluate the effects of a flat insole and two total contact insoles on peak and average normal stresses in the plantar areas. The nonlinear material property of the insole and frictional behavior of

the contact interface were considered. The results showed that total contact insoles could both effectively reduce high pressure peaks at the heel and metatarsal heads, and redistribute the pressure to the midfoot regions.
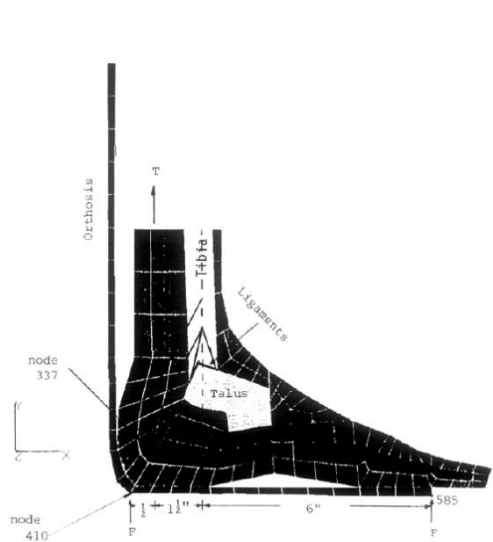
Figure 2-11. Vertical cross-sectional view of the 3D FE model of the ankle-foot orthosis system (Chu et al., 1995)
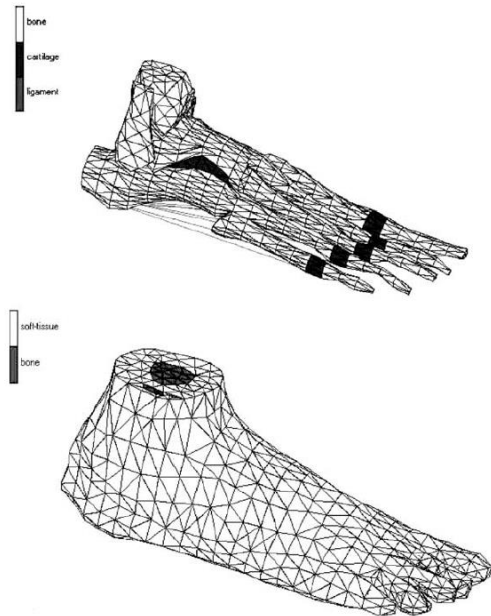
Figure 2-12. 3D FE model of bones, cartilage and major plantar ligaments (upper) and complete foot model combining of bones and soft tissues (Chen et al., 2003)

Since then, many researchers have incorporated a biomechanically detailed foot model in their foot-insole FE simulations (Cheung and Zhang, 2005, 2008; Hsu et. al, 2008; Antunes et al., 2008; Yu, 2009; Qiu et al., 2011; Franciosa et al., 2013; Sarikhani et al., 2016). While most foot models are created from CT scans from the feet of males and simulate only the foot and shoe sole interaction, Yu et al. (2008) developed a detailed 3D female foot model to simulate the biomechanical interactions between the foot and shoe sole of HHS with 2-inch heel (Figure 2-13 (a)) and evaluated the stresses within the bony structures during balanced standing. They extended the simulations to 3-inch HHS (Yu, 2009) and added upper shoe construction and simulated HHS donning and

walking (Yu et al., 2013). Qiu et al. (2011) also constructed a coupled foot-boot model for future studies and validated the model through balance standing experiments.
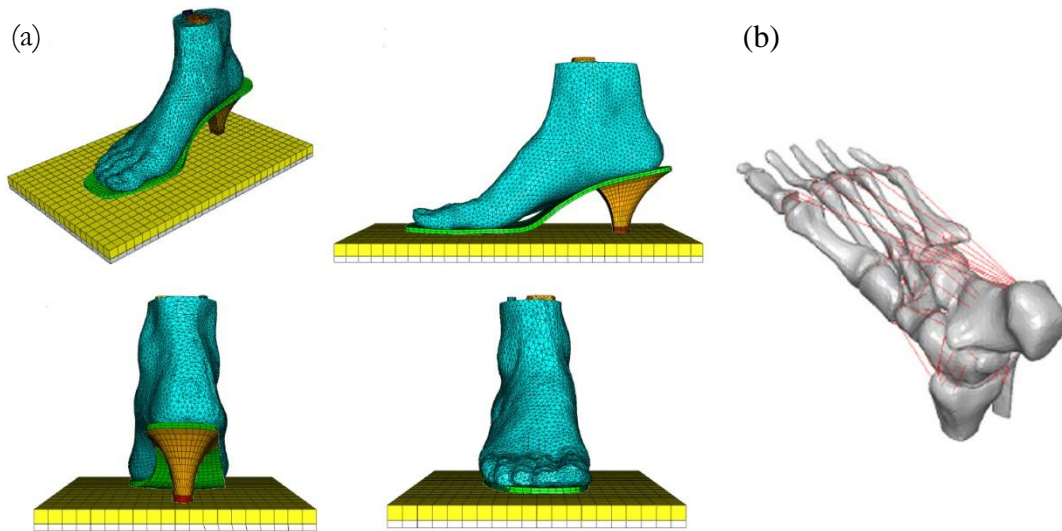
Figure 2-13. (a) Finite element model of female foot and 2-inch HHS (Yu, 2009) (b) bottom view of bony skeleton that shows ligaments and plantar fascia connections (Yu et. al, 2013)

Since FEA computation that involves a detailed foot model could take hours or even days, the search of an optimal design of multiple design factors that uses FEA could be an expensive process in terms of time. The number of design factors to be assessed is also limited.

Some researchers have evaluated all the design combinations in 2D FEA. Goske et al. (2006) developed a plane strain finite element model of the heel to quantify the effects of conformity, thickness, and material of insoles on pressure relief. A total of 27 designs were simulated during the early support phase of gait. These 27 designs covered all combinations of insole conformity (3 levels: flat, half conforming, and full conforming), insole thickness (3 thicknesses: 6.3, 9.5 and 12.7 mm) and insole materials (3 types: PORON Cushioning, Microcel Puff Lite and Microcel Puff). In another study on the relief of local plantar pressure in therapeutic footwear, Erdemir et al. (2005)

investigated all 36 plug design combinations of materials (3 levels), plug head geometries (6 designs), and placement position (2 levels) by using a 2D FE model.

Sarikhani et al. (2016) assessed the effects of each design parameter separately in their investigation on the optimal range of insole design parameters for two types of insoles (flat and custom-molded) through FEM and simulation of plantar stress distribution. The foot model was developed through CT scans. Insole thickness, inclination, and different materials were the design parameters applied to minimize the maximum stress and achieve the most uniform stress distribution. The effects of each design parameter were evaluated separately. A total of 18 designs were studied (5 thicknesses and 3 levels of inclinations for the custom-molded insole, 3 thicknesses and 4 heel heights for the flat insole, and 3 types of materials for custom-molded insole with a thickness of 2 cm).

Some researchers have therefore combined the techniques in the design of experiment (DOE) and optimization to evaluate multiple design factors at the same time while keeping the number of computation trials minimal.

Hsu et. al (2008) developed a detailed 3D foot model with bone and ligament structures to investigate the relationship between different shapes of insoles and the junction stress, so as to achieve an optimal insole design for lower fascia stress. A parametric analysis was carried out with 7 different insoles to predict the initial values for the optimization process. A subproblem approximation for an optimization analysis was then carried to determine the optimal insole design.

Cheung and Zhang (2008) presented a combined FE and Taguchi approach to identify the sensitivity of five design factors (arch type, insole and midsole thicknesses, insole and midsole stiffnesses) of foot orthosis on peak plantar pressure relief. By adopting the Taguchi method, which utilizes a fractional factorial design approach, 16 simulations

were required to identify the relative significance of different orthotic design factors for plantar pressure relief, while a total number of 1024 (4^5) analyses would be required for the full factorial approach.

Franciosa et al. (2013) investigated the sensitivity of geometric and material design factors on degree of perceived comfort by combining real experimental tests and CAD-FEM simulations. Eleven design factors (five 3-level factors and six 2-level factors) including materials and geometrical parameters were investigated. A full factorial design would require a large number of tests ($26 \cdot 35 = 15,552$). By employing the techniques in DOE, a fractional factorial design study was carried out and a set of 16 virtual prototypes with different combinations of design factors were developed for FE simulations. An analysis of the resulting plantar pressure identified the most prominent design factors. The findings showed that perceived comfort is highly related to the sole thickness and sole material. Softer materials and thicker soles were found to increase the degree of comfort.

As an alternative approach to wear trial evaluations, FEM is an effective means to systematically evaluate the parametric effects of different structural and material configurations of a new insole and biomechanical response of the foot under different loading conditions. The combined use of FE simulations and parametric models might be an ideal solution when a large number of design factors are involved, as this would require computation to identify the optimal design through experimental tests on product prototypes, which is extremely difficult and expensive. The development of a detailed biomechanical foot model from CT or MRI images allows assessments on tissue and bone stresses. However, it is also an expensive process to build such a complicated FE model and run the simulations in terms of time, and it is not practical to carry out CT or MRI scans for every patient or customer who needs a customized

orthotics design. A simpler and more practical method is required to extend the FEA approach from laboratory simulations to practical applications.

2.8. Chapter Summary

The fit of shoes is vital to foot health. While 3D scanning has already been adopted in the retail market for the fitting of flat shoes, a similar approach might be carried out for HHS. Due to the lack of suitable instruments to acquire 3D foot anthropometric measurements for HH positions, few research work has been done to assess the fitting of HHS. To scan the foot in HH positions, the scanning time must be short enough to minimize errors introduced by body sway. Jezeršek, and Možina (2009) developed a high-speed scanning system based on multiple-laser-plane triangulation to collect 3D foot measurements, but no textural information can be recorded in the scans. Schmeltzpfenning et al. (2009) developed the DynaScan 4D which is an ideal system for assessing the changes in foot morphology during gait but is not available on the market yet. In order to study the female foot morphology in HH positions, a fast and reliable scanning system has to be developed.

Furthermore, the literature related to the development of HHS insoles is limited. This might be due to the difficulties of designing an insole with very limited space inside the shoe sole. Although shoe inserts such as metatarsal pads might provide cushioning and or/ absorb shock at critical locations, without increasing the contact area of the midfoot and heel, they only redistribute pressure in a localized area, and so high plantar pressure is still found in the same region. A full-length insole, therefore, would be the only ideal way to redistribute plantar pressure across the entire foot.

In order to obtain information on the plantar pressure distribution and weight-bearing contact area for the new insole design, a thorough biomechanical study is necessary to

evaluate the effects of heel height on these measurements during standing and walking. Since the latest literature has shown that there are significant differences in kinetic and kinematic measurements when the heel reaches about 10 cm, the experiment would include this height as one of the test conditions. An EMG study on selected leg muscle activity would also allow the assessment of foot stability in both the AP and ML directions, thus providing scientific evidence for the need of extra insole features to enhance plantar support.

Although total contact insoles can effectively redistribute plantar pressure and hence reduce high forefoot pressure, they might not be a popular choice for HHS users considering the cost of fabricating a pair of custom-made insoles. A more generic design with specific features such as pads at metatarsal and heel region for pressure relief and cushions at the latitudinal and medial arch for better support might be a reasonable approach to be adopted for the new design.

Little has been done on the simulation of foot-shoe interactions in HHS with FEA. The study by Hsu et al. (2008) focused on flat foot conditions while that by Yu et al. (2009, 2013) focused on 2-inch heel shoes, which might not show the shoe-sole interaction in higher heels. Since the shape of the foot, contact area, and locations of the COM relative to the weight bearing plantar area would vary in different HH positions, FE models that simulate real HH conditions need to be constructed for subsequent analysis on HHS. Moreover, a simpler and more practical method is required for developing a foot model to extend the use of the FEA to more practical applications.

Chapter 3 - Research Plan and Methodology

The primary objective of the present study is to design an insole that could lower plantar peak pressure and at the same time provide optimal foot support in high-heeled shoes. To achieve this, a thorough scientific basis needs to be established at the first place to understand the heel-elevated foot anthropometry and the static and dynamic balance control in high-heeled shoes. Material properties for short-listed insole materials will also be evaluated. The flow diagram below briefly describes the research plan.
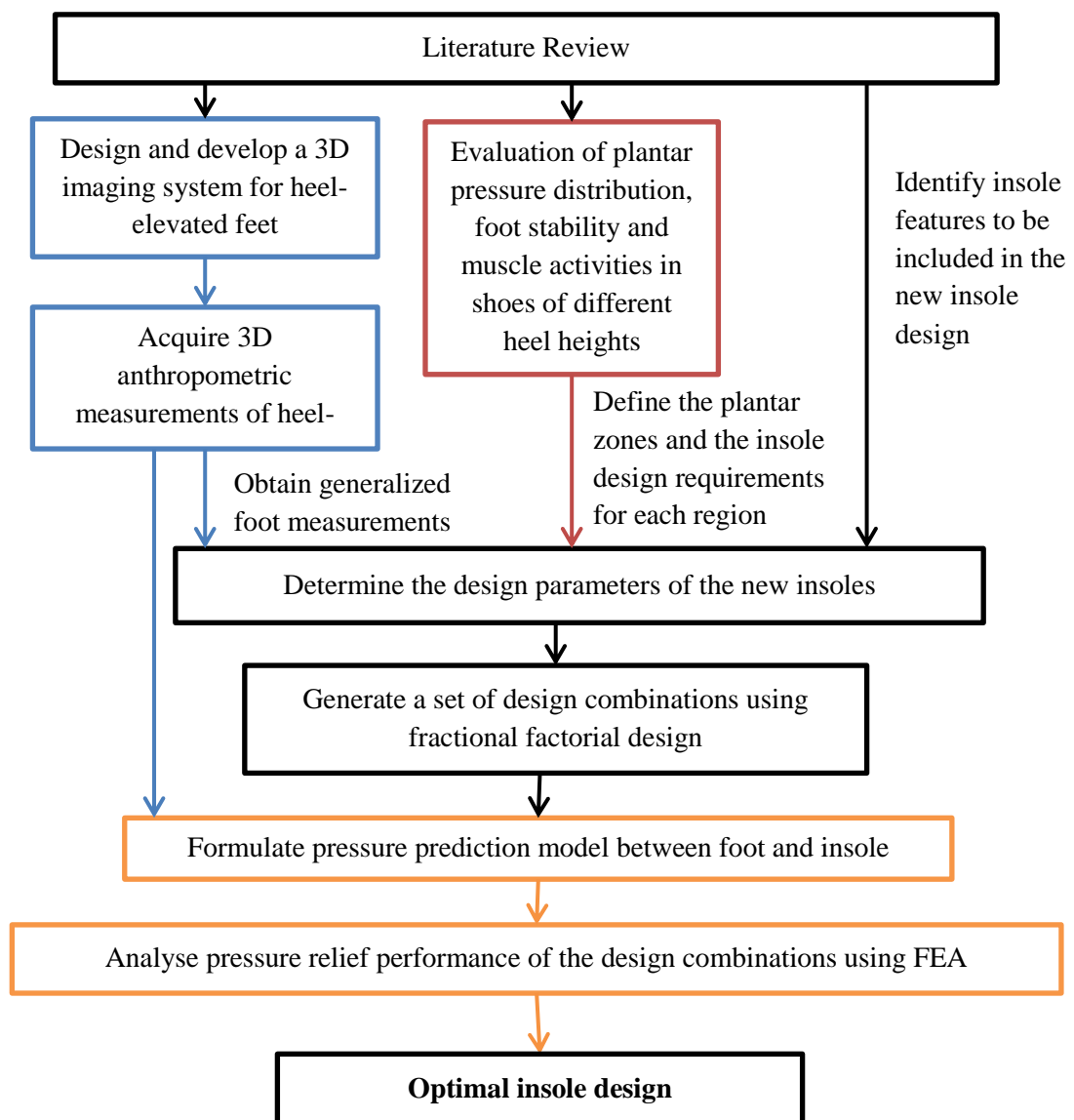
Figure 3-1. Flow diagram of research plan

3.1. Heel-elevated foot anthropometry evaluation

In order to assess the ability of current 3D scanning systems in scanning heel-elevated foot and the possibility to adopt these systems for the present study, an evaluation with Frontier's 3D Foot Scanner and NextEngine was carried out. The former system failed to scan foot in heel-elevated positions and the latter took too long to acquire a complete 360° scan image. Both systems were not considered suitable to be used in the present study.

In view of the lack of equipment to obtain foot anthropometric measurements, a 3D foot and Ankle Imaging System was designed and built. The development could acquire a 360° 3D foot scan within 1 second. It allowed both geometric and colour information to be recorded. Its repeatability was assessed. System accuracy were examined and benchmarked with Steinbichlar's Comet Vario Zoom Scanner, a market available pattern projection 3D scanner.

Massive 3D foot anthropometric measurements were taken on human subjects with their feet resting on foot supports at various heel heights. Information extracted from the scans would serve as a reference for the dimensional parameters of the new insole design

3.2. Plantar pressures distribution and foot stability analysis

Human subject experiments were carried out to collect plantar pressure information of HHS wearers during some of the most frequent daily activities, standing and walking. Four different testing conditions, HHS with heel heights of 1cm, 5cm. 8cm and 10cm, were tested.

Since experience in wearing high-heeled shoes may affect one's strategy in HHS balance control, two subject groups (regular and non-regular shoe wearers) of healthy young females were recruited. Shoe samples were provided to the subjects according to the subject's shoe size. They were required to perform tasks including bipedal quiet standing, single-leg standing and normal walking along a 6 meters straight path. Questionnaire was distributed and filled by each subject to evaluate their perceived comfort and fit of shoe samples.

General high-heeled gait parameters such as cadence, stride length, stance-swing phase percentage will be studied. Measurement parameters that are related to body balance such as the trajectories, excursions and variations of center of pressure in antero-posterior and medio-lateral directions will also be evaluated. The effects of heel heights and Findings would serve as a reference for the structural design and material selection of the new insole.

3.3. Muscle activities analysis

Wearing HHS significantly increases certain leg muscle activities and could lead to muscle fatigue. In order to analyse the effects of heel heights and high-heel experience on muscle activities of selected muscles when maintaining standing balance, surface electromyography (EMG) experiments were carried out on 24 healthy female subjects. Muscles governing standing balance control in medio-lateral and antero-posterior directions were identified and examined. High muscle activities and long activation periods of different muscle motor groups could indicate foot instability in the corresponding direction and thus better foot support might be required in the new insole design.

3.4. Design of New Insole and evaluation with Finite Element Analysis

One of the primary objectives of the present study is to design an insole that could lower plantar peak pressure and at the same time provide optimal foot support in high-heeled shoes. In conjunction with the results collected from foot anthropometry evaluation and high-heeled gait analysis, a new insole was designed with 7 design variables, including insole thickness, materials and dimension of cushions. Insole materials were selected based on the function requirements of the design feature. The effects of the 7 design parameters on the magnitude and location of peak pressures were analyzed using FEA. The optimal insole design is the one that performed the best in peak plantar pressure relief.

Chapter 4 – Evaluation on female foot anthropometry in heel-elevated posture

4.1. Introduction

The use of HHS alters the way how the body weight acts onto the foot. With elevated heel heights, the load of body weight is shifted to the forefoot and rearfoot areas (Mandato, 1999, Speksnijder et al, 2005) and changes the direction to which the load is applied to the foot arch and thus results in arch deformation and muscle strains. By studying the changes of foot geometry in different heel heights, we can better understand the effect of heel heights on human foot anatomically and biometrically.

With the evolutionary developments in digital imaging and computing technologies, 3D surface scanning is becoming a powerful means to acquire geometric measurements, especially for objects that are having complex and organic geometries and where geometries have to be recorded in high level of detail. The recent enabling 3D scanning technologies allow fast and accurate geometric measurements to be taken. In addition to 1D and 2D linear measurements such as lengths, angles and girths, more 3D measurements, such as surface area, and even volume information can be computed from the 3D scans. Some scanning systems even record real colour and textural information of the scan object. The technology serves a very useful means to study organic geometries such as the human bodies.

In order to determine whether the shape characteristics of the foot vary with heel height, a systematic study was carried out to collect 3D foot measurements during standing in different heel elevations. The shape characteristics of the foot were then evaluated by examining the linear dimensions and angles.

4.2. Evaluating the performance of current 3D scanning systems on scanning heel-elevated foot

Since all commercial 3D foot scanners are designed for scanning the foot that steps flat onto the scanning platform, a pilot study was carried out to examine the scanning performance if the heel of the foot to be scanned is elevated in different heights. In this pilot study, five women subjects have been recruited to perform foot scanning with two scanning systems: a 3D foot laser scanner developed by Frontier Advanced Technology Limited and a general-purpose scanner, the NextEngine 3D laser scanner. For each subject, both feet were scanned and four 3D foot scanned images were obtained on each foot for each scanning system. The four 3D foot images include one with the foot flatly resting on the floor (NextEngine 3D laser scanner) or the scan platform (Frontier 3D foot laser scanner), and three other scans for the foot resting on different heel supports at heights of 1, 5 and 8 cm When scanning with the NextEngine 3D laser scanner, six scans were performed at six different locations around the foot to combine a final 3D foot image with the software provided by NextEngine. The scanning performance of the two systems was then evaluated in consideration of data quality and completeness and scanning and processing time.

NextEngine's laser scanner gave full colour scans (Figure 4-1). Apart from shaded areas, such as the plantar surface and those in-between the toes, the scan quality is satisfactory. The level of details and completeness of the final 3D image, however, can be further improved by increasing the scanning resolution and adding more scans from more angles respectively, but this would significantly lengthen the scanning and processing time. There is always a trade-off between scan data quality and scan time.

Figure 4-1. Foot scanned images from the Frontier 3D foot laser scanner with foot of subject resting flat on the scanning platform (top left); foot heel resting on support that is 1 cm (top right), 5 cm (bottom left) and 8 cm (bottom right) in height.

Frontier 3D foot laser scanner allows the plantar surface to be scanned. The latter provided a quite complete 3D image of the foot and ankle area when scanning the foot in a natural resting position on the scanning platform. Undulations of the scan surface were observed along the cross-sectional projected laser lines, although this can be improved through system calibration or eliminated by simply smoothing the mesh. Outlier scan data points sometimes appeared at both ends of the foot image. When the heel was elevated, the scanner could still scan the plantar surface but the data quality became very poor towards the rear of the foot and the ankle area. A higher heel height means poorer quality of the scan data.
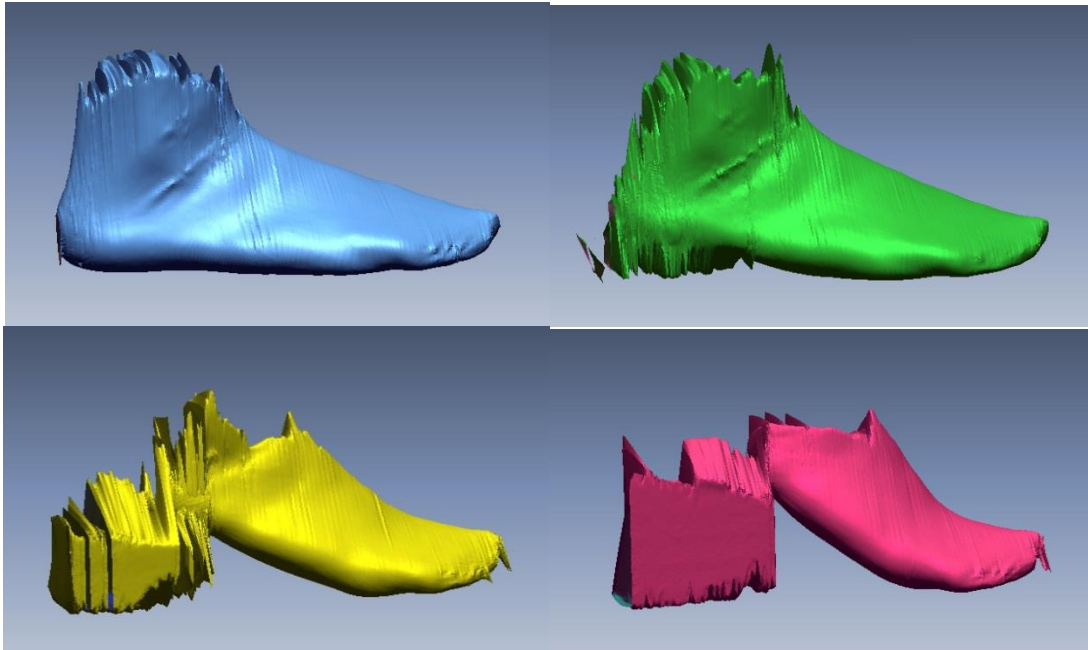
Figure 4-2. Foot scan images from the Frontier's 3D Foot Laser Scanner with subject's foot resting flat on the scanning platform (top left); foot heel resting on support of 1cm (top right), 5 cm (bottom left) and 8 cm (bottom right) in height

When performing the automated foot measurement functions provided in the Frontier scanning software package, it was found that many of the foot feature points and measurements were not correctly derived.
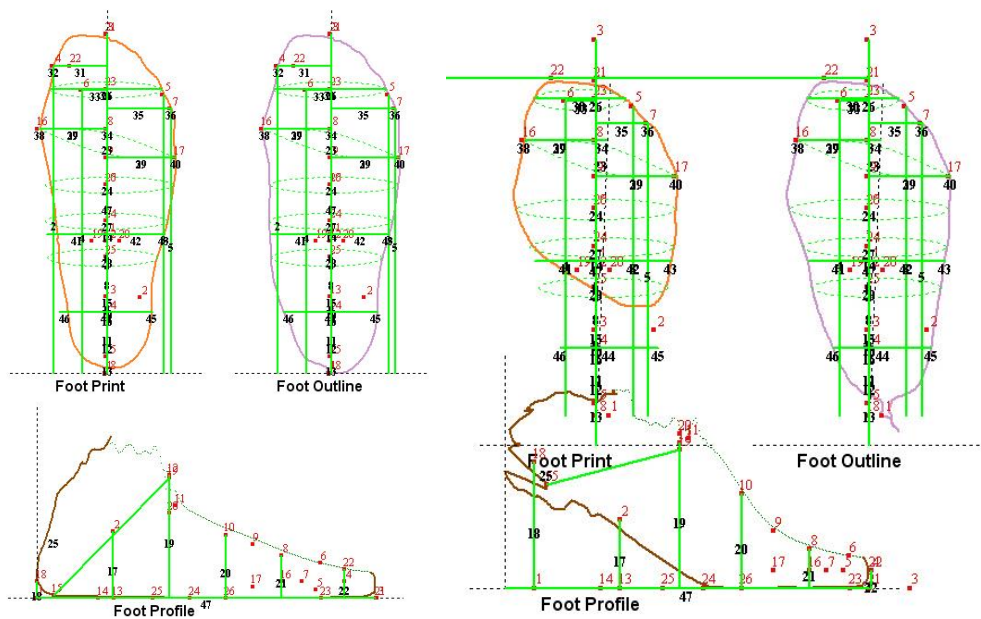
Figure 4-3. Automated foot measurements derived from a standard foot scan (left) and a 5 cm heel-elevated scan (right)

As shown in figure 4-3, since all automated height measurements are defined as vertical measurements from the scanning plate, and many other automated foot measurements are derived based on the foot length, uplifting the heel and failing to detect the correct foot length imply that all other automatic foot measurements are not reliable, thus taking away the merit of adopting a commercial 3D foot scanning system.

Current 3D foot scanning systems available in the market are easy to use, but the foot to be scanned has to be positioned in designated orientations and postures. Other general-purpose scanners take too long to scan the whole foot, which might result in data inconsistencies due to participant fatigue. Both the NextEngine and Frontier scanners in this research work do not adequately fulfill the requirements of scanning time and data completeness for foot scanning in heel-elevated positions.

4.3.   Development of the 3D Foot and Ankle Imaging System

Although 3D foot scanning has been extensively utilised in the footwear industry, specific information on foot anthropometric measurements of elevated heels is particularly scarce. The lack of scanning equipment might be one of the reasons for this deficiency of information. As described in the previous section, market available foot scanners only allow foot scanning to be performed in a designated foot flat position. Problems would arise when scanning a heel-elevated foot (Wan et al., 2014). In this study, a 3D foot and ankle imaging system (Figure 4-4) is developed. The system enables a 360° scan with full colour to be performed within a timeframe of one second.
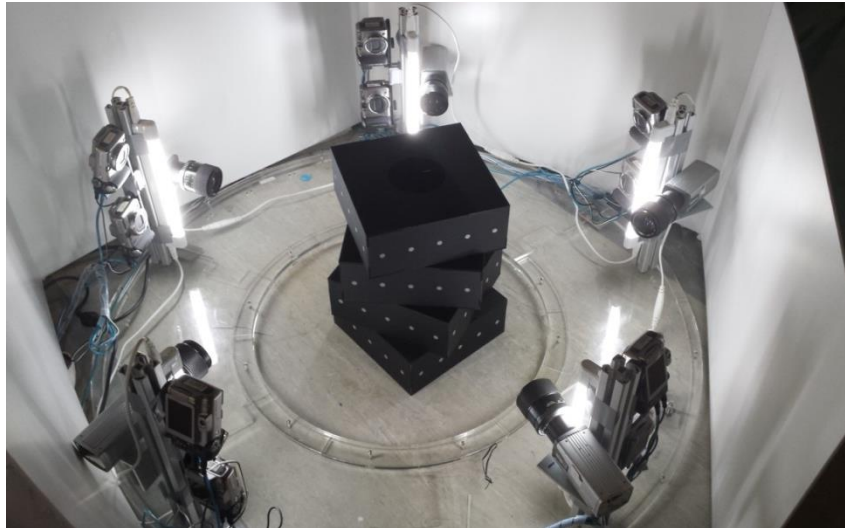
Figure 4-4. The newly developed 3D foot and Ankle Imaging System

4.3.1. Architecture of the 3D foot and ankle imaging system

The 3D foot imaging system is comprised of five scanning modules (See figure 4-4). Each module is consisted of a pair of Canon Powershot A650IS digital cameras, a pattern projector and a 12-inch fluorescent tube. Camera settings such as the shutter speed, zoom factor, aperture size were individually configured and stored in the cameras locally, which would be resumed automatically every time when the cameras were switched on.

All cameras were connected to two control units, through which the power supply and command signals were given to the cameras and images were transferred by means of USB cables. The two control units were separately connected to two laptop computers with USB cables, whereas the laptops were connected to each other by means of LAN cable.

The digital cameras, pattern projectors, control units, and the operation programme were previously developed by Industrial Centre of The Hong Kong Polytechnic University. In the present study, modifications were made to the instruments upon the size of the projected pattern, the number of scanning modules to be adopted, their

locations and orientations. These parameters were carefully examined so that the best scan coverage and level of detail can be attained in the final foot model.

Operation commands were given at one of the laptop computers (acting as an operation centre) and were then sent to the other laptop. Through the two laptops the command signals will be sent to the two control units separately, where the signals were synchronized and sent to the cameras. The cameras will finally execute the commands. Operator could control the following actions of each camera:

(1) Power on / off

(2) Focus

(3) Shutter / Image taking

(4) Switching between photo capture mode and data transfer mode

(5) Upload images from SD card to a designated location in the laptop computer

(6) Delete images stored in SD card

Images taken during a scan will be temporarily stored locally in the SD card inserted in the camera before being uploaded to the laptops.
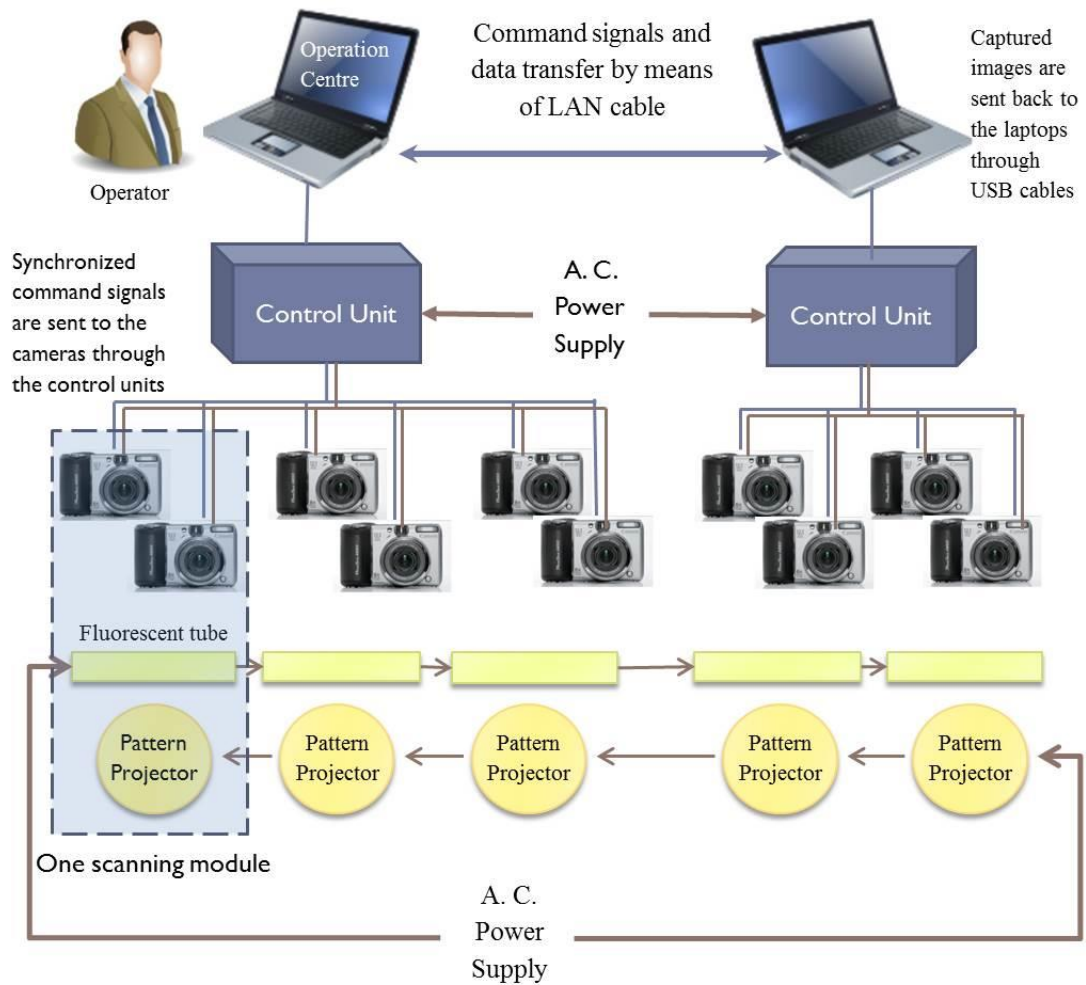
Figure 4-5. Diagram illustrating the architecture of the 3D foot and ankle imaging system

4.3.2. Camera Calibration

All cameras had to be calibrated prior to scanning. Their six exterior orientation parameters, which includes the camera positions and rotation angles about the x-, y- and z- axis, together with the interior parameters that describe the cameras' focal lengths, image centres, coefficients of radial lens distortions and tangential distortions will be determined during the calibration process. These parameters will be used to reconstruct the 3D model from 2D images during the scanning process. The camera calibration algorithm was written based on the work of Heikkilä and Silvén (1997).

Figure 4-6. Each camera has to take an image on the calibration range during camera calibration

A 4-layer calibration range of the shape of a twisted cuboid was designed and fabricated for camera calibration. The range was made up of 0.5 cm thick acrylic with black mat surface. Each layer had four sides. Five retro-reflective circular targets were attached on each side. A total of 80 circular targets were attached across the whole calibration range to serve as control points in the camera calibration. The positions of these circular targets in the 3D space were carefully surveyed by close-range photogrammetry.

Calibration accuracy would be affected if the observed targets lie on the same plane. The four layers were therefore rotated at 45 degrees as they stacked up. By doing so the targets captured in every camera would lie on various planes. Under this target array arrangement, at least 25 targets would be captured by each camera during calibration.

The camera calibration process is similar to a scanning process, just that the foot is replaced by the calibration range. After calibration, the scanning accuracy of the calibrated space (volume bounded by the targets) would be assured.

4.3.3. The 3D scanning workflow

Two images will be taken consecutively by each camera within 1 second during the scanning process. The first image records the real colour and texture information of the scanned foot while the second image will be used to reconstruct the 3D foot model. Figures 4-7 and 4-8 show the collections of first images and second images respectively taken during a scan. When taking the first image, fluorescent tubes were switched on to illuminate the scanning booth. The lights would then be switched off when speckle patterns were projected onto the foot before taking the second image. The diagram in Figure 4-9 describes the flow of the scanning procedures.
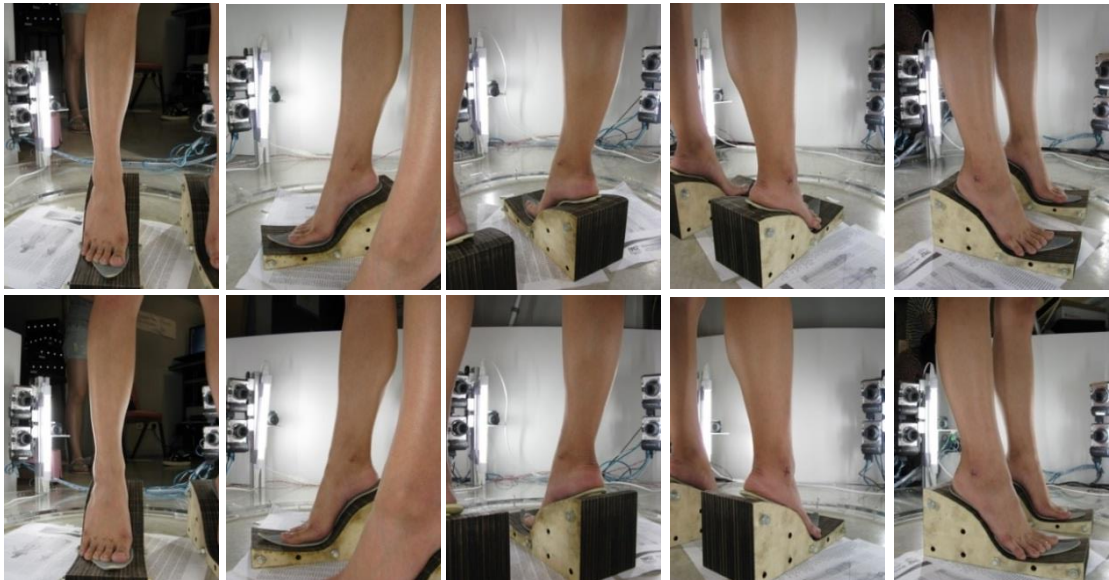
Figure 4-7. A collection of the first images taken by the 10 digital cameras

Figure 4-8. A collection of the second images taken by the 10 digital cameras
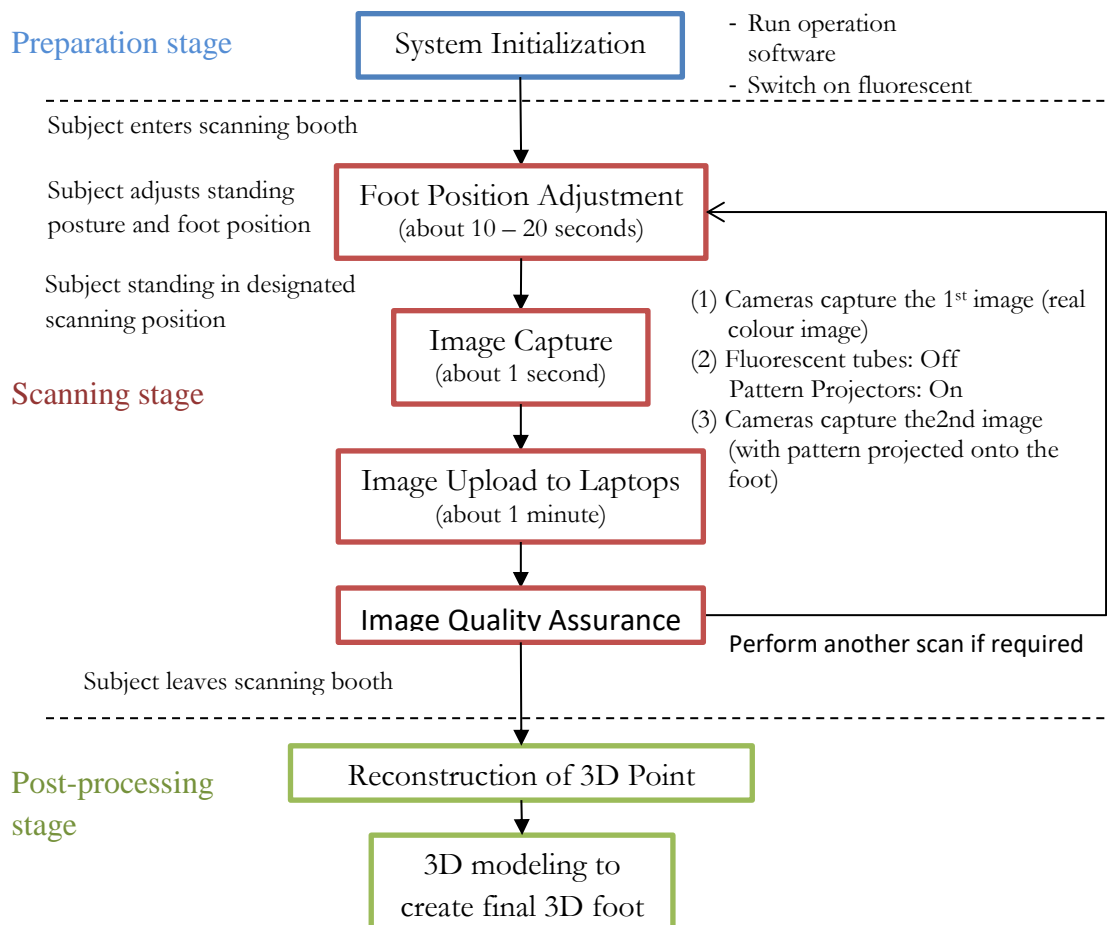
Figure 4-9. Flow diagram describing the scanning procedures

65

After taking the images, the operator could download all images that were stored locally in the cameras to the operation centre. The scanning stage was thus completed. These images, together with the camera calibration parameters calculated in the camera calibration, would be used to compute the 3D point models in the post-processing stage.
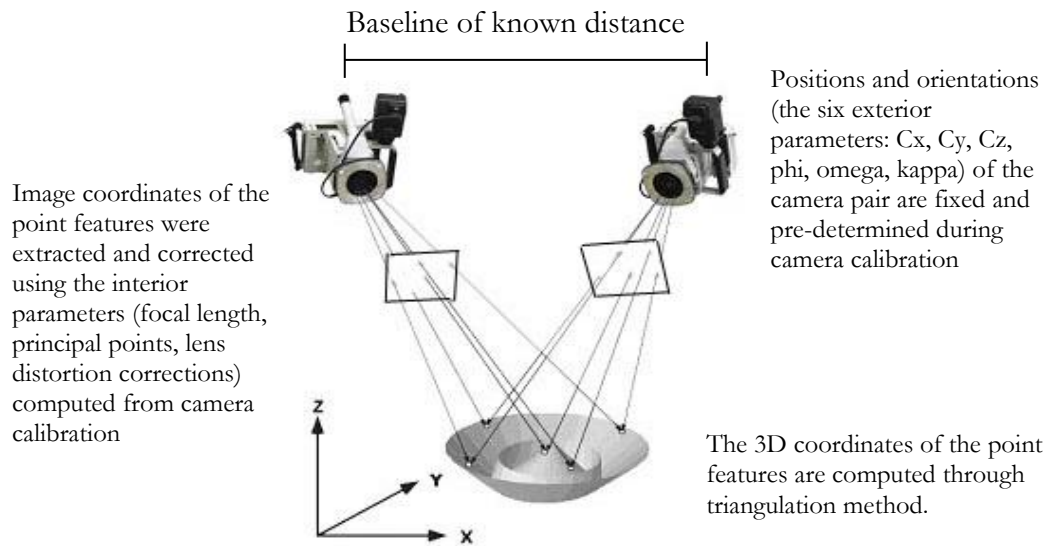
Figure 4-10. 3D point features were computed by the triangulation principles.

Reconstruction of the 3D models from the image pairs is an automated process. For each image pair, point features that can be identified in both images were extracted. Lens distortion corrections were then made to the image coordinates of these point features in accordance with the intrinsic parameters obtained from the camera calibration. (Please refer to section 4.3.2) The 3D coordinates of each identical feature point would then be computed based on the concepts of photogrammetry.

The raw data output of the 3D Foot and Ankle Imaging system was five aligned colour point clouds reconstructed from the second image pair (Figure 4-8) of each scanning module. Further post-processing can be carried out using any 3D modeling software to produce mesh models (Figure 4-11), surface models or solid models depending on the application requirements. High definition colour textural information was finally

mapped onto the 3D model (Figure 4-12) with the texture mapping algorithms of the system based on the camera calibration parameters.
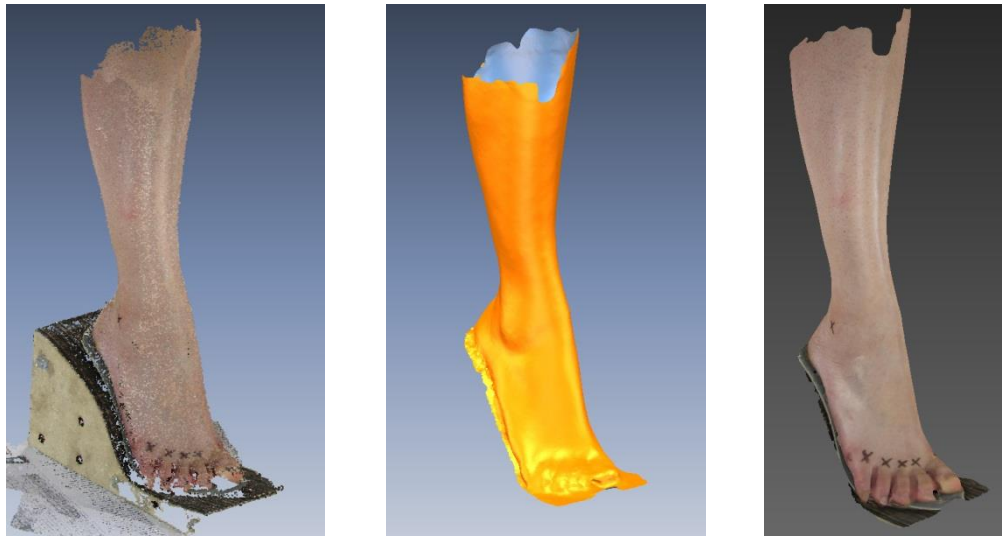
Figure 4-11. Five aligned colour point clouds exported from the 3D foot and ankle imaging system (left). Polygonal mesh model created from raw scanned data with Rapidform XOR3 (middle). High definition textural information mapped onto mesh.

Figure 4-12. The resulting real colour mesh model in different views.

4.4. Evaluating and Benchmarking the newly develop 3D Foot and Ankle Imaging System

4.4.1. Introduction

To evaluate the performance of the 3D Foot and Ankle Image System, the bottom half of a rigid mannequin (Figure 4-13) was chosen as the reference object to examine the system's repeatability and accuracy. This chosen mannequin had a mat surface with skin colour which better imitated the human skin conditions. In addition, its foot features such as toes, nails were more profound (Figure 4-14) and could provide features with greater level of detail (LOD) to assess the system performance.

The evaluation included three tests: (1) repeatability of scans, (2) accuracy of scans, and (3) accuracy of foot measurement extraction. The methods of the tests will be described in the following section. Results of the evaluation will be presented and discussed in Section 4.4.3.

Figure 4-14. Detailed Foot features can be found on the chosen mannequin

Figure 4-13. Bottom half of the chosen mannequin

4.4.2. Methodology

4.4.2.1. Repeatability test

A reliable scanning system should always give the same scanning result under the same scanning condition such as scan object position and lighting. An experiment was therefore designed and carried out to assess the repeatability of the 3D Foot and Ankle Imaging system.

A total of 10 sets of scan were captured on the mannequin in the repeatability test. The mannequin was first placed on the designated scanning position (P1), as shown in figure 4-15, where five scans were taken. The mannequin was then rotated about 30 degrees clockwise (P2), at which another five scans were performed. The systems were switched off and on in between each scan.
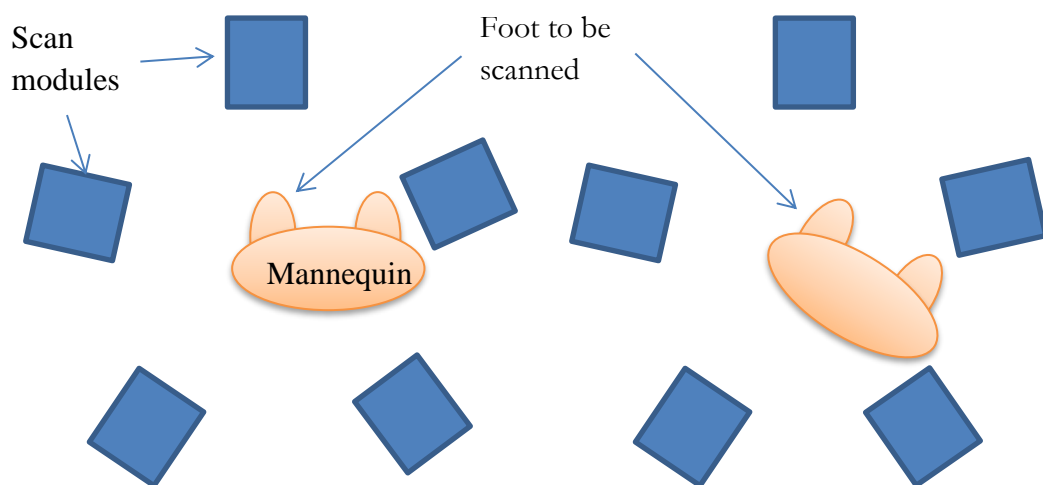
Figure 4-15. Mannequin at designated scanning position (P1) (left) and rotated position (P2) (right).

All of the raw scan data, that is, the point clouds, were processed by using Rapidform® XOR3™ under the same computation parameters to produce polygonal mesh models. These mesh models were then superimposed and the mesh deviations of three randomly selected pairs (1) among the scans acquired in P1; (2) among the scans

acquired in P2; and five randomly selected pairs (3) between scans obtained in P1 and P2, were evaluated. The accumulated areas (in percentage of the total mesh area) over the mesh deviations were computed for each pair at 0.1 mm increments (Psikuta et al. 2015).

4.4.2.2. Accuracy test– benchmarking with high quality optical scanner

After the developed imaging system proved to have good repeatability, its measurement accuracy was examined. In this test, the 3D foot and ankle imaging system was compared with a market-available optical scanner, the Comet Vario Zoom 400 Scanner (Steinbichler Optotechnik GmbH). The scanner provides sequentially projected binary fringes with white light as the projection pattern and data accuracy up to ±0.1 mm.

Figure 4-16. The mannequin was scanned by Comet Vario Zoom scanner by Steinbichlar Gmbh
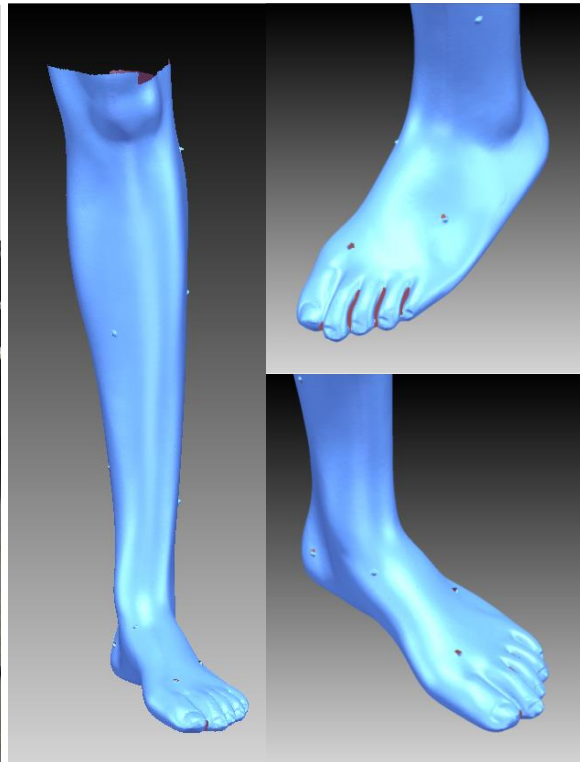
Figure 4-17. A collection of images showing the mesh model created from the scans of Comet Vario Zoom.

A total of 39 partial scans were performed by the Comet Vario Zoom scanner. These partial scans were then being merged to create a single mesh model with a modeling software, Rapidform XOR3. Figure 4-17 shows the final mesh output. This model was used as a reference model and compared against the six mesh models created from the 3D foot and ankle imaging system in P1 for the repeatability test. The accumulated areas (in percentage of the total mesh area) over the mesh deviations were computed for each pair at 0.1 mm increments. The mesh deviations could be regarded as the measurement errors of the tested imaging system.

4.4.2.3. Validating foot anthropometric measurements

The 3D foot and ankle imaging system was designed for scanning the foot with elevation of the heel such that anthropometric measurements could be extracted from the digital scan models. Apart from assessing the spatial accuracy of its resultant models, it is equally important to assess the accuracy of the colour and textural components of the scanned models, which would in turn affect the accuracy of locating any colour landmarks to be used in the foot scanning exercise. Thus, by evaluating the accuracy of the landmark distances extracted from the scans, the textural data accuracy could be validated.

Since the Comet Vario Zoom 400 Scanner does not record colour in its scans, a digital caliper was used to measure the landmark distances on the reference mannequin.

First, nine landmarks were identified on the right foot of the mannequin and marked with an "x" with a red ballpoint pen that has a 0.5 mm line weight. Eight linear distances between these nine landmarks (as shown in Figure 4-18) were then measured on the mannequin with a digital caliper (with precision of 0.01 mm) by a single examiner. These distances were later compared with those extracted from three

randomly selected mesh models acquired in P1 by the same examiner with the use of Rapidform XOR3. Three rounds of measurements were carried out and the average value of each distance measurement parameter was evaluated.
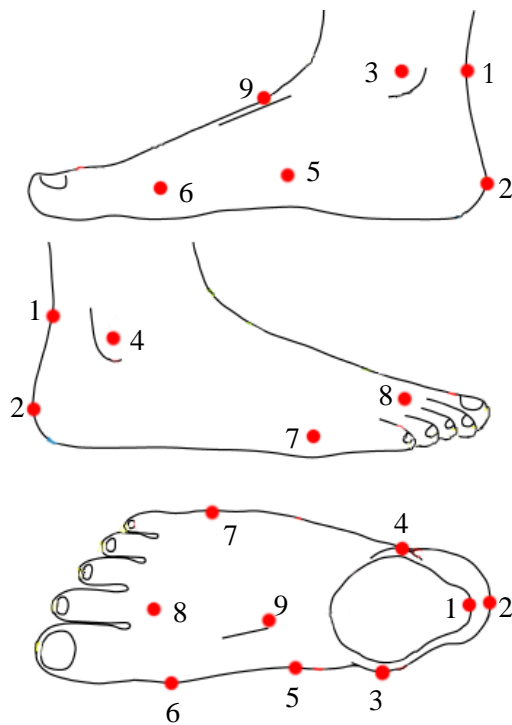
Figure 4-18. Medial (top), lateral (middle) and dorsal views that show landmark locations marked on mannequin.

Table 4-1. Linear measurement parameters extracted from mannequin.

Linear measurement (Dominant direction vector)	From Landmark	To Landmark
D1 (L)	3	8
D2 (L)	2	7
D3 (L)	8	9
D4 (W)	6	7
D5 (W)	3	4
D6 (W)	6	8
D7 (H)	1	2
D8 (H)	5	3

Statistical analysis was carried out on all of the measurement parameters. Independent sample t-testing was carried out to evaluate the statistical significance of the differences between the two different measurement methods. Significance was established at p =0.05.

4.4.3. Result and Discussion

4.4.3.1. Repeatability of 3D scans on mannequin

To evaluate the repeatability of the 3D foot and ankle imaging, the mesh deviations of three randomly selected pairs (1) among the scans acquired in P1; (2) scans acquired in P2; and five randomly selected pairs (3) between scans in P1 and P2 were evaluated.

For scans acquired in P1, 99.06% of the areas of overlap between the meshes have a deviation less than ± 0.5 mm, and 99.9% within ± 1 mm. Similar results were obtained in P2, where 99.34% of the areas of overlap between the meshes have deviations less than ± 0.5 mm, and 99.98% within ± 1 mm. Repeatability of the scans that are randomly selected pairs in P1 and P2 is similar (99% within ± 0.5 mm), thus indicating that the repeatability by this system is high when the scans are performed under the same conditions, such as the scan module settings and configurations, positioning of the scan object, and lighting. The system repeatability is comparable to that of a handheld scanner, Artec MHT (Artec Group, USA), which attained a repeatability of 0.6 mm as evaluated by Psikuta et al. (2015).

In comparing the scans acquired in P1 with those in P2, the repeatability is reduced. Deviations are less than ± 0.5 mm and ± 1 mm for 93.53% and 99.64% of the accumulated mesh area respectively. The reduced repeatability of the scans that are randomly selected pairs in P1 and P2 indicates that the orientation of the scan modules could affect the coverage and accuracy of the scans, and P1 has a better scanning orientation. This observation also shows that the current positions and orientations of the scan modules have positive effects on the accuracy of the system. Subjects should therefore position themselves on the position and orientation in P1.

4.4.3.2. Benchmarking - Accuracy of 3D scans on reference mannequin

In benchmarking the scanning results of the new imaging system against that of the Comet Vario Zoom scanner for accuracy assessment, it was found that 99.07% of the areas of overlap between the meshes have a deviation less than ± 0.8 mm and 99.59% within ± 1 mm. The accuracy of the system is therefore about ±0.8 mm for over 99% of the areas of overlap between the meshes (Figure 4-19). This value is well within the measurement tolerance for the designated applications in foot measurement, as the smallest measurement unit used in most conventional measuring equipment in anthropometry, such as rulers and tapes, is at the millimeter level.
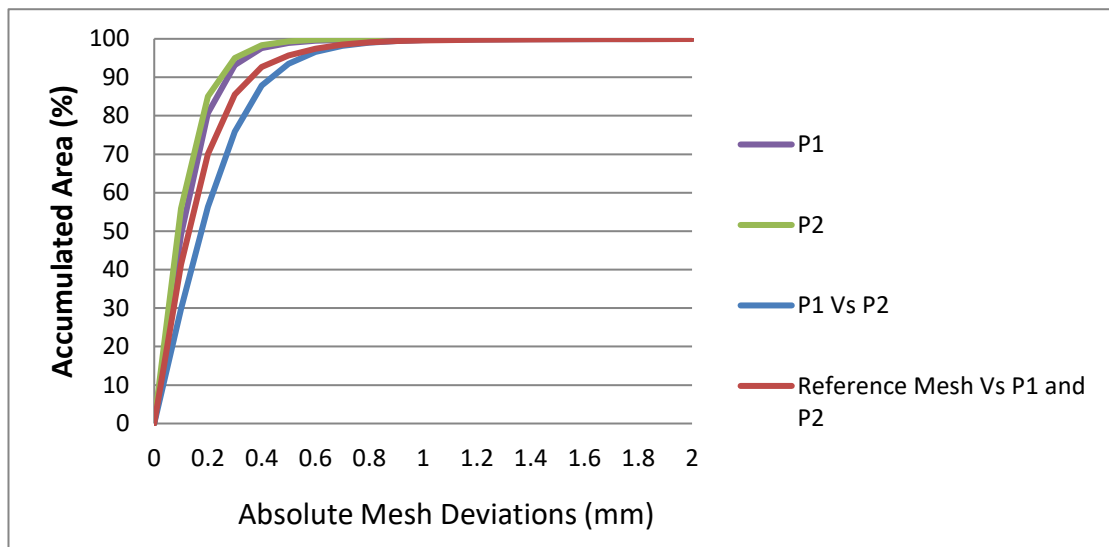
Figure 4-19. Graphical presentation of repeatability of scans in (1) P1, (2) P2, (3) randomly selected pairs in P1 and P2, and (4) between reference mesh captured by Comet Vario Zoom scanner and scans in P1

4.4.3.3. Validating 3D foot anthropometric measurements - comparison with manual foot measurements

In order to validate the accuracy of the colour and textural data of the imaging system, colour landmarks were drawn on a reference mannequin and their locations identified to extract certain foot measurements. Independent sample t-testing was carried to

evaluate the statistical significance of differences between the measurements obtained from a digital caliper and the 3D foot and ankle imaging system. The significance was established at p = 0.05. Table 4-3 shows the results of the independent sample t-tests.

Table 4-2. Results of independent sample t-tests that compare and evaluate the mean differences of the two methods. Significance established at p < 0.05.

Measurement variable	Digital Caliper		3D foot and ankle imaging system		Mean Diff.	Sig. (2-tailed)
	Mean (mm)	SD	Mean (mm)	SD		
D1 (L)	127.266	.0796	127.26778	.070	-.00178	.971
D2 (L)	**149.354**	**.0493**	**149.53032**	**.145**	**-.17632**	**.050**
D3 (L)	56.272	.0455	56.38236	.122	-.11036	.117
D4 (W)	**90.410**	**.0430**	**90.00369**	**.312**	**.40631**	**.022**
D5 (W)	**55.282**	**.0466**	**55.04092**	**.214**	**.24108**	**.022**
D6 (W)	**39.854**	**.0167**	**39.46194**	**.104**	**.39206**	**.000**
D7 (H)	27.314	.0416	27.32806	.150	-.01406	.848
D8 (H)	63.876	.0279	63.78989	.205	.08611	.403

For the length and height measurements, no significant differences were found between the mean values of the two methods, except at D2 (mean difference = -0.18 mm). All of the width measurements, D4 (90.00 ± 0.31 mm), D5 (55.04 ± 0.21 mm), D6 (39.46 ± 0.10 mm), which were taken from the 3D models, are less than those measured with the digital caliper, by 0.41 mm, 0.24 mm and 0.39 mm respectively. Moreover, the standard deviations with 3D imaging are generally greater than those with the use of the digital caliper.

The greater standard deviations can be explained by the mesh model resolution and the measurement extraction method used in the modeling software. In Rapidform XOR3, linear measurements can only be taken between mesh vertices, but not in any other part of the polygonal faces. The extraction accuracy, therefore, is dependent on the mesh resolution. Scanning is a sampling process. The mesh models are digital representations

that approximate real objects. Errors are highly possible over the whole digitization process. The mesh resolution of the models is about 0.5 mm while the precision of the digital caliper is 0.1 mm. The standard deviations of the measurements of the 3D foot and ankle imaging system are therefore greater than those of the digital caliper.

The reduced width measurements resulting from the mesh modeling might be related to the smoothing during the mesh building process. Smoothing is usually performed when a mesh is built from a point cloud and during mesh optimization in which the mesh vertices are redistributed to obtain better polygon regularities. Although the mean differences are statistically significant, the discrepancies are relatively small (<0.5 mm).

The test showed that the red landmarks could be easily identified and accurately located on the mesh models, thus indicating that the colour and texture are mapped onto the mesh model with good accuracy and resolution. The texture mapping algorithms adopted by the system are therefore qualified for applications in foot anthropometric measurements.

4.4.4. Conclusion

The results of the system evaluation has demonstrated that the newly developed 3D Foot and Ankle Imaging System has good scanning repeatability and its accuracy is well within the measurement tolerance for foot measurement in most anthropometric applications. Hence, with its fast scanning ability and availability of the colour and texture information, the new system is a reliable means to acquire foot measurements in the less stable heel-elevated postures.

4.5. Evaluation of foot measurements in heel-elevated postures

4.5.1. Foot scanning on human subjects

In order to study the foot anthropometry with elevated heels, a total of 45 subjects (21 – 35 years old, 160.3 ± 5.7 cm; 53.6 ± 5.8 kg) were recruited to undergo 3D foot scanning with the 3D foot and ankle imaging system. All of them did not have visible foot deformities and were free from foot injuries in the past three years. The study was approved by the Human Subjects Ethics Sub-committee of the Hong Kong Polytechnic University. All of the participants signed written informed consent prior to the implementation of the experiments.

Prior to scanning, the height and weight of the subjects were recorded by using a weight scale and a height rod respectively. Ten anatomical landmarks (Witana et al., 2006) were marked on their right foot with an eyebrow pencil. A total of three scans (with elevation of 0 cm, 5 cm and 10 cm of the heels) were performed for each subject. During scanning, the subjects were required to stand still on a flat wooden pile (elevation of 0 cm heel) or a pair of foot supports (with elevated heels) in a balanced position, with each foot supporting approximately half of the body load. The three conditions of the heels were scanned in random order. Figure 4-20 shows a subject who is standing on a pair of foot supports with an elevated heel of 10 cm. To minimise the scanning errors introduced by body swaying, all of the scanning was completed within two minutes and a two-minute break was allowed between the scans.
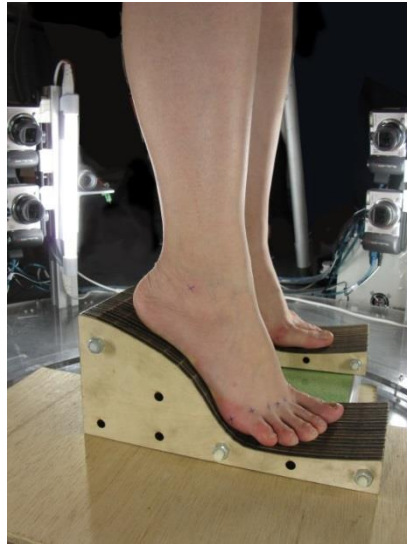
Figure 4-20. Subject standing on a pair foot supports with 10cm heel elevation

4.5.2. Production of the heel-elevated foot supports

To simulate the heel elevation condition similar to wearing HHS with corresponding heel heights, four pairs of foot supports were produced. The profiles of these foot supports were depicted based on the shoe profiles provided by the shoe manufacturer of our shoe sample. Figure 4-21 shows the side view of the foot support.
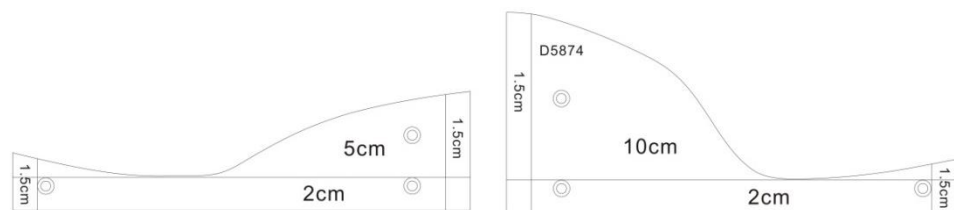
Figure 4-21. Design of foot supports with 5 cm and 10 cm heel elevation.

The foot supports (Figure 4-22) were made by stacks of wood piles of 1cm thickness. The wood piles were cut into designated shape by laser cutting. They were then stacked up to required width and fixed tight together by means of plastic rods and screws.

Figure 4-22. The two pairs of foot support

4.5.3. Foot anthropometric measurement extraction and evaluation

In order to study the shape characteristics of the forefoot area, 18 measurement parameters including two toe angles, two toe lengths, three widths across the metatarsal head area, five metatarsal-phalangeal joint (MPJ) heights and five distal interphalangeal (DIP) joint heights were extracted from each scan. These measurements were selected based on the measurements of the flattened shoe last patterns around the forefoot area (Chen, 2005). The ball girth was excluded in this study because it does not provide much detailed information about the shape characteristics of the forefoot. We replaced this measurement with the width and MPJ height measurements of each toe. Definitions of the measurement parameters are provided in Table 4-2 and illustrated in Figure 4-23.

Table 4-3. Definitions of forefoot measurement parameters

Definition of foot dimensions			
Foot Axis			Vector that runs from the pternion to the second MPJ projected on the x-y plane
Ball Axis			Vector that joins the most laterally prominent point of the first and the fifth MPJs on the x-y plane
Tread Point			Intersecting point between the foot axis and ball axis
Angle	A1	Flex Angle	Angle between the foot axis and ball axis measured on the horizontal plane
	A2	Hallux Angle	Angle between the orthogonal ball line and the line that passes through the medial edge of the ball width to the contact point on the hallux side measured on the horizontal plane
	A3	Small Toe Angle	Angle between the orthogonal ball line and the line that passes through the lateral edge of the ball width to the contact point on the side of the small toe measured on the horizontal plane
Length	L2	Hallux Length	Distance from the tread point to the tip of the hallux along foot axis
	L3	2nd Toe Length	Distance from the tread point to tip of the hallux along foot axis
Width	W1	Orthogonal Ball Width	Horizontal distance measured between the most laterally prominent point of the first and the fifth MPJs
	W2	Medial Ball Width	Distance between the tread point and the most medially prominent point of the fifth MPJ along the x-axis
	W3	Lateral Ball Width	Distance between the tread point and the most laterally prominent point of the first MPJ along x-axis
Height	H1 – H5	MPJ Height	Distance measured from the surface of the foot platform to the top of the MPJ of each toe, along the normal of the surface of the foot platform.
	H6 – H10	Height at the DIP Joint	Distance measured from the surface of the foot platform to the top of the distal interphalangeal joint of each toe, along the normal of the surface of the foot platform.
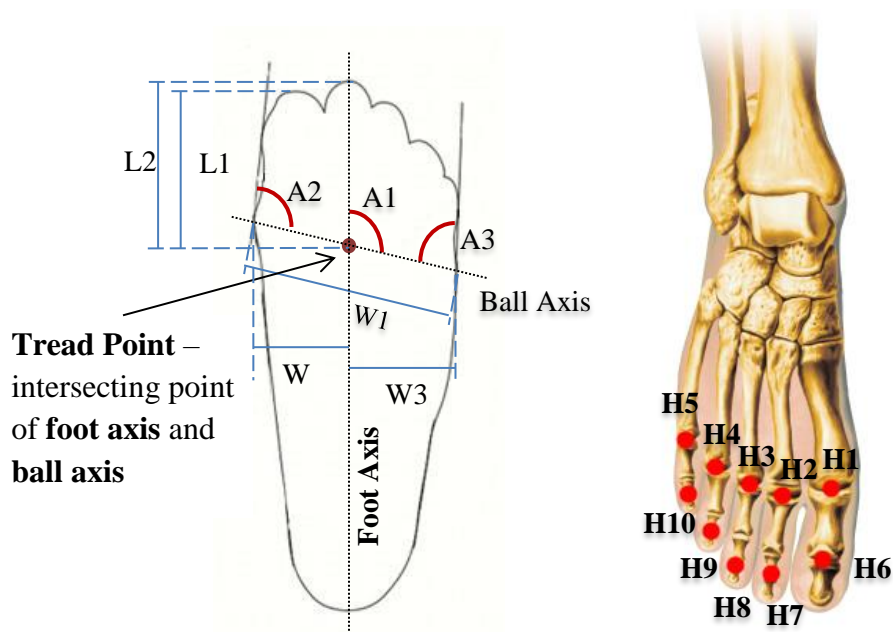
Figure 4-23. Dorsal view of measurement parameters: L1-3, A1-3 (left). Dorsal view of locations where H1 to H10 are measured (right).

Statistical analysis was carried out for all 18 measurement parameters with IBM SPSS Statistics 21 software. Repeated measures of analysis of variance (RANOVA) was carried out to evaluate the statistical significance of the differences in the foot measurements measured for the three different heel-heights. Bonferroni post-hoc testing was also carried out to compare the means of all possible pairs of variables measured under the three different heel-heights. Significance was established at $p = 0.05$.

4.5.4. Results and discussion

Three angle measurements and fifteen linear foot measurements that encompass all three dimensions were extracted and statistically analysed. Table 4-4 is a summary of the results from the RANOVA and the Bonferroni post-hoc tests.

Table 4-4. Mean, standard deviations, significance of mean differences (RANOVA results) and pairwise significance (Bonferroni post-hoc test results) of each foot measurement parameter for three different heel heights

Measurement Parameter		0 cm Mean (S.D.)	5 cm Mean (S.D.)	10 cm Mean (S.D.)	Sig. of mean difference F	p
Hallux Length	L1	72.301 (±4.51)*°	73.698 (±4.37)*§	70.788 (±4.54)°§	25.265	.000
2nd Toe Length	L2	66.753 (±5.10)*	68.473 (±5.18)*°	65.492 (±5.32)°	16.032	.000
Orthogonal Ball Width	W1	90.475 (±5.05)*	90.277 (±5.63)°	89.046 (±5.10)*°	12.288	.000
Medial Ball Width	W2	38.162 (±2.45)	38.482 (±2.77)	37.861 (±2.41)	2.907	.075
Lateral Ball Width	W3	49.617 (±3.10)*	48.816 (±3.17)*	49.189 (±3.02)	3.538	.037
Flex Angle	A1	103.714 (±2.92)*	104.415 (±2.96)°	101.557 (±3.60)*°	15.682	.000
Hallux Angle	A2	96.729 (±3.69)	97.001 (± 4.85)*	95.191 (±5.86)*	7.577	.005
Small Toe Angle	A3	76.686 (±6.00)*°	78.496 (± 6.44)*§	81.857 (±7.85)°§	28.196	.000
Hallux MPJ Height	H1	26.802 (±1.90)*	26.914 (±1.73)*	26.941 (±1.90)	4.861	.018
2nd MPJ Height	H2	24.569 (±1.52)*°	24.154 (±1.44)*	24.079 (±1.54)°	12.974	.000
3rd MPJ Height	H3	23.247 (±1.41)*°	23.662 (±1.58)*	23.737 (±1.56)°	12.974	.000
4th MPJ Height	H4	22.418 (±1.59)*°	23.635 (±1.63)*§	25.101 (±1.94)°§	86.581	.000
5th MPJ Height	H5	20.216 (±2.05)*°	22.570 (±2.16)*§	25.450 (±2.18)°§	112.706	.000
Hallux DIP Joint Height	H6	18.667 (±1.22)*	18.039 (±1.31)	17.888 (±1.16)*	4.469	.017
2nd DIP Joint Height	H7	13.548 (±1.52)*°	12.600 (±1.37)*	12.889 (±1.32)°	12.677	.000
3rd DIP Joint Height	H8	12.737 (±1.42)	12.453 (±1.29)	12.511 (±1.04)	.986	.381
4th DIP Joint Height	H9	12.256 (±1.33)	12.008 (±1.19)	12.114 (±1.27)	.482	.580
5th DIP Joint Height	H10	12.793 (±1.57)	12.595 (±1.43)	12.699 (±1.26)	.176	.839

All linear measurements are measured in mm, and angle measurements in degrees.
Significance = $p < 0.05$.
Mean difference pairs with statistical significance: *, ° and §.

Toe lengths: Two toe lengths were extracted in the test: the hallux (first toe; L1) and the second toe (L2) lengths. For both parameters, the longest toe lengths were observed on heels elevated at 5 cm, with 73.7 mm for L1 and 68.5 mm for L2. The shortest toe lengths were found on heels elevated at 10 cm, with 70.8 mm and 65.5 mm for L1 and L2, respectively. Statistically significant differences (p=0.000) were observed for both L1 and L2. The significantly shorter toe lengths for a 10 cm heel elevation (approximately 5 mm shorter than those on heels elevated at 5 cm) might probably indicate an anterior shift of the tread point. This hypothesis will be further discussed and verified with other foot measurements later in this section.

Ball widths: Three width measurements were taken in the testing, amongst which significant differences were observed in the orthogonal ball width (W1) and lateral ball width (W3). The greatest orthogonal ball width was found on foot resting on a flat surface (90.475 ± 5.05 mm), followed by heels elevated at 5 cm (90.277 ± 5.63 mm), and finally, heels elevated at 10 cm (89.046 ± 5.10 mm). Although the mean differences were found to be statistically significant in RANOVA (p=0.000), the differences are small (greatest difference is 1.43 mm) when compared with the standard deviation (around ±5 mm). The level of mean differences could be considered as negligible.

Flex angles: The flex angle (A1) was found to be the greatest on an elevated heel of 5 cm (104.415° ± 2.96°), followed by an elevated heel of 0 cm (103.714° ± 2.92°) and finally an elevated heel of 10 cm (101.557° ±3.60°). The flex angle value for the an elevated heel of 10 cm was found to be significantly different from that for the lower heels of 0 and 5 cm, thus indicating that either (1) the pternion medially shifts relative to the forefoot as the heel is lifted, thus resulting in rotation of the foot axis in the clockwise direction or (2) the ball axis rotates in an anti-clockwise direction on the horizontal plane as the heel is increased, or (3) both situations happen at the same time. More supplementary information will be provided to support (2) when examining the toe angles and MPJ heights later.

Toe angles: Two angle measurements were extracted to explain for the toe spread. For the hallux angle (A2), a significant difference was found between an elevated heel of 5 cm (98.00° ± 4.85°) and 10 cm (95.19° ± 5.86°), with the largest and smallest values among the three heel heights, whilst the small toe angle (A3) increases with heel elevation. The mean small toe angles increased from 76.69° of the 0 cm heel to 78.496° on an 5 cm heel, and the highest angle is 81.86° on a 10 cm heel.

It is interesting to observe that with a 10 cm heel elevation, the hallux angle is the lowest but the small toe angle is the greatest, and the increase in the angle of the small toe (5.171° compared with 0 cm heel) is greater than the reduction in the angle of the hallux (-1.538° compared with 0 cm heel). This phenomenon possibly indicates that (1) the ball axis rotates in an anti-clockwise direction, and (2) the fifth toe spread farther out with increased heel elevation.

MPJ heights: Although statistically significant differences were observed in all of the MPJ heights for all three tested heel heights, the mean differences for the hallux, and second and third toes are very small, which are less than 0.5 mm. More obvious increasing trends were observed for the fourth and small toes as the heel height was increased. The MPJ heights of the fourth toe increased from 22.42 ± 1.59 mm on a 0 cm heel, to 23.64 ± 1.63 mm on a 5 cm heel, and the greatest on a 10 cm heel (25.10 ± 1.94 mm). The same trend of increase was observed for the MPJ heights of the small toe. The MPJ height for 0 cm, 5 and 10 cm heels are 20.22 ± 2.05 mm, 22.57 ± 2.16 mm and 25.45 ± 2.18 mm respectively. The increase in the MPJ heights in the fourth and smallest toes indicates that the lateral forefoot is lifted as heel elevation is increased, thus resulting in a smaller contact area between the plantar and the sole, and also shifting the body load to the metatarsal heads of the remaining three toes. This explanation accords with previous studies in which plantar pressures were found to be the highest on the hallux and medial forefoot (Speksnijder et al., 2005; Lee and Wong, 2005; Mandato and Nester, 1999) with increased heel height.

Lifting of the lateral forefoot also indicates a shift in the ball axis. By combining this observation with the aforementioned observations in the angle measurements (A1 to A3), it can be concluded that the ball axis rotates in an anti-clockwise direction as the

heel is elevated. This also explains why the toe lengths are shorter when the heels are elevated to 10 cm. As the ball axis rotates in the anti-clockwise direction, the tread point, based on which the toe lengths are measured, moves towards the direction of the toes. Therefore, shorter toe lengths are observed.

DIP joint heights: Significant differences were identified only in the DIP joint heights of the hallux and second toes. The DIP joint height for both toes on 0 cm heel was found to be greater and significantly different as opposed to an elevated heel of 5 and 10 cm. This indicates that the hallux and the second toes are pressed downward as the heel is elevated. This observation, however, only describes a "general" situation. When examining the digital models, it was observed that the shape of the toes changes quite differently as the heel is elevated. Instead, a number of hammer and mallet toes were found on an elevated heel of 10 cm (Figures 4-24 and 4-25). Of the 50 subjects, mallet toes were observed in four subjects, while hammer toes were found in another eight of the subjects. Such deformities were mainly observed in the second (12 out of 12 occurrences), third (6 out of 12) and fourth (3 out of 12) toes. The occurrence of mallet toes explains the comparatively larger deviations of the DIP joint height measurements of the second toe compared to the other toes.

Figure 4-24. Hammer toes observed in 2nd, 3rd and 4th toes of another subject.

Figure 4-25. Mallet toes observed in 2nd, 3rd and 4th toes of another subject.

It is interesting to note that the standard deviations of the linear foot measurements are comparatively greater in consideration of the level of mean differences detected. This is not surprising as these measurements are not normalised to the foot length of the subjects. Measurements of larger magnitudes would therefore result in larger standard deviations in the ratio for a normally distributed dataset.

Generally, the results of this study demonstrate that the forefoot shape changes with different heel elevations as statistically significant mean differences are identified in many of the foot measurements. With increased heel elevation, the toe spread is greater with the fifth toe moving to the lateral side of the foot, and the MPJ height of the fourth and fifth toes is increased.

Moreover, the toes might "deform" with an overly high heel. Toe deformations are observed on the second toe on an elevated heel of 10 cm in almost one quarter of the subjects in this study. The forefoot experiences greater load as the heel elevation is increased, and the shape and placement of the toes change from their natural foot flat position to cope with the extra load exerted.

The findings suggest that slight compensations might be required in the toe box design for better shoe fit and comfort with shoes of different heel heights. The design of a shoe last might involve over 30 foot measurements (Chen, 2005; Hawes et al, 1994).

However, these measurements were usually taken in barefoot in the natural foot flat position. Changes in the forefoot shape characteristics such as a wider small toe angle due to changes in heel height were not considered when fabricating the shoe last for HHSs.

The toe box design is important in footwear as most of the design work takes place at the toe region (Luximon and Luximon, 2013). On one hand, the toe box should have enough allowance to account for the movement of the foot inside the shoe and any swelling after long hours of wear. On the other hand, it should not be overly spacious because it needs to grip the foot and restrict the foot into a proper position. As the forefoot bears greater loads and swelling might be increased when wearing HHSs, the toe box design is particularly critical in HHSs.

Limitations of the study

Reliability and accuracy are evaluated based on mesh models produced in Rapidform XOR3. The results might vary if different post-processing software is used.

Shifting and rotation of the ball axis were observed with increased elevation of the heels. Thus, the ball axis, together with its child component, the tread point, do not appear to be the best reference for the alignment of foot models. A more reliable foot alignment method, which is developed based on anthropometric features with minimal changes over different heel elevations, would be required to bring the foot models of different heel elevations to the same coordinated space for better comparison and description of their shape changes.

Moreover, the foot plantar is not included in the scans in this study. If accurate scanning of the foot plantar is carried out, more information such as the contact area

could be obtained. This would help researchers to understand how the toes "deform" with different heel elevations and help improve the foot-bed design in HHS.

4.6. Conclusion

The newly developed 3D foot and ankle imaging system has demonstrated repeatability and accuracy for extraction of anthropometric foot measurements. The system even has the capability to detect minor changes in the forefoot dimensions with variations in the heel height in the foot scanning experiments. With the availability of colour and texture information, easy landmarking (use of 2D markers instead of 3D markers) is possible during foot scanning; any skin conditions of the foot, such as blisters, corns and calluses, cand also be easily identified in the foot scans. The short capture time (within 1 second) is also an advantage of the system when human subjects are involved in the scanning process. Since scanning is completed in a very short time span, measurement errors introduced by unintentional body swaying can be minimised.

The current study is the first to focus on forefoot measurements with different heel heights. The shape of the forefoot, as illustrated by the various length, width and height measurements, is shown to change with different heel elevations. The most obvious observation is a wider toe spread in the horizontal plane, thus indicating slight compensations might be required in the toe box design when fabricating shoes of different heel heights, especially in the MPJ regions of the fourth and fifth toes and the DIP region of the hallux and second toes.

The deliverable of this study provides a reliable means for anthropometric measurements and can further contribute to the field of footwear design. With a fast scanning speed and ease of module reconfigurations, the new imaging system will greatly contribute to the evaluation of:

- fit of shoes (especially HHS) by comparing foot scans with different shoe last models,

- changes in the foot dimensions due to swelling after running or wearing of HHSs for long hours,

- changes in the foot shape at different stages of the stance phase in gait (as a series of 3D measurements can be captured over time by replacing the digital cameras with high-speed cameras), and

- postural studies in scoliosis or breast research where human subjects are to be scanned at specific body bending angles.

Chapter 5 – Evaluation of plantar pressure and foot stability with high-heeled shoes

Previous research has shown that the use of high-heeled shoes (HHSs) changes the plantar pressure distribution and foot stability. These changes could have critical impacts on the design parameters of new insoles, such as the definition of the plantar zones, material property requirements of the insole materials, and insole features for providing additional foot support. Therefore, in order to provide a better understanding of how plantar pressure distribution and foot stability change with heel height, a comprehensive biomechanical evaluation is carried out on 24 healthy young females in this study by using an in-shoe pressure sensing system.

The experiment in this study aims to evaluate:

(1) the effects of heel height on **plantar pressure distribution** during quiet standing and normal walking, and

(2) the effects of ***heel height*** and ***HHS experience*** on **foot stability** during quiet standing and normal walking.

Four heel heights that are the most commonly found in everyday commonly worn shoes are examined: 1 cm, 5 cm, 8 cm and 10 cm. During the experiment, the recruited subjects are required to wear four pairs of shoes with a 1 cm, 5 cm, 8 cm and 10 cm heel respectively, and perform two tasks of walking along a straight pathway and quietly standing.

The experimental design, including the subjects, shoe samples, instrumentation, and experiment protocol adopted will be presented in the methodology session. The methods of data post-processing and statistical analysis will be described separately for each objective, followed by the results and discussions. These findings will be used to

formulate the design requirements of the new insoles and will be described in the last session of the chapter.

5.1. The shoe samples

Shoes with a 1 cm, 5 cm, 8 cm and 10 cm heel are tested in this study. They were supplied by the same manufacturer, with the same shoe style and sole materials, so as to minimize the difference of variance that would contribute to the measured variables. Figure 5-1 shows the side view of the four pairs of shoes used in the study. These four pairs of shoes comprise the most common heel height worn by women on a daily basis, which range from a low heel of 1 cm, medium heel of 5 cm, and high heels of 8 cm and 10 cm. The size of these shoes ranged from EU 36 to 38.

Figure 5-1. (left to right) Side view of the shoes with 1 cm, 5 cm, 8 cm and 10cm heel

5.2. Equipment

The plantar pressure measurements were recorded by using the Pedar®-X in-shoe pressure measurement system (Novel GmbH, Munich, Germany) (Figure 5-3). The reliability of this system has been verified in previous work (see for example, Debbi et al., 2012; Ramanathan et al., 2010; Putti et al., 2007). A pair of Pedar insoles (EU size 36/37) which contained 99 pressure sensors embedded into each insole was used and calibrated by using a standard protocol prior to the implementation of the experiment. The measurements were recorded at a frequency of 50 kHz (Mittlemeier and Morlock, 1993).

Figure 5-2. Pedar®-X in-shoe pressure measurement system

Figure 5-3. Setup of Pedar®-X in-shoe pressure measurement system

5.3. Subjects

Prolonged wear of high heels can change normal body posture and shorten the calf muscles which may result in a different plantar pressure distribution patterns and perceived comfort. It is also assumed that women who wear high-heels regularly would adopt a different gait pattern from the non-regular high-heel wearers, thus resulting in different plantar pressure distribution and subjective comfort. Therefore, two subject

groups were recruited for the experiment: regular HHS wearers and non-regular HHS wearers.

Twenty-four young females (12 regular HHS wearers and 12 non-regular HHS wearers) aged from 21 to 28 were recruited for the experiment. Regular HHS wearers are defined as those who have worn HHSs with a minimum heel height of 5cm for three or more times a week and at least 18 hours each week in the past two years. All subjects have a foot size of EU 37 or 38 and self-reported that they have not suffered from lower-extremity pain and injury for a minimum of one year prior to the study. Table 5.1 summarises the demographics of the participants. The mean differences between the two subject groups have been estimated using independent sample t-tests and the p-values are presented in the last column of the table. All participants gave informed written consent prior to the experiment.

Table 5-1. Demographic data of participants

	Regular HHS wearers (Mean ± SD)	Non-regular HHS wearers (Mean ± SD)	p-value
Number of subjects	12	12	
Age (years)	24.6 ± 2.1	23.2 ± 2.3	0.169
Body height (cm)	159.0 ± 3.8	160.5 ± 4.7	0.441
Body mass (kg)	52.53 ± 6.94	49.15 ± 4.15	0.063
BMI (kg/m^2)	21.57 ± 2.63	21.32 ± 1.22	0.530

5.4. Experimental Protocols

The recruited subjects were required to perform two tasks: balanced stance (BS) and normal walking (NW) for each heel height during the experiment. The experimental protocols were approved by the Human Subjects Ethics Sub-committee of the Hong Kong Polytechnic University.

Prior to the experiment, a shoe-fitting session was carried out to identify the best-fitting shoes for each heel height. Subjects were given sufficient time to try on different shoe

samples (with the Pedar® insole sensors inserted) and were asked to walk around to ensure that there was no heel slippage during push off.

The four testing heel heights were assessed in random order. A two-minute break was given in-between the tasks and testing conditions to prevent fatigue. For each heel height, the subjects were required to wear the HHS with the Pedar® insole sensors inserted. They were then required to perform the following tasks.

 (1) Balanced stance (BS)

Subjects were required to perform a standardized quiet standing posture -- to stand still with their feet 17 cm apart from the heel centres, toe-out angle 14°, arms by their sides, and eyes looking at a visual target placed approximately 3 m in front of them at eye level (Mclloy et al., 1997). The plantar pressure measurements were recorded in three 30 s trials. (Landry et al., 2010)

 (2) Normal walking (NW)

The subjects were required to walk at their own selected pace along a 6-meter long straight pathway for 5 "successful trials" after 5 practice trials to adjust the shoe/insole combination. During each trial, the subjects were required to stare at a visual reference placed in front of them at eye level. The self-selected walking pace was monitored by two pairs of automatic timing gates placed at both ends of the pathway. Figure 5.4 shows the experimental setup.
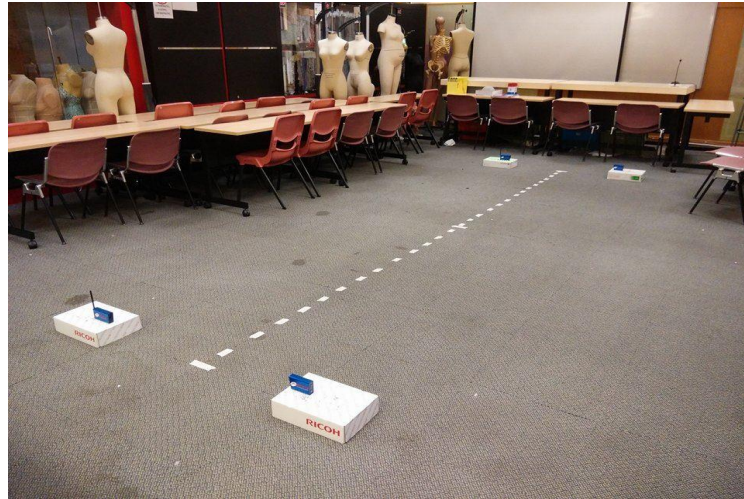
Figure 5-4. Six-meter straight pathway and automated timing gates.

5.5. Data processing and analysis

5.5.1. Evaluating plantar pressure distribution

To evaluate the changes in the plantar pressure distribution across the different heel heights, the foot plantar was divided into eight regions: the heel, lateral mid-foot, arch, first metatarsal head (MTH 1), second and third metatarsal heads (MTHs 2, 3), fourth and fifth metatarsal heads (MTHs 4, 5), hallux and lesser toes (See Figure 5-5). The areas of each foot region defined on the insole sensors are shown in Table 5-2.
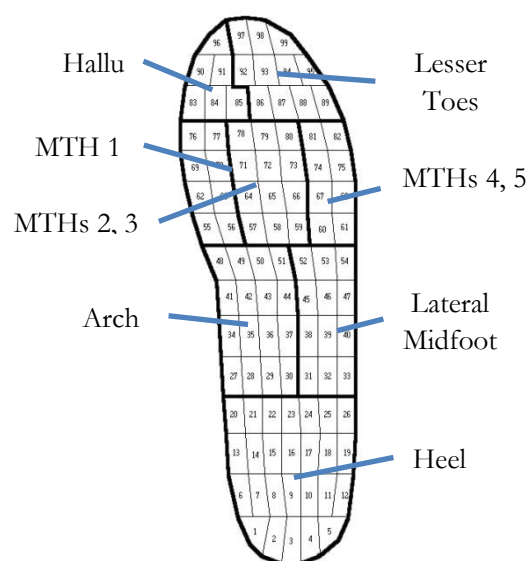
Figure 5-5. Eight regions of foot plantar

95

Table 5-2. Insole areas of eight plantar regions and their percentage to total insole area.

Plantar Region	Sensor Area (cm^2)	% area to total insole area (%)
Hallux	7.49	5.95
Lesser Toes	13.75	10.92
MTH 1	10.25	8.14
MTHs 2, 3	15.4	12.23
MTHs 4, 5	10.24	8.13
Arch	20.37	16.18
Lat. Midfoot	15.29	12.15
Heel	33.10	26.29
Total	**125.89**	**100**

Four variables were extracted from the measurements of plantar pressure for BS: force (F) in % of body weight, peak pressure (PP) in kPa, mean pressure (MP) in kPa, and pressure contact area (CA) in cm^2 of each plantar region, which were calculated for each 30 s trial and averaged among the three trials of the same tested heel height. These variables were statistically analysed with IBM SPSS Statistics v21. The effects of heel height on the changes in the mean value of the four variables were examined by using one-way repeated measures ANOVA (RANOVA) followed with Bonferroni post-hoc tests for pairwise comparisons. Differences between the parameters of each height were considered significant if $p < 0.05$. The effects of HHS experience were not considered. In order to highlight the differences between heeled-shoes and flat-heeled shoes, only the comparison results of the 1 cm versus 5 cm heel, 1cm versus 8 cm heel, and 1 cm versus 10 cm heel are reported.

For the NW experiments, 3 consecutive steps of the right foot that were extracted in the middle of the pathway of each walking trial were analyzed. The first and last 3 steps in each trial were excluded to avoid discrepancies due to gait initiation and termination. Pedar measurements, such as the PP and CA of each plantar region were calculated for each step and averaged among the 15 steps (5 trials x 3 steps) extracted for each heel

height. The pressure time integral (PTI), a commonly measured variable that defines the amount of pressure applied onto the foot plantar during foot contact, was not reported as the subjects performed the NW experiment in their own selected pace instead of a standardized speed. The walking speed, thus the duration of foot contact, varied among different heel heights within the subjects, as well as among the subjects themselves. The effects of heel height on the two plantar pressure variables were analyzed with IBM SPSS v21 by using RANOVA, followed with Bonferroni post-hoc tests for pairwise comparisons. Differences between the parameters of each height were considered significant if $p < 0.05$.

5.5.2. Evaluating foot stability by analyzing trajectories of COP

It is impossible to stay completely motionless when standing because the human balance control system is working continuously to maintain body balance. Continuous balance control adjustments result in body sways and thus changes the location of the centre of mass (COM). Changes in the COM would result in changes to the centre of pressure (COP) of the foot. By analysing the trajectories and variations of the COP, the static stability of the subjects when in wearing shoes with different heel heights can be assessed.
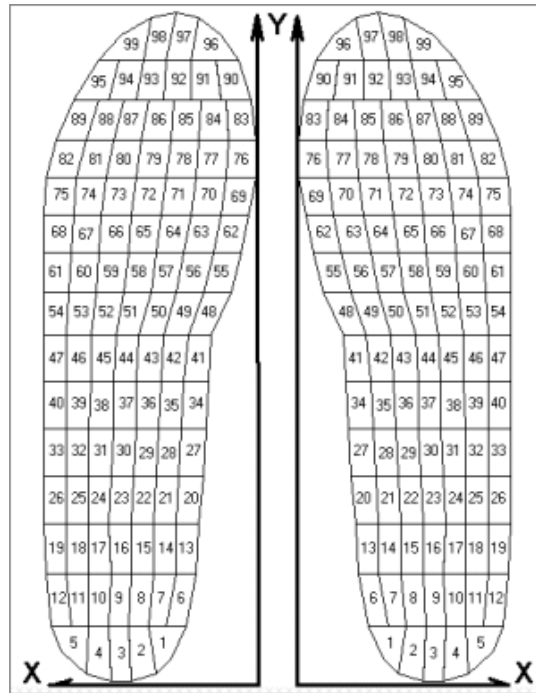
Figure 5-6. Coordinate system of COP in Pedar system

The location of the COP is described as a pair of coordinates (COPx, COPy), where COPx is the distance between the COP and the origin in the medio-lateral (ML) direction and COPy is the distance between the COP and the origin in the antero-posterior (AP) direction. Figure 5-6 shows the coordinate system of the COPs and locations of the origins for both the left and right insoles.

For the BS experiment, the mean COPx and COPy and their standard deviations (which describe the variability of the COP) and the mean velocity of the COP in the medio-lateral (x-direction) and antero-posterior (y-direction) directions of the three 30-second trials were calculated for the right foot in each BS trial. The effects of heel height and high-heel experience on these six variables were assessed by conducting a mixed between-within-subjects RANOVA, followed with a Bonferroni post hoc test for pairwise comparisons.

In order to assess the dynamic stability of the subjects when they are walking in shoes with different heel heights, the trajectories of the COPs during the stance phase of each

98

step were analysed. At heel strike, the COP would appear in the heel and develop towards the forefoot regions as the stance phase progresses. At the end of the stance phase, the COP would be found at the medial forefoot area around the second and third metatarsal heads. If the gait was stable, the trajectories of the COPs would be rather smooth and very consistent for each step. Fluctuations of the trajectories or large variations from the mean trajectory indicated less stable steps.

As the subject was moving forward at a direction very close to the in-foot y-direction during walking, the COP motions along the y-direction were more affected by the mechanical movements rather than stability. Therefore in this study, only the COPx component is analysed to assess stability.

Five COPx parameters including the mean, minimum, maximum, range (i.e. maximum – minimum) and, velocity of the COPx were calculated for each selected step. The variability of the steps was also quantified by calculating the root mean square (RMS) of the residual of each COPx record to the mean COPx trajectory.

To formulate the mean COPx trajectory, the locations of the COPx recorded over the stance phase for all steps were normalized against the percentage of completion of the stance phase. The blue dots in Figure 5-7 shows the COPx values obtained from 15 steps taken when wearing the shoes with a 1 cm heel. The data were normalized from 0 to 100% of the stance phase.
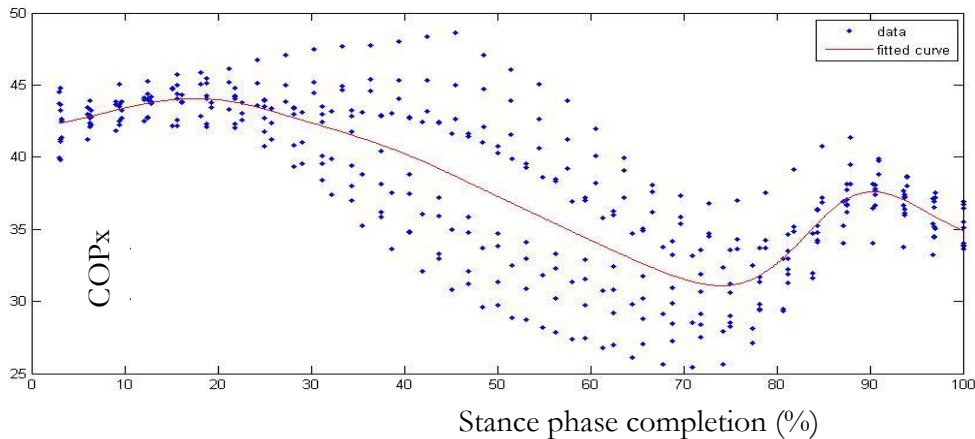
Figure 5-7. Plot that shows the COPx values (blue dots) and fitted mean curve (smoothing spline curve).

A smoothing spline curve was then fitted with the dataset. This curve can be regarded as the mean curve for the dataset. The residual of each data point, that is, the distance between the data point to the fitted curve, can be exported and analysed. By assessing the residuals of the dataset, the variations of the dataset could be quantified. The curve fitting and calculating of the residuals were carried out with MATLAB R2008a.

Since the subjects were required to walk at their own pace, the differences in their walking speed might have certain effects on their dynamic stability. Temporal variable must also be taken into account. Seven variables, including the four temporal variables related to gait characteristics, which are the walking speed (m/s), cadence of gait (steps/min), stance duration (duration of the stance phase, ms), and stance percentage (percentage of the time spent on the stance phase in a gait cycle) and standard deviations of the latter three variables which indicate variability in gait were also calculated for each selected step.

For each trial, the first and last three steps in each trial were excluded. Three consecutive steps of the right foot were selected in the middle of the pathway for analysis. The RMS of the COPx and mean value of the other variables of the 15 selected

100

steps (3 steps x 5 trials) of each subject with the same heel height were calculated and analysed by using IBM SPSS 21. The effects of the heel height and heel experience on these variables were examined by conducting a mixed between-within-subjects RANOVA, followed with a Bonferroni post hoc test for pairwise comparisons.

5.6. Results

5.6.1. Plantar Pressure Distribution

(1) Balanced stance

The general statistics and p-values of the ANOVA and Bonferroni tests of the four measured variables including the average PP, average MP, average CA, and average force (F) in percentage of the body weight (BW) of the eight plantar regions for all subjects are summarized in Table 5-3.

Table 5-3. - Descriptive statistics of peak pressures, mean pressures, contact area and force (in % body weight) of the eight plantar regions.

Main Effects	Plantar Regions	ANOVA p-value	1 cm		5 cm				8 cm				10cm			
			Mean (A)	S. D.	Mean (B)	S. D.	p-value	% of change (B) – (A)	Mean (C)	S. D.	p-value	% of change (C) - (A)	Mean (A)	S. D.	p-value	% change (D) – (A)
Peak Pressure (kPa)	Hallux	.002	38.17	15.56	53.75	19.65	.003	40.83	56.80	16.89	.003	48.82	43.31	15.58	.672	13.46
	Lesser Toes	.001	22.35	9.42	34.90	12.89	.006	56.13	41.64	22.19	.012	86.28	33.07	9.50	.002	47.95
	MTH 1	.000	48.45	20.68	62.50	22.94	.001	29.01	86.56	26.66	.000	78.67	111.03	47.66	.000	129.17
	MTHs 2, 3	.000	39.27	11.69	64.43	45.89	.000	64.06	89.38	18.52	.000	127.60	112.62	28.24	.000	186.77
	MTHs 4, 5	.000	34.39	12.32	37.60	13.81	1.000	9.34	56.25	14.83	.000	63.59	55.26	20.57	.000	60.70
	Arch	.000	30.83	8.41	40.71	14.81	.000	32.02	27.24	11.72	.894	-11.66	19.96	12.08	.000	-35.28
	Lat. Midfoot	.000	31.59	7.72	42.93	12.00	.000	35.90	28.47	10.79	.910	-9.89	29.60	9.84	1.000	-6.29
	Heel	.000	115.16	25.18	108.62	29.09	.632	-5.68	101.63	15.76	.026	-11.75	82.10	21.23	.000	-28.71
Mean Pressure (kPa)	Hallux	.000	17.45	9.10	25.80	12.17	.002	47.85	29.26	11.24	.001	67.66	17.07	7.15	1.000	-2.18
	Lesser Toes	.000	6.35	4.01	11.95	9.00	.045	88.29	15.93	10.14	.001	150.89	11.61	4.90	.001	82.89
	MTH 1	.000	22.38	12.65	27.05	10.87	.199	20.88	41.45	11.55	.000	85.19	48.84	15.80	.000	118.22
	MTHs 2, 3	.000	20.71	8.75	26.93	14.01	.041	30.04	41.59	7.19	.000	100.82	50.63	12.04	.000	144.49
	MTHs 4, 5	.000	18.53	9.29	16.59	8.79	1.000	-10.45	25.27	9.26	.006	36.36	23.21	11.22	.286	25.25
	Arch	.000	7.02	3.32	6.69	4.36	1.000	-4.69	3.89	2.62	.004	-44.64	2.77	2.64	.000	-60.48
	Lat. Midfoot	.000	13.01	5.68	13.10	6.32	1.000	0.68	7.57	4.19	.002	-41.81	8.66	5.75	.007	-33.47
	Heel	.000	50.05	10.16	47.46	9.21	1.000	-5.17	42.08	5.76	.001	-15.94	33.40	8.84	.000	-33.27
Pressure contact area (cm²)	Hallux	.000	4.43	1.62	5.30	1.35	.074	19.69	5.68	1.02	.012	28.29	4.10	1.23	1.000	-7.40
	Lesser Toes	.000	4.44	2.58	6.66	2.92	.016	50.13	7.87	3.27	.001	77.25	7.35	2.42	.003	65.61
	MTH 1	.001	6.97	1.78	6.85	1.41	1.000	-1.71	8.13	1.00	.118	16.69	8.02	0.95	.101	15.20
	MTHs 2, 3	.326	11.43	2.98	10.67	1.33	1.000	-6.63	11.53	1.35	1.000	0.88	11.51	1.56	1.000	0.66
	MTHs 4, 5	.263	7.16	2.66	6.48	2.46	1.000	-9.48	7.57	1.25	1.000	5.74	6.98	1.92	1.000	-2.51
	Arch	.000	6.17	2.24	5.33	3.15	1.000	-13.60	3.78	2.59	.012	-38.77	2.92	2.38	.000	-52.73
	Lat. Midfoot	.000	8.75	3.26	7.73	2.70	.452	-11.64	5.32	2.71	.001	-39.13	5.87	3.82	.017	-32.89
	Heel	.000	27.87	2.04	27.57	2.25	1.000	-1.10	26.11	2.22	.002	-6.32	25.01	2.38	.000	-10.26
	Total	.129	77.22	14.42	75.66	9.70	1.000	-0.80	76.00	9.90	1.000	-1.58	72.70	13.03	.508	-7.06
Force (% of Body Weight)	Hallux	.000	4.41	2.10	5.88	1.97	.011	1.47	6.44	1.85	.007	2.04	4.26	1.80	1.000	-0.15
	Lesser Toes	.000	2.81	1.58	4.81	2.52	.013	1.99	6.20	3.04	.001	3.38	5.19	1.64	.001	2.38
	MTH 1	.000	7.67	3.61	8.70	3.15	.598	1.03	12.76	3.28	.000	5.08	16.45	4.32	.000	8.78
	MTHs 2, 3	.000	10.62	3.67	12.35	3.39	.086	1.73	19.33	3.54	.000	8.71	26.14	4.97	.000	15.52
	MTHs 4, 5	.000	6.19	2.57	5.39	2.55	.688	-0.81	7.65	2.03	.098	1.46	7.44	2.67	.443	1.25
	Arch	.000	4.74	1.88	4.47	2.38	1.000	-0.28	2.27	1.38	.000	-2.48	1.57	1.24	.000	-3.17
	Lat. Midfoot	.000	6.60	2.59	6.57	2.55	1.000	-0.03	3.35	1.67	.000	-3.25	3.89	2.25	.002	-2.71
	Heel	.000	56.95	11.44	51.84	9.46	.009	-5.11	42.01	5.66	.000	-14.94	35.06	6.65	.000	-21.89

Peak Pressure (PP) - Due to the regulatory body sway that serves to maintain balance during standing, the plantar pressure of each plantar region would vary during standing. The PP depicts the highest pressures recorded in each plantar region during the timed trials. According to the RANOVA results (see Table 5-3), significant mean differences can be observed for all eight plantar regions across the tested heel heights. The PP over the forefoot area which consists of the hallux, toes and MTH regions generally increase with heel height. The percentage of increase was highest in MTHs 2, 3 region (187% increase from 1 cm to 10 cm and 128% increase from 1 cm to 8 cm) and MTH 1 region (129% increase from 1 cm to 10 cm and 79% from 1 cm to 8 cm). On the other hand, a significant decrease in PP was observed in the arch (-35%) and heel (-29%) regions when the 1 cm heel was compared to 10 cm heel. The average PP of the eight plantar regions of all subjects when performing BS in the shoes with different heel heights is plotted in Figure 5-8.
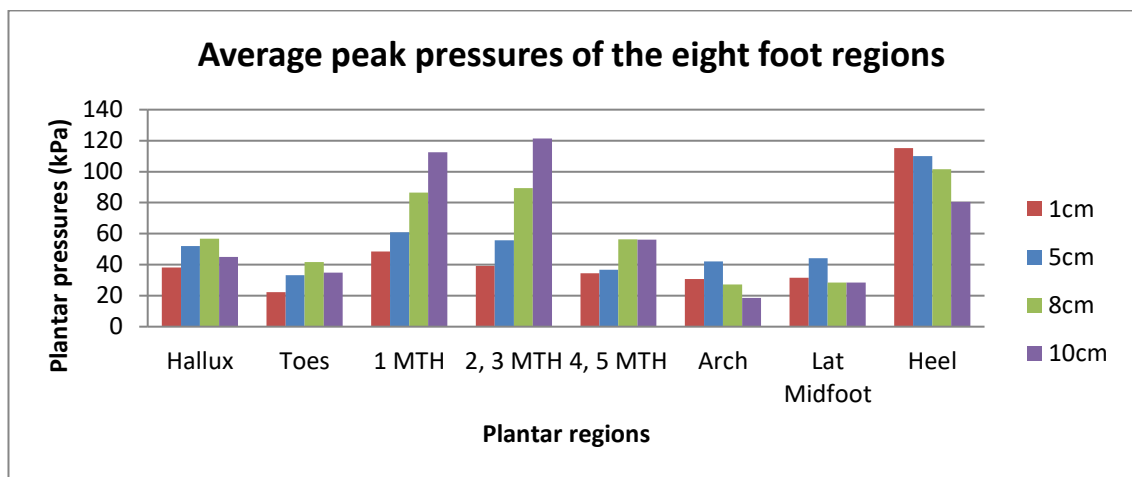
Figure 5-8. Average peak pressure of the eight plantar regions during BS in shoes with different heel heights.

Mean Pressure (MP) – The MP depicts the average pressure value observed in each plantar region during the BS trials. According to the RANOVA results shown in Table 5-3, significant mean differences can be observed for all plantar regions except for MTHs 4, 5 across the tested heel heights. The trend of the MP across the tested heel

heights is similar to that of the PP, but the values are smaller; that is, about 15 - 25% of the peak values for arch and about 40 - 50% of the PP for the other regions. Again, the percentage of increase is the highest in the MTHs 2, 3 region (144% increase from 1 cm to 10 cm and 101% increase from 1 cm to 8 cm) and MTH 1 region (118% from 1 cm to 10 cm and 85% increase from 1 cm to 8 cm). For the hallux and lesser toes regions, the MP was found highest for a heel of 8 cm and significantly higher than that of the 1 cm heel. A significant decrease in MP was observed in the rear-foot region when the 1 cm heel was compared to the 10 cm heel (-60% for the arch and -33% for the heel) and 1 cm heel to the 8 cm heel (-45% for the arch and -16% for the heel). The average MP of the eight plantar regions of all of the subjects during BS in shoes of different heel heights is plotted in Figure 5-9.
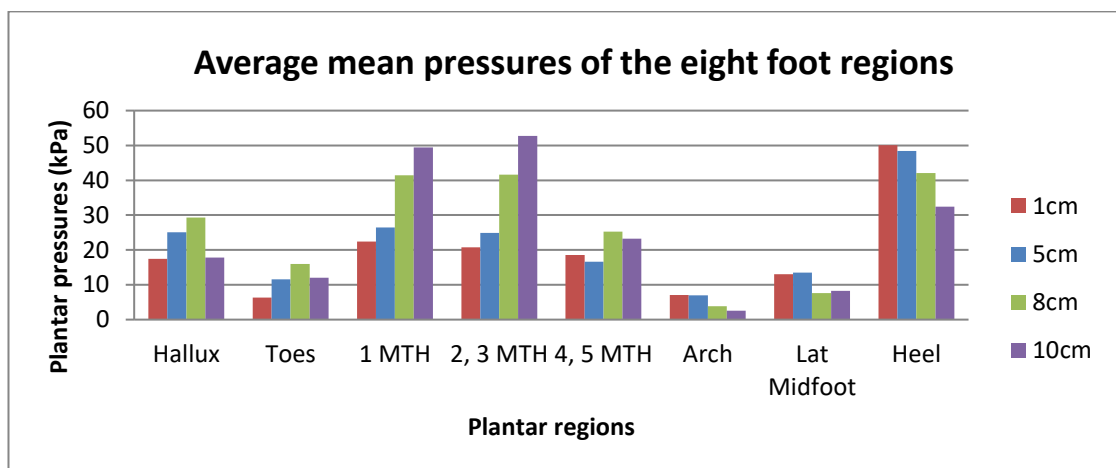
Figure 5-9. Average mean pressure of the eight plantar regions during BS in shoes with different heel heights.

The PP and MP values presented above are the primary measurements obtained from the Pedar system, without any normalization to counter the influence of the group average introduced by the different body weights. The effects are obvious when referring to the comparatively high standard deviations.

Pressure contact area (CA) – The CA depicts the insole area that is actually in contact with the foot plantar during the timed trials. This is defined as the sum of the areas

covered by the sensors with non-zero pressure measurements. For BS, the CA could provide numerical information on how the foot plantar comes into contact with a pair of flat insoles for each heel height. According to the results of the RANOVA, surprisingly, no significant changes were identified in the middle and lateral MTH regions, as well as the total CA across the different heel heights. However, the contact footprint varied with increase in heel height. With the 8 cm and 10 cm heels, a significant reduction in the CA was recorded for the arch (-39% and -53% for 8 cm and 10 cm heels respectively), lateral mid-foot (-40% and -33% for 8 cm and 10 cm heels respectively) and heel (-6% and -10% for 8 cm and 10 cm heels respectively) regions when compared with the 1 cm flat-heeled condition. The reduction in CA of the rearfoot was compensated by the increase in CA of the hallux and toe regions. A significant 28% increase in CA was recorded in the hallux at 8 cm heel. The percentage of increase is even greater for the lesser toes. A 50%, 77% and 66% increase was observed for the 5 cm, 8 cm and 10 cm heels respectively. The average CA of the eight plantar regions of all subjects during BS in shoes with different heel heights is plotted in Figure 5-10.
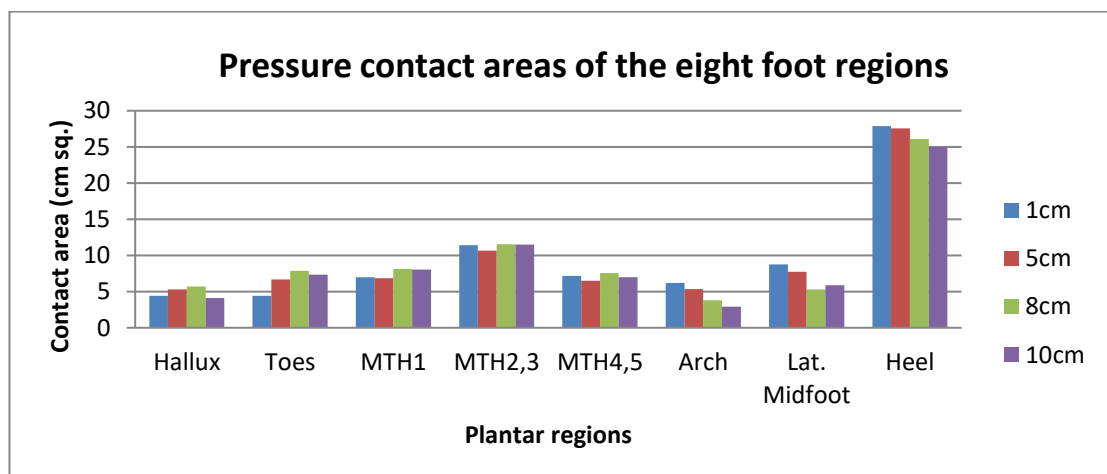
Figure 5-10. Average pressure contact area of the eight plantar regions during BS in shoes with different heel heights.

In examining both the MP and CA values (Figures 5-9 and 5-10), it can be observed that the changes in these two variables across the different heel heights are quite similar for most plantar regions except for MTH 1 and MTHs 2,3. For these two regions, the MP increases significantly with increase in heel height, but the corresponding changes in the CA are negligible. This observation shoes that the MTH 1, MTHs 2, 3 bore greater forces with higher heels, but the increased force acting on these areas is not accompanied with extra CA. The impact of the increased force on these regions during the use of HHS therefore requires extra attention in the new insole design.

Force in % of Body Weight (F) – In order to examine the distribution of the forces acting on each plantar region at different heel heights, the force (N) values recorded in each of the plantar region were taken as a percentage of the total force (body weight) that is acting on the foot. The percentage of force distribution is graphically presented in Figure 5-11.
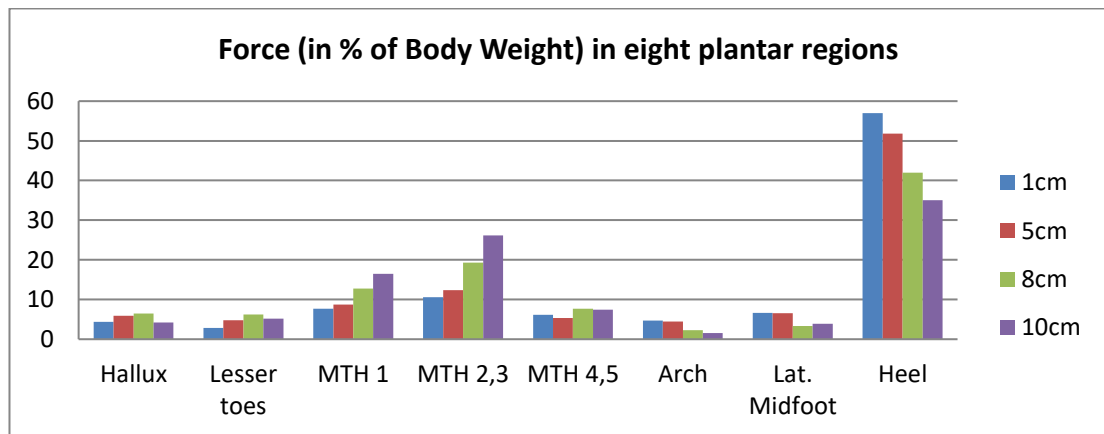
Figure 5-11. Force (in % of body weight) on the eight plantar regions during BS in shoes with different heel heights.

The RANOVA results showed significant changes in the force distribution for all plantar regions among the different heel heights. The most significant increase was found in the MTH 1 and MTHs 2, 3 regions. When the heel height reaches 8 cm, MTH 1 bears 5% more of the body weight and MTHs 2, 3 bear 8.8% more of the body

weight. This is a 66% and 114% increase when compared to the 1 cm heel. This trend continues with the 10 cm heel. The MTH 1 region bears 8.7% more of the body weight and MTHs 2, 3 region bears 15.5% more of the body weight, which is equivalent to 82% and 146% increase respectively when compared the 1 cm heel. On the other hand, significant decreases were found in the arch (8 cm: -2.5% BW, 10 cm: -3.2% BW), lateral mid-foot (8 cm: -3.3% BW, 10 cm: -2.7% BW) and heel (8 cm: -15% BW, 10 cm: -21.9% BW) regions in high-heeled conditions.

The loads that acted on the heel with the 1 cm flat-heeled conditions were mostly transferred mostly to the MTH regions as height of the heel increased. Figure 5-12 is a simplified visual of the force distribution on the plantar. The plantar is divided in four regions by combining (1) the hallux and lesser toes to become the region "Toes"; (2) the three MTH regions into one "MTH" region; and (3) the arch and lateral mid-foot into the region "Midfoot".
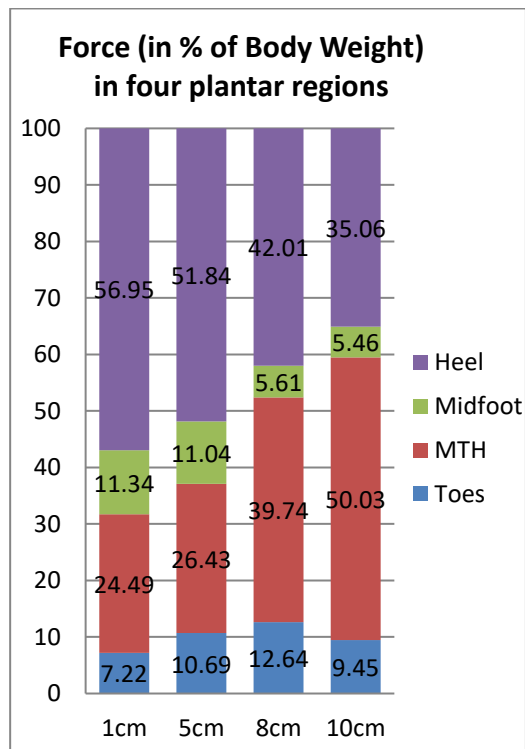
Figure 5-12. Stacked bar chart of the force distribution (in %) of four plantar regions with different heel heights.

As shown in the figure, the force distribution changes as the height of heel increases. With the 1 cm heel, the heel and mid-foot regions bear nearly 70% of the body weight. The forefoot region increased its share of the body weight as heel height increases. With a 8 cm heel, the forefoot region bears more than half of the body weight and with a 10 cm heel, almost 60% of the body weight is supported by the forefoot region.

(2) Normal Walking

The general statistics and results of the RANOVA and Bonferroni tests of the two Pedar variables including the PP, CA, and PTI of the eight plantar regions for all of the subjects are summarized in Table 5-4.

Table 5-4. - Average and standard deviation of PP and CA of each plantar region in relation to 1cm heel

Main effects	Plantar Regions	ANOVA p-value	1 cm		5 cm				8 cm				10cm			
			Mean (A)	S. D.	Mean (B)	S. D.	p-value	% of change (B) – (A)	Mean (C)	S. D.	p-value	% of change (C) - (A)	Mean (A)	S. D.	p-value	% change (D) – (A)
Peak Pressure (kPa)	Hallux	.000	272.52	94.6	335.20	124.1	.069	23	267.18	92.2	1.000	-2	202.13	70.4	0.26	-26
	Toes	.241	110.09	35.4	108.99	34.1	1.000	-1	101.46	29.0	.524	-8	97.67	36.5	.334	-11
	MTH 1	.000	236.87	93.1	329.08	128.2	.011	39	370.57	127.8	.000	56	393.66	168.9	.002	66
	MTHs 2, 3	.007	242.46	89.9	217.58	103.4	.519	-10	245.25	91.7	1.000	1	278.46	102.7	.289	15
	MTHs 4, 5	.000	129.04	39.4	85.76	35.6	.000	-34	106.47	48.7	.225	-17	108.87	33.7	.194	-16
	Arch	.000	67.10	17.3	71.34	16.3	1.000	6	43.55	17.4	.000	-35	36.26	14.5	.000	-46
	Lat. Midfoot	.000	48.24	10.2	70.55	14.2	.000	46	52.71	14.6	1.000	9	33.08	15.5	.002	-31
	Heel	.000	271.64	68.1	222.49	34.7	.003	-18	205.87	44.1	.001	-24	142.37	22.7	.000	-48
Pressure contact area (cm²)	Hallux	.002	20.94	3.2	22.29	2.3	.099	6	23.40	3.1	.017	12	19.70	4.0	.320	-6
	Toes	.577	32.17	8.9	34.29	6.0	.184	7	34.92	9.4	.215	9	33.38	8.6	.590	4
	MTH 1	.000	28.88	4.0	27.23	3.8	.147	-6	32.04	4.6	.006	11	29.09	3.8	.847	1
	MTHs 2, 3	.000	47.24	5.9	39.55	4.5	.000	-16	44.09	5.8	.056	-7	39.68	5.7	.001	-16
	MTHs 4, 5	.000	32.12	4.0	24.81	5.9	.000	-23	25.70	6.6	.001	-20	22.47	7.2	.000	-30
	Arch	.000	18.80	8.4	18.66	7.9	.934	-1	13.58	6.9	.019	-28	8.43	6.8	.000	-55
	Lat. Midfoot	.000	37.52	10.0	27.81	9.4	.000	-26	17.23	9.4	.000	-54	15.27	10.3	.000	-59
	Heel	.027	92.78	12.6	92.82	9.2	.989	0	90.82	11.2	.456	-2	86.64	13.2	.039	-7
	Total	.000	310.46	46.6	287.45	29.3	.015	-7	281.78	36.3	.006	-9	254.67	39.7	.000	-18

Peak Pressure (PP) – When compared to BS, the PP values obtained during NW were much higher. With the 10 cm heel, apart from the mid-foot regions, the PP recorded in each plantar region during walking was at least twofolds of that in quiet standing apart from the mid-foot regions. According to the RANOVA result, the mean differences in the PP due to heel heights were found to be statistically significant (p<0.001) for all plantar regions except for the toe region. The most significant increase was found in MTH 1, and a 39%, 56% and 66% increase was observed with the 5 cm, 8 cm and 10 cm heels respectively when compared to the 1 cm heel. The most obvious trend of decline in the PP was found in the heel region, in which a -18%, -24% and -48% were recorded for 5 cm, 8 cm and 10 cm heels respectively. The decrease in the PP was found to be also significant in MTHs 4, 5 (-34%) for the 5 cm heel, in the arch region for the 8 cm (-35%) and 10 cm (-46%) heels, and the lateral mid-foot for the 10 cm heel (-31%). The mean values of the PP measured during NW for all subjects with the different shoes are graphically presented in the bar chart in Figure 5-13.
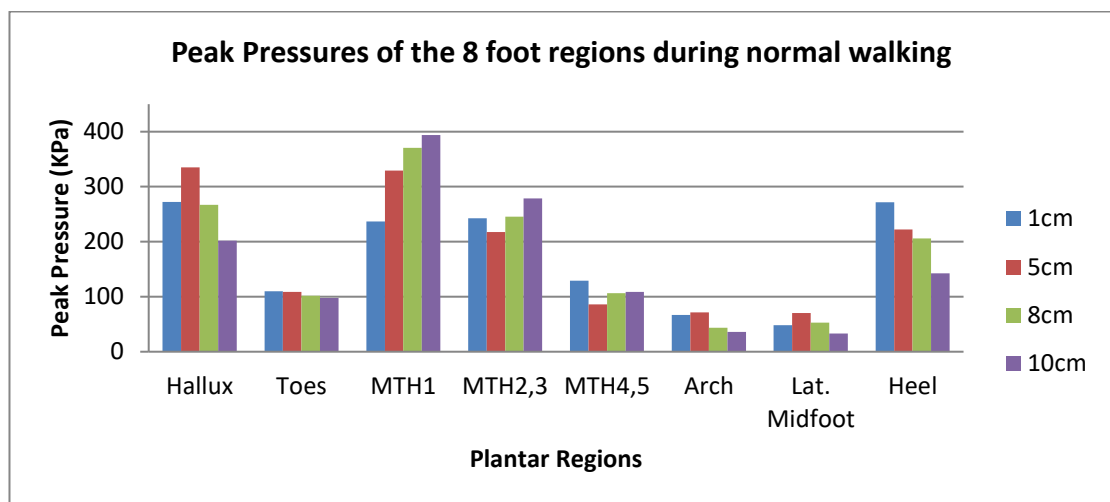
Figure 5-13. Average peak pressure of the eight plantar regions during NW in shoes with different heel heights.

Contact Area (CA) – Significant decreases in CA were observed in five out of the eight foot plantar regions. A significant 16% drop was observed in MTH 2, 3 for both 5 cm and 10 cm when compared to flat-heeled condition. While 20-30% decrease was

observed in MTH 4, 5 for all heeled conditions, the decreasing trends became more obvious in the mid-foot and heel regions. For the arch region, a -28% and -55% change were observed 8 cm heel and 10 cm heel respectively. For the lateral mid-foot region, a -26%, -54% and -59% drop were observed in 5 cm heel, 8 cm heel and 10 cm heel respectively. A 7% drop was also observed in the heel region at 10 cm heel. The resultant effect of the decrease of CA in these foot plantar regions was a decrease in the total CA, despite the fact that a significant increase was recorded at hallux (+12%) and MTH 1 (+11%) for 8 cm heel. Total CA was found to decrease with increasing heel height. When compared to flat-heeled condition, a -7%, -9% and -18% change were recorded for 5 cm, 8 cm and 10 cm heels respectively. %). Mean values of the contact areas measured during normal walking for all subjects were graphically presented in the bar chart in figure 5-14.
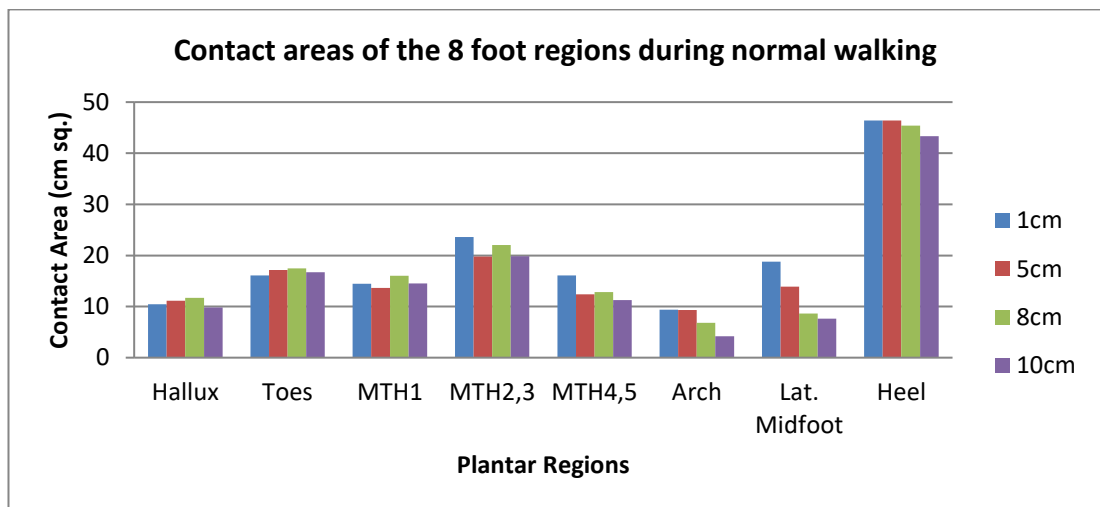
Figure 5-14. Average contact areas of the eight plantar regions during NW in shoes with different heel heights.

5.6.2.   Examining foot stability examination with COP trajectory analysis

(1) Balanced stance

Effects of Heel Height

The effects of heel height on the mean values of the COPx, COPy, standard deviation (S. D.) of the COPx and S. D. of the COPy, and mean velocity of the COPx and COPy were examined by using a mixed-between-within subjects RANOVA with heel heights being the within-subjects factor. The data were screened to ensure that the assumption of normality was met prior to the tests. Table 5-5 gives a summary of the mixed RANOVA results. The mean difference was considered statistically significant when $p<0.05$.

Table 5-5. Summary of RANOVA results of the within-subject effect (heel height) and interaction effect between within-subject and between-subject effect (high-heel experience) on static stability measures.

Main effects	Variables	F	df	p	η^2
Heel Height	Mean COPx	31.13	1.86	**.000**	.57
	Mean COPy	57.47	1.52	**.000**	.72
	S. D. COPx	9.06	3	**.000**	.29
	S. D. COPy	2.74	3	.063	.10
	Mean COPx Velocity	6.25	3	**.001**	.22
	Mean COPy Velocity	7.85	3	**.000**	.26
Heel Height *	Mean COPx	.35	1.86	.694	.02
High-heel	Mean COPy	.83	1.52	.418	.04
experience	S. D. COPx	5.89	3	**.001**	.21
	S. D. COPy	6.59	3	**.001**	.23
	Mean COPx Velocity	.44	3	.726	.02
	Mean COPy Velocity	1.21	3	.313	.05

Note: Significant values (p<0.05) in bold.

The results of the mixed RANOVA show an overall significant difference due to heel height in five out of the six measured variables, namely, the mean values of the COPx (F = 31.13, p = .000, η^2 = .57), COPy (F = 57.47, p = .000, η^2 = .72) and S. D. of the

COPx (F = 9.06, p = .000, η^2 = .29), mean velocity of the COP in ML (F = 6.25, p = .001, η^2 = .22) and AP (F = 7.85, p = .000, η^2 = .26) directions.

The results of Bonferroni pairwise comparisons showed that significant differences are found in all comparison pairs except the 8 cm and 10 cm pair of mean COPx, and all comparison pairs of mean COPy (Figure 5-15). In general, the values of the COPx decrease as the heel height increased, that is, the COP shifts towards the medial direction as the heel height is increased. When compared with the 1 cm flat-heeled condition, the mean of the COPx shifted medially by 1.68 mm with a 5cm heel, 3.96 mm with an 8 cm heel and 5.14 mm with a 10 cm heel. The mean of the COPy increased as the heel height increased, which means that the COP shifts forward as the heel height is increased. When compared to the 1 cm heel, the mean of the COPx shifts anteriorly by 11.93 mm with the 5 cm heel, 27.70 mm with the 8 cm heel and 36.39 mm with the 10 cm heel.
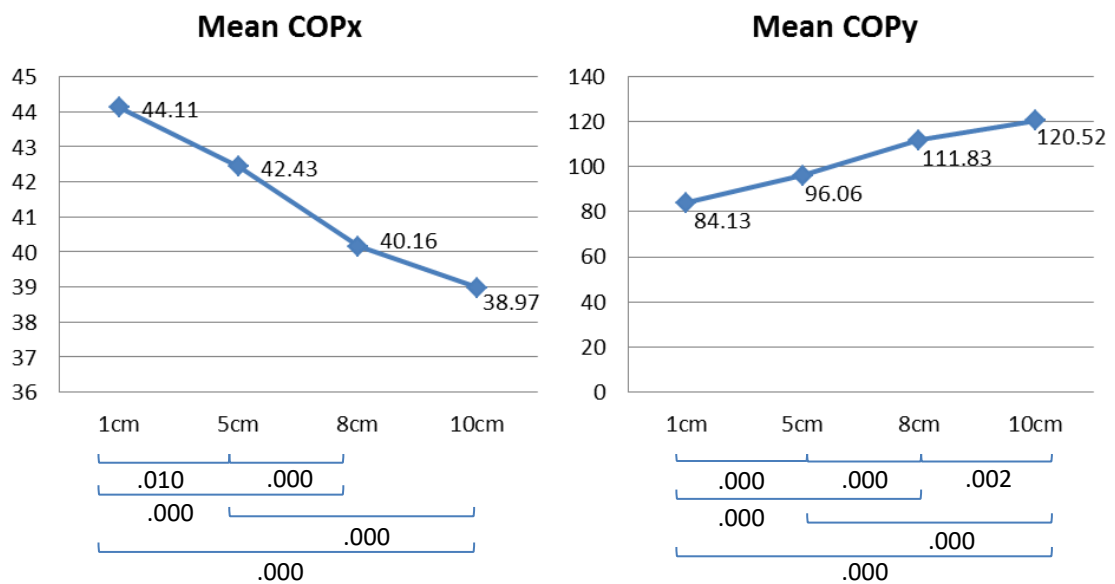
Figure 5-15. Mean values of COPx (left) and COPy (right) for all subjects and significant differences (p<0.05) found for each compared pair of shoes in Bonferroni post hoc test.

Since interaction effects (Table 5-5) were found significant in the S. D.s of COPx ($F = 5.89$, $p = .001$, $\eta^2 = .21$) and COPy ($F = 6.59$, $p = .001$, $\eta^2 = .23$), the effects of heel height on these two variables were evaluated separately for the two subject groups by one-way RANOVA and Bonferroni post hoc tests (Abu-Bader, 2010). Results of the pairwise comparisons were plotted in Figures 5-16 and 5-17.

For non-regular HHS wearers, significant differences were identified in both the S. D. of COPx (($F = 13.06$, $p = .000$, $\eta^2 = .54$) and S. D. of COPy (($F = 8.61$, $p = .000$, $\eta^2 = .44$) while the effect of heel height was not significant ($p < .05$) in these two variables for regular HHS wearers.

For non-regular HHS wearers, the mean S. D. values of both the COPx and COPy increased with heel height (Figures 5-16 and 5-17). The mean S. D. value of the COPx was the lowest for the 1 cm flat-heeled condition (S. D. $COPx_{1cm} = 0.39$) and it was significantly different from all heeled conditions. A 62.8% increase was recorded for the 5 cm heel (S. D. $COPx_{5cm} = 0.63$), 87.5% increase for the 8 cm heel (S. D. $COPx_{8cm} = 0.73$), and a 141% increase (S. D. $COPx_{10cm} = 0.93$) for the 10 cm heel. The increase of the mean S. D. in the AP direction is relatively smaller. When compared to the lowest value for the 1 cm heel (S. D. $COPy_{1cm} = 3.17$), only 41.2%, 51.8%, and 74.7% increases were observed for the 5 cm (S. D. $COPy_{5cm} = 4.48$), 8 cm (S. D. $COPy_{5cm} = 4.81$) and 10 cm (S. D. $COPy_{10cm} = 5.54$) heels respectively. Significant differences were identified between the 1 cm heel with 8 cm ($p = .017$) and 10 cm ($p = .003$) heels.
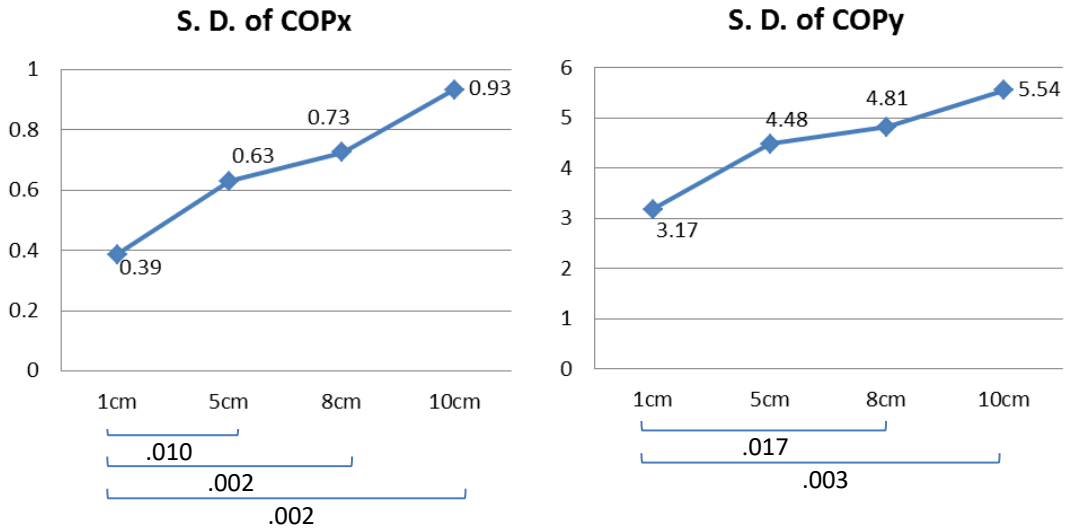
Figure 5-16. Mean values of S. D. of COPx and S. D. COPy of the non-regular HHS wearers and significant differences (p<0.05) found in Bonferroni post hoc test.
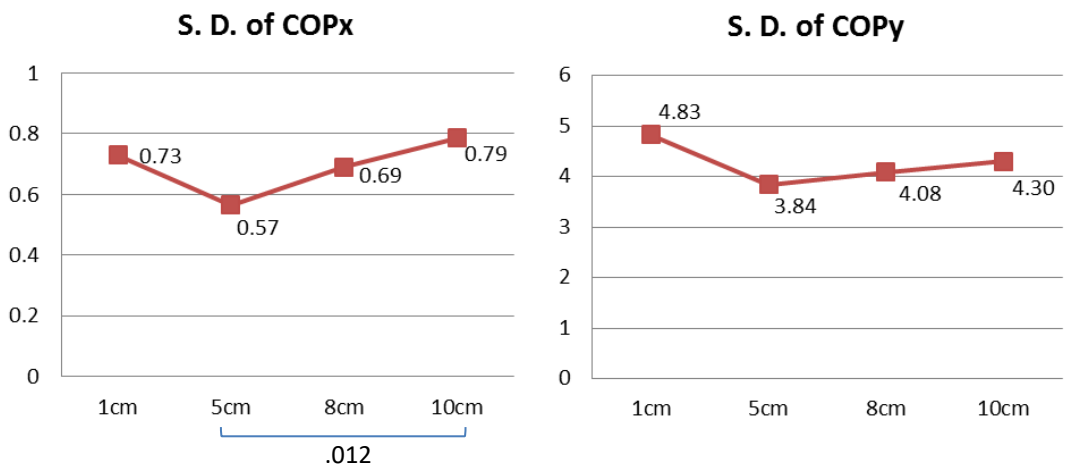
Figure 5-17. Mean values of S. D. of COPx and S. D. of COPy of the regular HHS wearers and significant differences (p<0.05) found in Bonferroni post hoc test.

The mean velocity of the COP in both the ML and AP directions (Figure 5-18) was the highest and significantly higher for the 1 cm heel (COPx velocity$_{1cm}$ = 6.54mm/s; COPy velocity$_{1cm}$ = 27.29mm/s). The mean velocity decreased as the heel height increased to 5 cm (COPx velocity$_{5cm}$ = 5.37mm/s; COPy velocity$_{5cm}$ = 22.68mm/s), and the lowest with the 8 cm heel (COPx velocity$_{8cm}$ = 5.27mm/s; COPy velocity$_{8cm}$ = 19.81mm/s). The mean velocity increased again with a heel height of 10 cm (COPx velocity$_{10cm}$ =

5.82mm/s; COPy velocity$_{10cm}$ = 23.33mm/s). The changes due to the effects of the heel height were more significant in the AP direction.
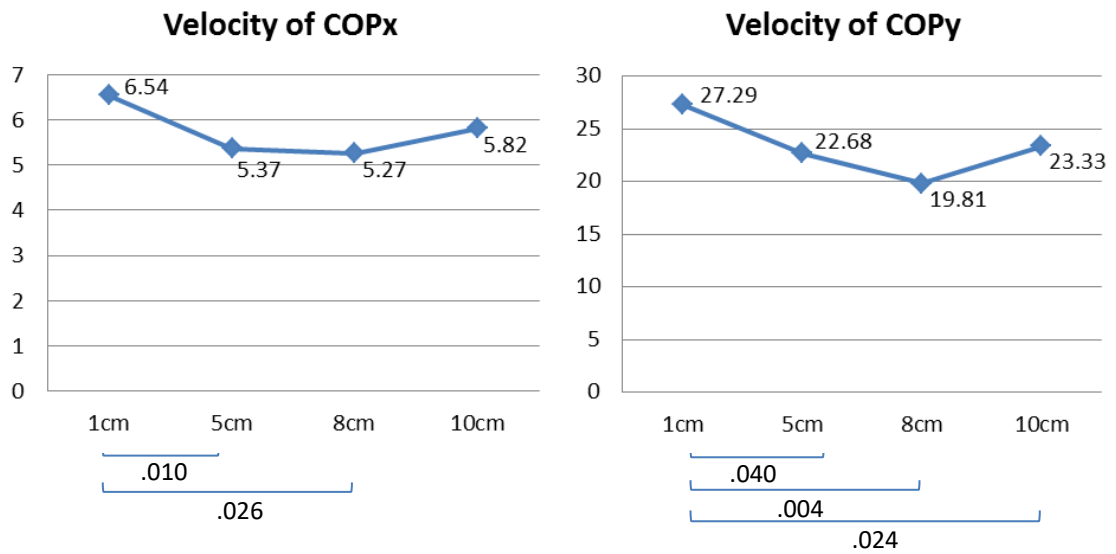
Figure 5-18. Mean velocity of COPx (left) and COPy (right) for all subjects and significant difference (p>.05) found in Bonferroni post hoc test.

Effects of HHS experience

As described above, the interaction effects identified in both the S. D. of COPx and COPy had indicated the significantly different performance of the two subject groups on these two variables due to changes of heel height. Figure 5-19 shows the interaction effect between heel height and HHS experience on these two variables.
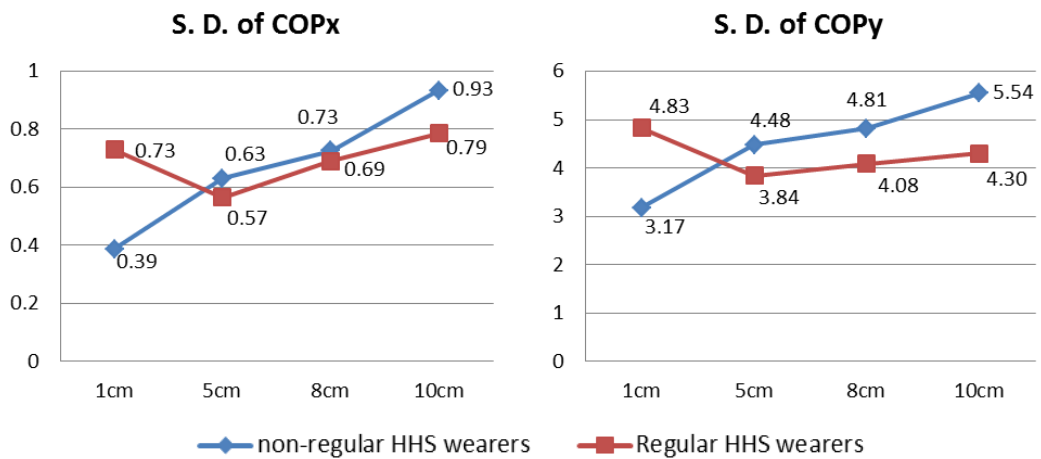
Figure 5-19. Plots showing the interaction effect of heel height and HHS experience on S. D. of COPx (left) and S. D. of COPy (right) for balanced stance.

It is interesting to note that HHS experience does not always improve static stability. With a lower heel of 1 cm, the S. D.s of both the COPx and COPy of regular HHS wearers are higher than that of both the COPx and COPy of the non-regular HHS wearers, although the differences are not statistically significant.

The effect of high-heel experience, the between-subject factor of the mixed RANOVA, on the rest of the variables was presented in Table 5-6. No significance was identified for these tested variables.

Table 5-6. Results of the mixed RANOVA showing the effect of HHS experience on the COP variables in balanced stance

Main effect	Variables	F	p	η^2
Heel Experience	Mean COPx	.01	.912	.001
	Mean COPy	.04	.850	.002
	Velocity of COPx	2.15	.157	.089
	Velocity of COPy	3.73	.066	.145

Note: Significant values (p<0.05) in bold.

(2) Normal Walking

To assess the variability of the COPx, four smoothing spline mean curves were plotted for each subject, with one for each heel height. The sum of the RMS of the residuals of each curve was calculated to quantify the variations of each dataset. Figure 5-20 shows the curve fitting results of the four heel heights of a non-regular (left column) and a regular (right column) HHS wearer.

117
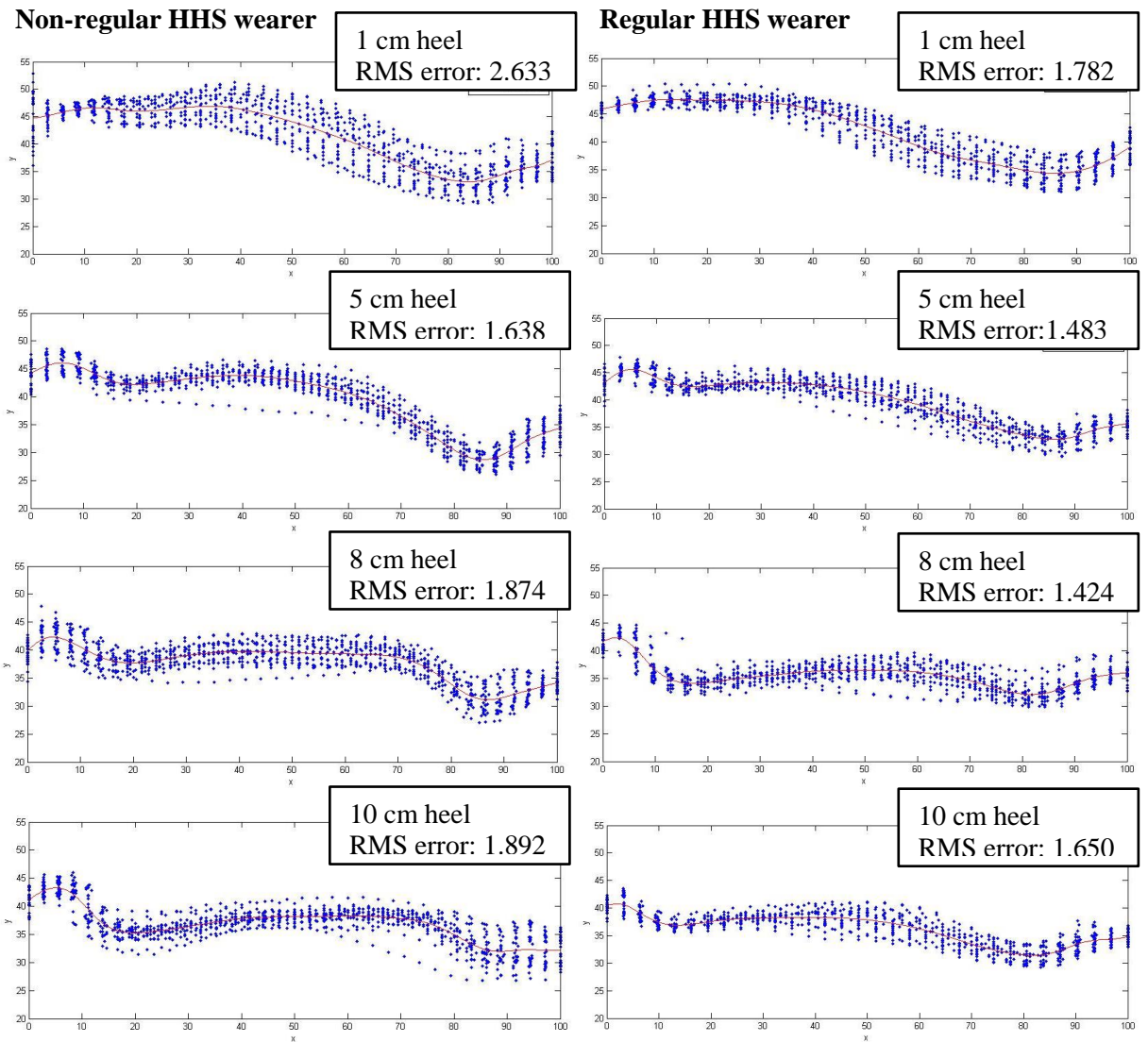
Figure 5-20. Plots of COPx distribution (15 steps) and fitted smoothing spline curves across the entire stance phase for four heel heights of a non-regular (left column) and regular (right column) HHS wearer.

Shape of fitted curves

In general, the fitted curves are the smoothest for the 1 cm heel. The COPx values during the loading response (0 – 20% of the stance phase) and mid-stance (20 – 70% of the stance phase) were the highest with the 1 cm heel and decreased with higher heels. With a heel height of 5 cm and higher, the COPx shows an upward shift right after heel strike followed with a decline towards the end of the loading response. The smallest

COPx values were found at push-off (about 80% - 90% of the stance phase) for all heel heights, in which the COP is located mostly around on the MTHs.

Effects of heel height

A mixed between-within-subjects RANOVA was conducted to examine the effect of heel height and heel experience on the six COPx variables and other seven temporal variables measured during normal walking trials. The data were screened prior to the tests to ensure that the assumptions of the RANOVA were met. Table 5-7 summarises the RANOVA test results.

Table 5-7. Summary of the mixed RANOVA results on the effect of heel height (within subject factor) on six COPx and seven temporal variables

	Measured effects	F	df	Sig.	Partial Eta Squared
COPx variables	RMS of COPx	5.56	3	**.002**	.236
	Mean COPx	83.68	1.94	**.000**	.823
	Min COPx	19.50	1.62	**.000**	.520
	Max COPx	98.15	2.08	**.000**	.845
	Range of COPx	15.86	1.69	**.000**	.468
	Velocity of COPx	7.50	1.96	**.002**	.294
Temporal variables	Mean Walking Speed	12.65	1.92	**.000**	.413
	Mean Cadence	2.33	3	.084	.115
	S.D. Cadence	3.25	3	**.029**	.153
	Mean Stance Duration	2.45	3	.066	.120
	S.D. Stance Duration	5.53	3	**.002**	.235
	Mean Stance Time Percentage	2.01	3	.123	.101
	S.D. Stance Time Percentage	4.75	3	**.005**	.209

Note: Significant values (p <.05) are shaded and bolded.

The results show overall significant differences (p <.05) in all six COPx variables. Among the seven temporal variables, overall significant differences were found in mean walking speed (p = .000), S. D. of cadence (p=0.029) S. D. of the stance duration (p =.002) and S. D. of the stance percentage (p=.005) among the four tested heel heights.

Interactions effect was identified in S. D. of cadence (F = 3.53, p = .021, η^2 = .16), the effect of heel height on this variable was evaluated separately for the two subject groups by one-way RANOVA and Bonferroni post hoc tests.

From the results of the Bonferroni pairwise comparisons, significant differences in the RMS of the COPx (Figure 5-21(a)) were found between the 1 cm and 8 cm (p = .020), 1 cm and 10 cm (p = .018) heels. Significant differences were found in all comparison pairs of the mean COPx and maximum COPx (Figure 5-21(b)). For the minimum, values of the 1 cm heel were found to be significantly different from those of the other heel heights. These four variables were found to be the highest with the 1 cm heel and decrease as the heel height increases.

For the range of COPx, the highest value of 18.67 mm was found with the 5 cm heel, followed by the 1 cm heel (18.03 mm), and then the 8 cm (15.94 mm). The lowest value of 14.58 mm was identified with the 10 cm heel (Figure 5-21(c)). Significant differences were found between the 1 cm and 10 cm (p = .008), 5 cm and 8 cm (p = .001), 5 cm and 10 cm (p = .000) heels. The mean velocity of the COPx (Figure 5-21(d)) was also found to be the highest with the 5 cm heel (48.99 mm/s), while the lowest value was found with the 1cm heel (41.17 mm/s). The difference between the two heel conditions was found to be significant (p=.000).

120

(c) Range of COPx

	1 cm	5 cm	8 cm	10 cm
	18.03	18.67	15.94	14.58

(d) Mean Velocity of COPx

	1cm	5cm	8cm	10cm
	41.17	48.99	44.78	45.45

Significant pairs (p <.05)
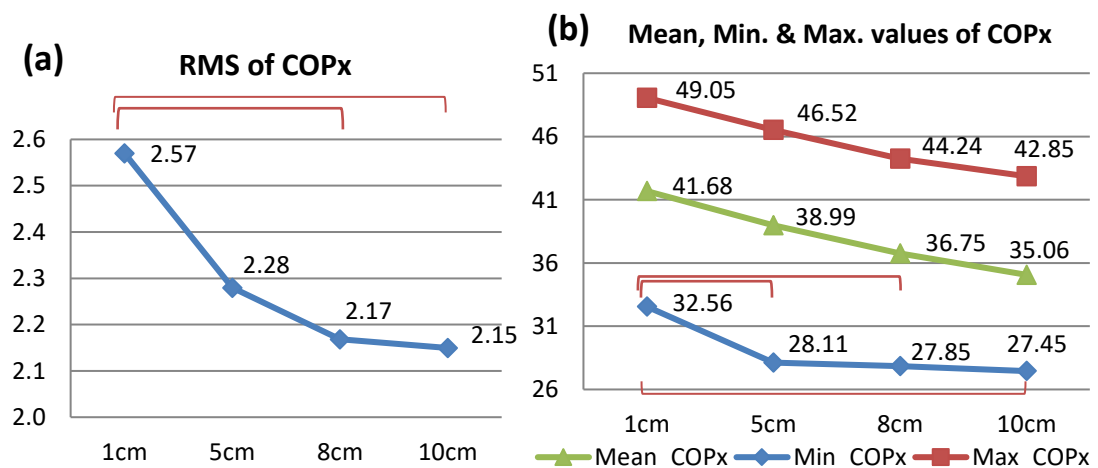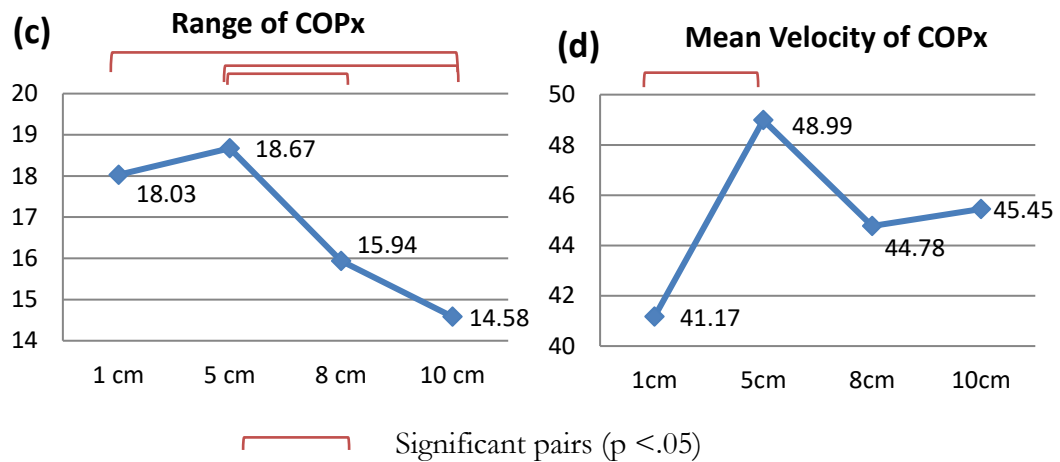
* For the mean and maximum values of COPx, all comparison pairs are significantly different (p < .05)

Figure 5-21. (a) Mean RMS values, (b) mean of mean, minimum, and maximum values of COPx, (c) mean ranges of COPx, and (d) mean velocities of COPx wth four heel heights.

For the temporal gait variables (Figure 5-22), significant differences in the mean walking speed were found between the lower heel heights (1 and 5 cm) and higher heel heights (8 cm and 10 cm). The subjects walked the fastest in the shoes with a 5 cm heel and slowest in the shoes with a 10 cm heel. Although the mean differences across heel heights are statistically significant, the trend of the change is not obvious. While the effects of heel height are not statistically significant in the mean cadence, mean stance duration, and mean stance percentage, significant differences were found between the 5 cm and 8 cm heels, and the 5 cm and 10 cm heels in the standard deviations of stance duration (Figure 5-22(e)), as well as the 5 cm and 10 cm heels in the standard deviations of stance percentage (Figure 5-22(g)).

For S. D. of Cadence, the effect of heel height was evaluated separately for the two subject groups by one-way RANOVA and Bonferroni post hoc tests. Effect of heel height was found to be significant in non-regular HHS wearers (F = 5.99, p = .003, η^2 = .40) only. Results of the post hoc tests showed that values from 1cm and 10 cm heel

are significantly different (p = 0.31). Figure 5-22(c) shows the plots of the two subject groups and the significant pair of the non-regular HHS wearer.
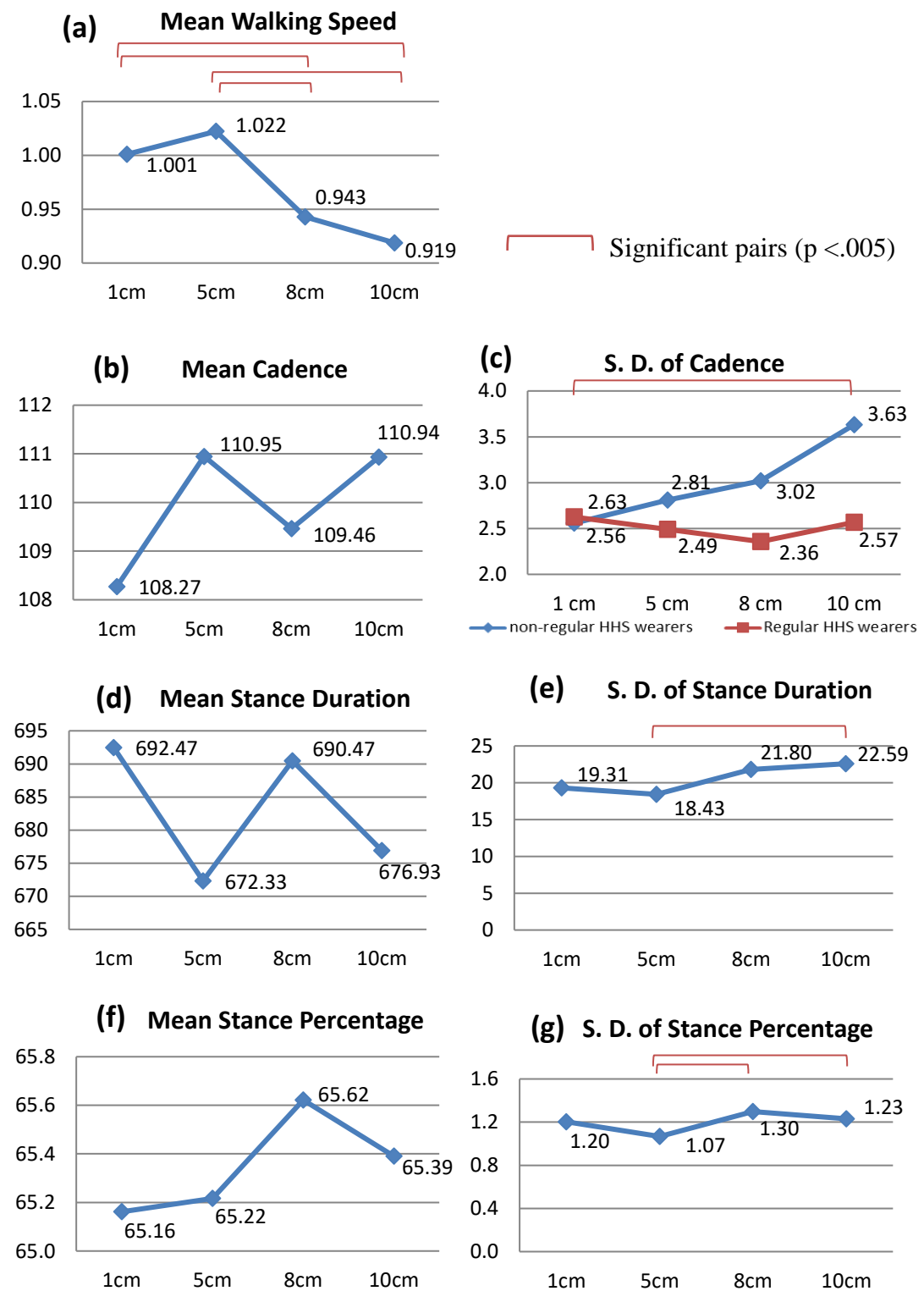
Figure 5-22. (a) Mean walking speed, (b) and (c) mean values of cadence and their standard deviations, (d) and (e) mean values of stance duration and their standard deviations, (f) and (g) mean values of stance percentage and their standard deviations for the four heel heights.

Effect of HHS experience

Results of the mixed RANOVA (Table 5-8) showed that no significant differences were identified between regular and non-regular HHS wearers in all COPx variables. The results indicated that high heel experience did not contribute significant percentage to the variance in these COPx variables.

Table 5-8. Summary of the mixed RANOVA results on the effects of HHS experience (between subject factor) on six COPx and seven temporal variables

	Measured effects	F	Sig.	Partial Eta Squared
COPx variables	RMS of COPx	1.096	.309	.057
	Mean COPx	2.286	.148	.113
	Min COPx	1.206	.287	.063
	Max COPx	.012	.913	.001
	Range of COPx	1.227	.283	.064
	Velocity of COPx	1.015	.327	.053
Temporal variables	Mean Walking Speed	1.778	.199	.090
	Mean Cadence	1.041	.321	.055
	S.D. Cadence	5.002	**.038**	.217
	Mean Stance Duration	1.230	.282	.064
	S.D. Stance Duration	2.966	.102	.141
	Mean Stance Time Percentage	1.879	.187	.095
	S.D. Stance Time Percentage	6.203	**.023**	.256

No significant differences were observed between the two subject groups on five out of the seven temporal variables, namely, the mean walking speed, cadence, stance duration and its standard deviations, and stance percentage measurements for all heel heights. However, the standard deviations of cadence (Figure 5-22(c)) and stance percentage (Figure 5-23) were observed to be significantly higher in non-regular HHS wearers for high-heeled gait.

S. D. of Stance Percentage
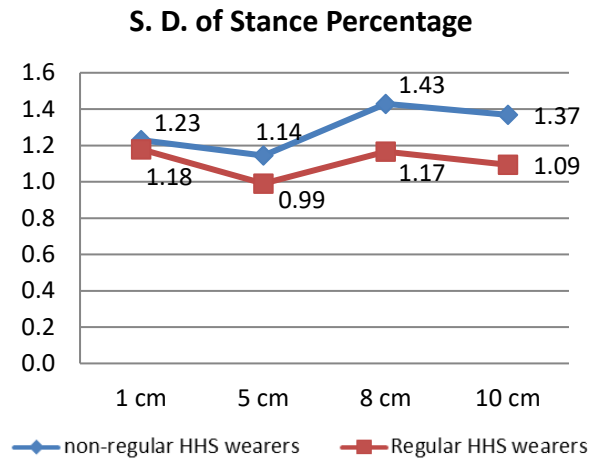
Figure 5-23. Mean values of standard deviations of stance percentage of the two subject groups for the four heel heights

5.7. Discussion

After examining the plantar pressure distribution patterns in the shoes during standing and walking, it was found that the forefoot pressure increases significantly with increases in heel height. This observation echoes those of many previous studies. (see for example, Schwartz et al., 1964; Snow et al., 1992; Corrigan et al., 1993; Mandato and Nester, 1999; Speksnijder et al., 2005) In this study, the plantar pressure distribution completely changes when the heel height is increased to 8 cm. At this height, the MP values of all eight regions of the plantar foot significantly change when compared to quiet standing in 1 cm heels (see Table 5-3). The body load shifts from the mid and rear-foot regions to the toes and MTH regions, thus causing the forefoot to bear over 50% of the body load with an 8 cm heel and almost 60% with a 10 cm heel. Apart from the anterior shift of load, the plantar pressure also appears to be more evenly distributed in the 1 cm heel. While the heel region bore the greatest share of the body load, other planar regions bore a similar amount of body load with the 1 cm heel. As heel height increases, a greater amount of body loading accumulated on the medial and central MTH region. When the heel height reached 10 cm, the MP values of the medial and centre MTH regions more than doubled that of the 1 cm heel. These findings suggest that functional requirements such as pressure relief and shock absorption of materials that are used in the insoles for HHSs in specific regions of the plantar foot, especially MTHs 1, 2, and 3, should be different from those that are used in common everyday shoes.

Peak pressures recorded during walking also indicated higher forefoot load in higher heel heights. With a 10 cm heel, PP could reach 200 kPa in the MTH 1 and 400 kPa in the MTHs 2, 3 region, indicating the presence of clinical pain as PP exceeded 255kPa (25.5N/cm^2) (Silvino et al., 1980). These findings suggested that the functional

requirements such as the pressure relieving and shock absorption abilities of materials to be used in the insoles for HHS at specific plantar regions, especially MTH 1, 2, and 3, should be different from those for use in flat lady shoes.

The pressure measurements also indicated the approximate locations of the forefoot PP. According to Table 5-3, the forefoot PPs are found at MTHs 2, 3 for BS and MTH 1 for NW. The CA measurements were found to increase in the toe region, remain approximately the same in MTH regions, and decrease in the mid-foot and rear-foot regions with a higher heel. These observations correspond to the findings of Speksnijder et al. (2005) and suggest that increasing the CA in the mid- and rear-foot regions might be one of the more effective strategies of redistributing the plantar pressure more evenly.

This study has also evaluated the effects of heel height and HHS experience on balance during standing in both the AP and ML directions. The four different heels height encompass the most commonly worn heel heights by women on a day to day basis. In comparison to previous studies, the results in this study showed that during quiet standing, the COP values shift medially and anteriorly as the heel height is increased. Variations of the COP (standard deviations of COP) in both directions increase with increasing heel height for non-regular HHS wearers only. Regular HHS wearers even had the largest standard deviations in flat-heeled condition. Since the effects of heel height are not statistically significant for regular HHS wearers, this observation only partially validates the first hypothesis which states that foot stability decreases with increased heel height. Disregarding the exceptional high S. D. values at 1 cm heel, the mean S. D. of the COP_y generally increases with heel height, which is basically in line with the observations of Hapsari and Xiong (2016) and Gerber et al. (2012) in which the standing balance (in AP direction) were found to be worse with a 10 cm heel in the

former, and larger COP oscillations were observed for a 7 cm heel than standing barefoot in the latter.

It is worth noting that the effects of heel height on standing balance are very significant in the ML direction, especially for non-regular HHS wearers. When comparing the mean standard deviation of the COPx for a 10 cm heel (0.93) to the 1 cm heel (0.39), a 141% increase was recorded for non-regular HHS wearers. This suggests that the ML components of the COP measures should always be included in the examination of standing balance in HHSs.

The instability introduced by HHSs can be explained by the increase in height in the COM as well as the reduction in the area of the support base (Chien et al., 2013). When standing in HHSs, the COM shifts upward and forward, thus resulting in a less stable balancing model. Due to aesthetics, HHSs often have a narrow heel base, which fails to provide stable plantar support (Luximon et al., 2015) to the wearer, thus making postural control a more challenging task.

Aside from the changes in the COM and support base, the feet are more supinated and plantar-flexed when standing in HHSs. These changes in the foot posture not only changes the weight bearing conditions of the feet (Ko et al., 2009; Speksnijder et al., 2005; Snow et al., 1992), but also reduce the range of motion of the ankle plantar flexion and calcaneal eversion. Hence, the feet might not be able to evert as naturally and efficiently to maintain balance as heel elevation is increased (Ebbeling et al., 1994).

The collective results of the instability demonstrate that a different strategy for balance is necessary, one that would involve different hip and ankle motor skills to maintain body equilibrium. The previous literature indicated that when perturbations are small and the supporting surface is firm, an ankle strategy is adopted by the body, and when perturbations are rapid and larger, and the supporting structure is deficient or cannot

accommodate the feet, while a hip strategy would be adopted by the body (Horak et al., 1990). During quiet standing, an ankle strategy is the first strategy used to counteract the small perturbations of the center of gravity. As instability increases with heel height, larger perturbations of the center of gravity might result. Therefore, the hip strategy is adopted if the ankle strategy fails to maintain balance. This explanation is provided in Hapsari and Xiong (2016), who observed that a hip strategy is used when the subject is standing in HHSs, although the ankle strategy is still predominantly used.

It is also interesting to find that although there are the least overall variations in the COP with a flat heel of 1 cm, the mean COP velocity is the highest. This observation suggests that with flat shoes, static balance is maintained through minor but highly frequent body sway, which might be the result of using the ankle strategy. As the height of the heel is increased to 8 cm, the COP oscillates farther but at a slower pace, thus indicating that the standing posture is less stable and corrective movements are made accordingly. With an increase of heel height to 10 cm, both the magnitude and velocity of the postural sway are increased. Greater COP oscillations and more rapid rate of change in the COP movement indicate very poor static stability. Greater efforts and more intensive corrective body sway, as a result of both ankle and hip movement, are thus necessary to maintain body balance.

The current study negates the findings in Hapsari and Xiong (2016) who concluded that the HHS experience has no significant effect on standing balance, and finds statistically significant effects of the HHS experience on standing balance in both the ML and AP directions, especially with higher heels of 8 and 10 cm. Moreover, a significantly lower velocity of the COP were observed in regular HHS wearers in the AP direction for all heel heights, which suggests that they might have better muscle strength in their anterior and posterior postural muscles, and hence a more efficient balance strategy is

adopted when wearing HHSs. This explanation is supported by previous EMG studies (Stefanyshyn et al., 2000; Hapsari and Xiong, 2016) where experienced HHS wearers were found to exert different muscle effort from certain lower extremity muscles.

It is also worth noting that while regular HHS wearers generally have better static stability than non-regular HHS wearers in both the ML and AP directions for all heel heights, their stability when they wear shoes with low heels (1 cm) is inferior to that of the non-regular HHS wearers, although the difference is not statistically significant. This suggests that the HHS experience might have negative effects on static stability with flat heels, and could be attributed to the chronic adaptations of the muscle-tendon architecture of frequent high heel wearers as suggested in other studies, such as shorter calf muscles in experienced HHS wearers during standing (Csapo et al., 2010; Cronin et al., 2012).

In NW, all cadence and stance time variables fall within the normal range (Levine et al., 2012). A mean curve that shows the changes in the COPx locations over the entire stance phase was determined for each subject for each heel height. The upward fluctuations observed in the loading response with a 5 cm heel and higher indicate that the COPx shifts frequently and thus there is instability of gait. Taking into account the narrow width of the heel, the magnitude of the fluctuations increase in significance and might have greater effects on stability. The fluctuations might also suggest that regular HHS wearers tend to "correct" their COP towards the medial direction during loading response.

The mean COP in the ML direction was found to increase with heel height. As the COPx can be regarded as a measure of the tilting movement of the foot (Hoogvliet et al., 1997), shifting of the COP towards the lateral side in high heels indicates eversion of the foot (Gefen et al., 2002). If the wearer fails to correct the COP and retain her

129

balance at heel strike, there might be the risk of falling or spraining of the ankle. The ability to stabilize the foot during loading response, therefore, is vital for maintaining balance in the HH gait.

Another important dynamic stability measure, the RMS of the COPx, has been also evaluated in the present study. The largest RMS values were observed with a lower heel of 1 cm, and found to be significantly different from the RMS values of the higher heels of 8 cm and 10 cm. This finding is in line with those of Hyun et al. (2016) but seems to contradict the assumption that stability decreases with increasing heel height; however, the phenomenon might be explained by the difference in the area or width of the base of support (BOS) of the HHSs in this study (Luximon et al., 2015).

Since all of the shoe samples have an identical toe box style and shape, the remaining variable, which is the BOS, lies in the heel area. According to Winter (1995), the vertical projection of the COM should fall within the BOS to maintain balance, in which the BOS was defined as the "possible range" of the COP. Hence, it is easier to maintain balance in shoes with a larger BOS. The BOS at the heel of the shoes with a 1 cm heel is the largest, thus allowing larger variations in the COP without the risk of falling.

Without taking into consideration the 1 cm heel, the RMS value still decreases as the heel height increases, while the width of the base of the heel remains the same for all the other heel heights of 5 cm, 8 cm and 10 cm. This can be explained by another factor – the walking speed. As the subjects were asked to walk at their preferred pace, with the assumption that they were walking at a pace that reflected their best stability (Beauchet et al., 2009), they might have sacrificed the walking speed for better stability when walking in high-heels. This explanation is supported by observations of the mean walking speed, in which the subjects walked faster in low heels and slower in high heels.

These observations are also in agreement with those in previous studies (Annoni et al., 2014; Esenyel et al., 2003, Opila-Correia, 1990a).

It is interesting to find that the RMS of the COPx is highest with a heel of 1 cm but its velocity of the COPx is the lowest. The RMS value accounts for the variance among the steps taken while the velocity of the COPx relates more to the walking speed and the pattern of the progression of the COP in each step. This observation is in agreement with the plots in Figure 5-19 where the shape of the mean curve with a heel of 1 cm fluctuates less but the variations among the steps are greater compared to the other heel heights. The walking speed might also be the reason why the range and velocity of the COPx were found to be significantly higher with a heel of 5 cm, as the mean walking speed recorded is the highest.

Apart from the mean walking speed, other temporal variables including cadence, stance duration and stance percentage did not change significantly from a flat-heel to high-heel gait. Although several previous studies (Esenyel et al., 2003, Han et al., 1999; Opila-Correia, 1990a) also did not find a significant difference between these two gaits in terms of the cadence, however, the stance percentage was found to be significantly higher in high-heel gait in a study by Opila-Correia (1990a).

High-heel experience is not found to have significant effects on the COPx values, their variability (RMS), and the temporal variables in this study, including the mean walking speed, cadence, stance time and stance percentage, although non-regular HHS wearers did show different HH gait characteristics compared to the regular HHS wearers — greater variance (standard deviations) was observed in the temporal measurements of their gait, thus indicating that their gait is less consistent temporally. The current findings somewhat agree with a study by Chien et al. (2014) in which no significant

effects of the HHS experience were found in walking speed and cadence, but the effects on stance time percentage were significant.

There are several limitations in this study. Due to the demographic characteristics of the participants recruited, the results are only valid for young healthy females. The Definition of regular HHS wearer adopted in this study is also a determinant factor that affects the result of the effects of high-heel experiences.

5.8. Chapter Summary

Due to the changes in foot morphology and the shifted COM, the use of HHSs redistributes the body load bearing pattern of the plantar foot, thus forcing the vulnerable regions - the medial and centre metatarsal regions, to bear most of the body load which originally acted on the heel region with shoes that have a flat heel. On the other hand, due to changes in the foot morphology with higher heels, the CAs, PP and force of the midfoot and rearfoot regions decrease as the height of the heel increases.

Moreover, wearing HHSs negatively affect foot stability in quiet standing as the variations of the COP in both the AP and ML directions increase with heel height. The adverse effects start to accumulate when the heel height reaches 8 cm and increase in severity with a heel of 10 cm. High heel experience, however, appears to help to maintain postural control in high heeled conditions. As poor stability in quiet standing indicates greater risks of fall, non-regular HHS wearers should avoid occasional use of HHSs with heels higher than 8 cm. The findings enhance understanding on how postural sway varies with heel height in both the ML and AP directions during quiet standing. For NW, the study has presented a method to quantify and analyse walking stability. By constructing a mean curve of the COP in the medio-lateral direction during

the stance phase, the pattern of the COPx progression, the intra-subject COPx variance among strides, and thus the walking stability could be determined.

The pressure measurements collected in this study provide reliable information such as the pressure range of each plantar region, location of PP, and regions to improve CA. All of these could help to determine the design parameters of the new insole in this study.

Chapter 6 – Evaluation of muscle activities and balance control strategies in HHS

In the foot stability analysis reported in Chapter 5, it was found that HHS experience could improve one's static foot stability in HHS. This suggested that regular HHS wearers might adopt different balance strategies from non-regular HHS wearers. Different balance strategies, such as hip strategy or ankle strategy, involve different levels of activity and coordination from different lower extremity muscles. In order to investigate how static balance strategies change with heel height and whether heel experience would affect one's balance strategies, an experiment was carried out on twenty four healthy young females (twelve regular HHS wearers and twelve non-regular HHS wearers) when performing balanced stand (BS) and single-leg stand (SLS). Centre of pressure (COP) measurements and Surface electromyography (SEMG) measurements were collected to examine postural steadiness and muscle activities of six selected muscles: rectus femoris (RF), vastus medialis (VM), vastus lateralis (VL), tibialis anterior (TA), Peroneus Longus (PL), medial gastrocnemius (MG) of the supporting leg.

As mentioned in the literature review, the vast majority of research that focused on standing balance was performed in flat-heeled condition, aiming to predict the fall risks of certain patient groups and to evaluate the effect of shoes, external perturbations, stance widths and age on postural control. Since the feet in HHS are always in a plantar-flexed condition, the range of motion of the ankle joint are restricted (Mika et al. 2012; Son et al., 2008) and hence might affect the efficiency of adopting the ankle strategy in regulating the COP to maintain standing balance. Being regarded as one of the critical indicators on one's balance control ability and a reliable tool to evaluate the effects of unstable shoes on muscle training and rehabilitation purposes, balanced stance was

performed in the present study to evaluate the balance control strategies in HHS through muscle activities and postural steadiness measurements. In order to induce greater challenge to the balance system in the ML direction, SLS was also included in the study. Not only putting full body load on the standing leg, width of the base of support (BOS) in SLS also reduced significantly. By examining BS and SLS together, we could examine activities of selected muscles and balance control ability in less stable standing equilibriums in both AP (introduced by heel height) and ML (introduced by narrower BOS in SLS) directions.

While RF, VM and VL covering the front and sides of the thigh are knee extensor muscles that help stabilizing the knee and assisting hip movements during standing; TA (dorsi-flexor and evertor), PL (evertor) and MG (plantar-flexor) are the lower leg muscles that are responsible for ankle movements and stabilization. Higher muscle activation of the selected muscles has been associated with the increase of heel height (please refer to Section 2.4.5) during gait. In this study we would like to investigate the effects of heel height on their activation levels in static balance.

Although both the knee and ankle are primarily hinge joints allowing movements on sagittal plane (AP direction), there are evertors and invertors on the lower leg that provide active control at the ankle for ML stability. Hence, higher muscle activities would be expected in the ankle evertors and invertors as the instability in ML direction increases in SLS.

Apart from the effect of heel height, the effect of HHS experience on muscle activation level during static balance would also be examined in this study as this issue was less explored in literature. Although chronic adaptations in muscle-tendon architecture (Csapo et al., 2010; Cronin et al., 2012) and different muscle activations during high-

heeled gait (Csapo et al., 2010) and postural balance (Hapsari and Xiong, 2016) were observed in experienced HHS wearers, the findings were not always consistent.

In this study, we hypothesized that (i) the electromyographic (EMG) muscle activity of selected extrinsic lower extremity muscles and postural sway increase with heel heights; and (ii) activation levels of muscles associated to ankle movements, especially PL, the evertor, would be significantly higher in SLS than BS; and (iii) experienced HHS wearers adopt different balance strategies and have better postural steadiness than non-regular HHS wearers in high-heeled conditions.

6.1. Subjects

Twenty-four young, adult female of age 21–28 years were invited as the participants for this study. Twelve are regular HHS wearers and twelve are non-HHS wearers. Regular HHS wearers were defined as participants who had worn HHS with a minimum heel height of 5cm, for at least 18 hours weekly, three or more times a week, for the past two years. All participants had EU 37 or 38 feet and were self-reported free from lower-extremity pain and injury for a minimum of one year prior to the study. Please refer to Table 5-1 for the demographic data of the participants. The experimental protocol was approved by the University's Human Subjects Ethics sub-committee and all participants gave informed written consent prior to the test.

6.2. Instrumentation and preparation prior experiment

Surface Electromyography (EMG) is the most widely used method in examining muscle activities in gait analysis. It measures the electrical activity of a contracting muscle. The magnitude of EMG signal, which describes the amount of electric activity during a contraction, would be used to quantify the level of muscle activities in this study.

In the experiment, surface electromyography (SEMG) of rectus femoris (RF), vastus medialis (VM), vastus lateralis (VL), tibialis anterior (TA), peroneus longus (PL), and medial gastrocnemius (MG) from the standing leg (Figure 6-1) were collected using a wireless EMG system (Noraxon USA Inc., Scottsdale, AZ, USA) at an initial sample rate of 3000 Hz. Raw EMG signal was high-pass filtered at 10 Hz and the root mean squared EMG was computed at a 100ms window before transmission.
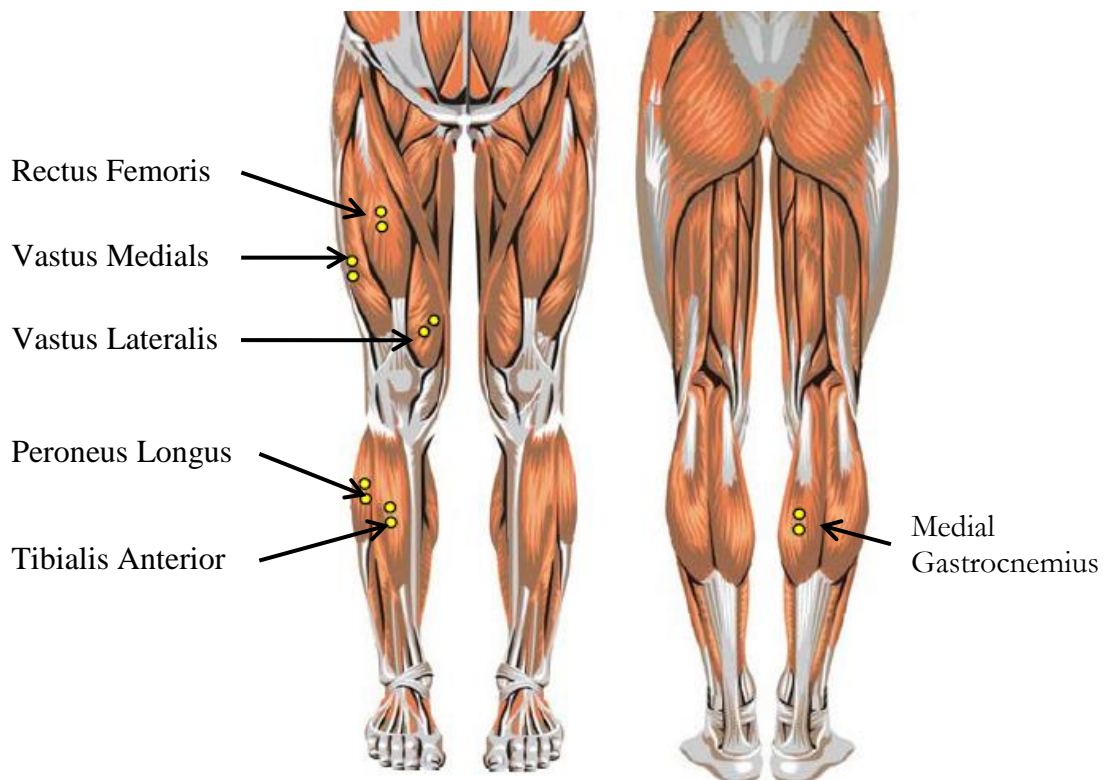
Figure 6-1. Anatomical positions of selected muscles and corresponding electrode sites, front view (left) and dorsal view (right)

Light shaving and cleaning with alcohol of the electrode placements area was performed prior to electrode placement. EMG electrode pairs were placed with a 20 mm inter-electrode distance parallel to the muscle fibre orientation, on the most prominent point of the muscle belly. Three trials of maximum voluntary contractions (MVC), each lasted for 3 seconds, were performed for each muscle. A recovery period of 1 minute was given between each trial. The RMS EMG signals were smoothed using a 500 ms sliding

window and the highest value among the 3 trials were used for data normalization. RMS EMG recorded during SLS was expressed as the percentage of the MVC values.

The in-foot COP locations were recorded by Pedar®-X insole measuring system (Novel GmbH, Munich, Germany). A pair of 2mm-thick Pedar® insole sensors (EU size 36/37) with 99 pressure sensors embedded to each were used to record the measurements at 50 Hz.
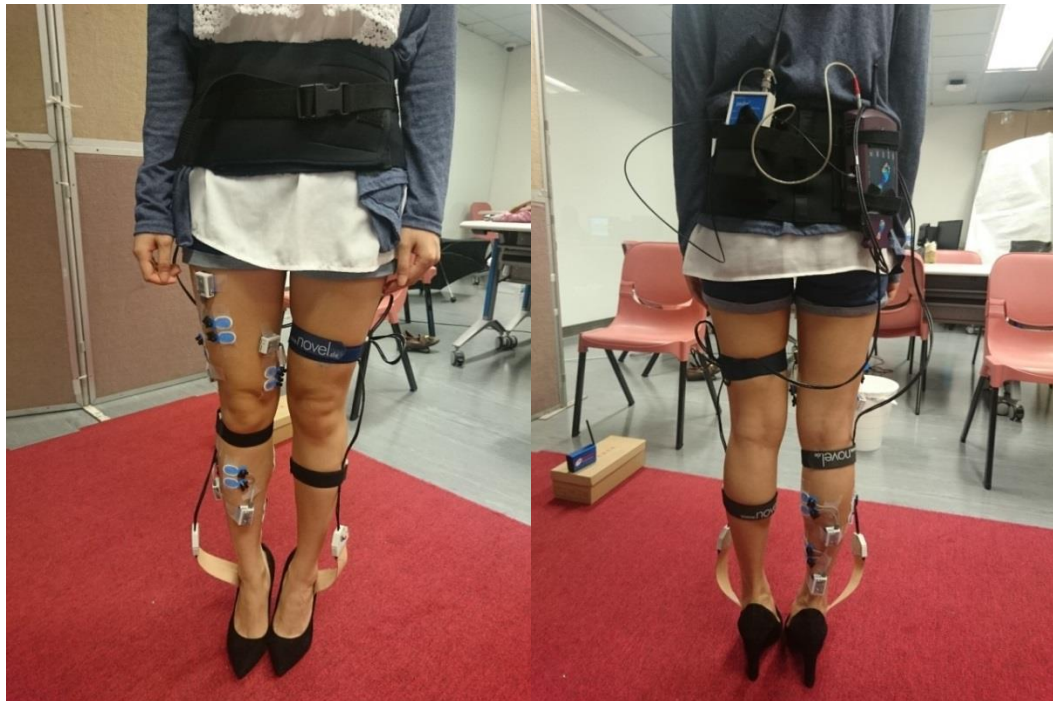
Figure 6-2. Front view and dorsal view of a subject after putting on the Pedar-X insole measuring system and having EMG electrodes attached on the skin surface of selected muscles

6.3. Experimental protocol

Four different heel heights were tested in the study. This combination covered the most common heel heights in daily use, ranging from low-heels (1cm), mid-heels (5cm) to high-heels (8cm and 10cm). The sizes of the shoe samples range from EU 36 to 38. Please refer to Figure 5-1 for the side views of the shoe samples.

Prior to the experiment, participants were asked to identify their best-fitted size of sample shoes for each condition. For each condition, subjects were required to wear our HHS samples with the Pedar® insole sensors inserted. They were then required to perform the following tasks:

(1) Balanced stance (BS)

Subjects were required to perform the standardized quiet standing posture -- to stand still with feet 17 cm apart from the heel centres, toe-out angle 14°, arms by their sides, eyes looking at a visual target placed approximately 3 m in front at eye level (Mclloy et al., 1997) Plantar pressure measurements were recorded in three 30s trials. (Landry et al., 2010)

(2) Single-leg stance (SLS)

Participants were initially standing relaxed with eyes open and weight evenly distributed between both feet. They were then instructed to stand only with their dominant legs and lift up another leg and for 30s. Measurement was stopped after 30 s of the SLS, or if the participant's swing leg touched the floor. The participant was instructed to keep her arms along the side of the body during initial standing and throughout the task. Compensatory arm movements were accepted during SLS (Jonsson et al., 2004). To prevent falls or injuries, a chair with a high chair back was put close to the participant throughout the experimental session. Participants were allowed to practice before testing. Three trials were performed for each heel height condition.

Figure 6-3. Posture of Single-Leg Stance (SLS)

The four testing conditions were assessed in randomized order. A two-minute rest was given in-between each condition to prevent fatigue.

6.4. Data Processing and Analysis

The SLS task involves switching from bipedal to unipedal standing. The process requires an initial voluntary action of moving the COP over the standing leg, followed by the task of maintaining postural orientation in space (Jonsson et al., 2004). The first 5s was therefore regarded as the dynamic phase and thereafter a static phase. Since the aim of this experiment was not to access individual postural steadiness but the general effects of heel heights and HH experience on postural control, only measurements from the static phase (25s) were evaluated.

For the postural steadiness evaluation, seven COP-related variables, namely, the mean COP values, their excursions (which denote the largest magnitude of oscillations) in both medio-lateral and antero-posterior directions, and the mean COP velocity were computed for the static phase of each trial. The mean values of the three trials of the same heel elevation condition of each subject were calculated.

To evaluate the muscle activity, the mean RMS values of the six muscles, as well as their standard deviations were calculated over the static phase of each trial. Data obtained from the experiment were statistically analysed with the SPSS Statistics 21 (IBM Corp., Armonk, New York) software. The effect of heel height and HHS wearing experience on the muscle activities and COP was analysed by repeated measures analysis of variance (ANOVA). The mean difference between variables obtained in BS and SLS were compared through paired-samples test. Significance of the statistical analysis was set at $p < 0.05$.

6.5.   Results

For balanced stance, heel height of HHS significantly increased the level of muscle activities of all selected muscles ($p < 0.05$). The percentage of change of all measured variables when compared to 1cm heel and results of the pairwise comparisons of the post-hoc Bonferroni test is summarised in Table 6-1. As shown in the table, the muscle activities %MVC increased significantly with heel height. When compared with flat-heeled condition, the mean of %MVC of thigh muscles increased 31 to 52%, and significant 67%, 70% and 54% increase were identified in PL, TA, and MG in 8cm respectively. When the heel reached 10cm, the increase in muscle activities were all statistically significant, percentage of increase ranged from 58 – 81%.

Table 6-1. Percentage of change of the measured variables in BS when compared to 1cm heel and results of the pairwise comparisons of the Bonferroni post-hoc test. Significant difference (P<0.05) identified between the two subject groups were in bold and marked with an asterisk.

Measured variables	5cm	8cm	10cm
RF	-18	31	**58***
VL	14	52	**73***
VM	11	47	**68***
PL	40	**67***	**74***
TA	37	**70***	**81***
MG	**31***	**54***	**60***
COP ML	**-4***	**-10***	**-13***
COP AP	**12***	**25***	**30***
COP Excursion ML	9	17	**34***
COP Excursion AP	5	6	21
COP Velocity ML	**-22***	**-24***	-13
COP Velocity AP	**-20***	**-37***	**-18***

The muscle activities of regular HHS wearers is significantly higher on VL ($p=0.011$ <0.05) and lower on TA ($p=0.043 <0.05$) than that of non-regular HHS wearers. No significant difference is found between the two subject groups on the muscle activities of other muscles.

The mean COP, maximum excursions and mean COP velocities in both ML and AP directions are significantly different when wearing the shoes with different heel height ($p<0.05$). As described in the last chapter, COP increases in AL direction and decreases in ML direction with increasing heel height, indicating a forward and medial shift of COP. No significant difference was identified between regular and non-regular HHS wearers in the COP and the COP excursions, but the former had significantly smaller COP velocity in AP direction ($p = 027 < 0.05$).

The mean and standard deviation of each measured variable collected from the two subject groups were plotted in figures 6-4 and 6-5. Significant difference (P<0.05) identified between the two subject groups were marked with an asterisk in the chart title.

Figure 6-4. Mean and S. D. of the EMG (%MVC) of the six selected muscles in BS
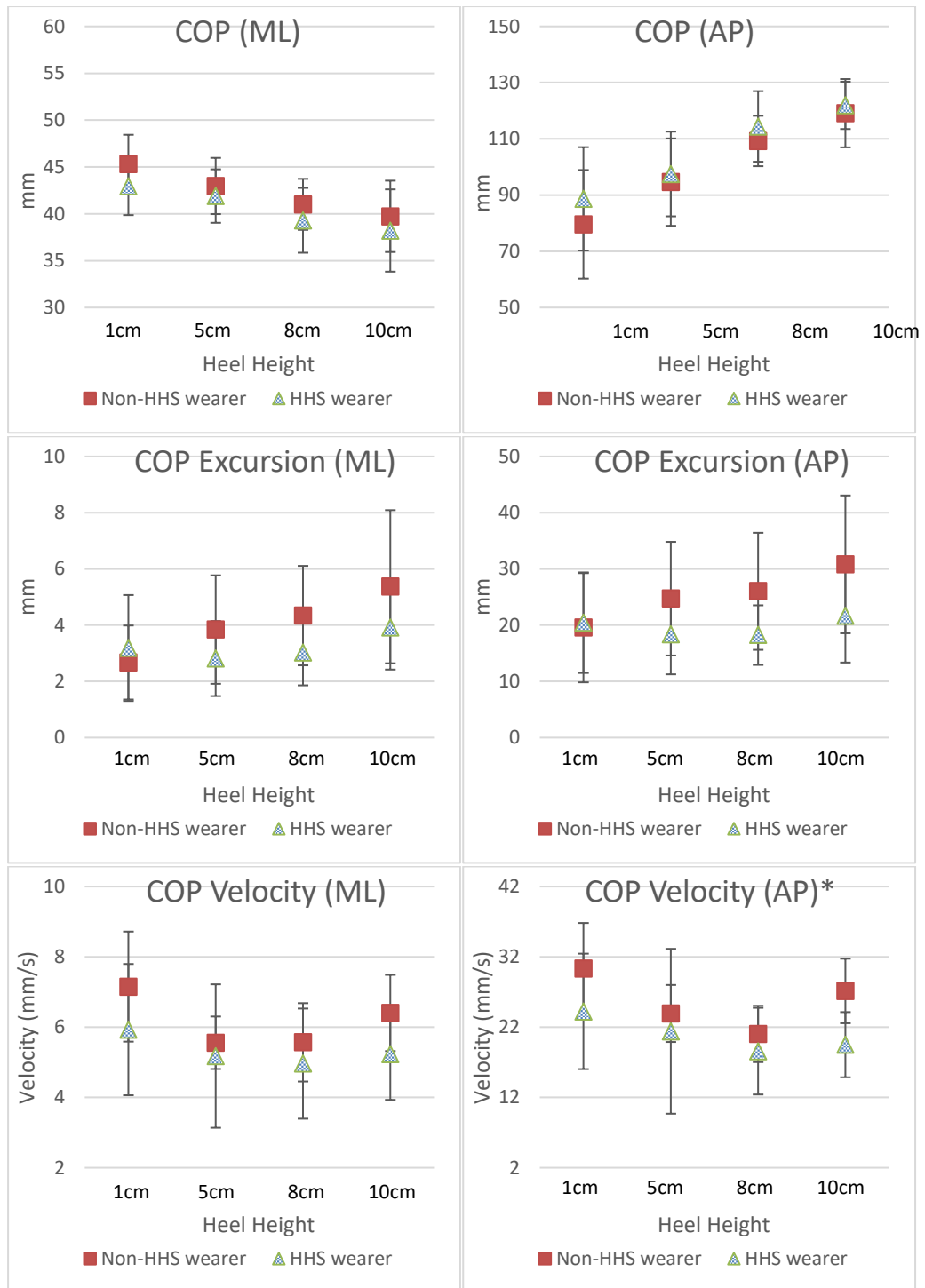
Figure 6-5. Mean and S.D. of the six COP-related variables in BS

Similar to BS, heel height of HHS significantly increased with the level of muscle activities ($p<0.05$) in SLS. The percentage of change of all measured variables when compared to 1 cm heel and results of the pairwise comparisons of the post-hoc Bonferroni test is summarised in Table 6-2. As shown in the table, the muscle

activities %MVC of thigh muscles increased significantly with heel height. When compared with flat-heeled condition, the mean of %MVC of thigh muscles significantly increased 55 to 57%, and a significant 28% increase was found in PL. When the heel reached 10 cm, the percentage of increase in muscle activities rose to 75 – 78% for the thigh muscles, and to 41% for PL.

Table 6-2. Percentage of change of the measured variables in SLS when compared to 1cm heel and results of the pairwise comparisons of the post-hoc Bonferroni test. Significant difference (P<0.05) identified between the two subject groups were in bold and marked with an asterisk.

Measured variables	5cm	8cm	10cm
RF	14	**55***	**75***
VL	17	**55***	**76***
VM	22	**57***	**78***
PL	12	**28***	**41***
TA	1	12	34
MG	18	31	43
COP ML	**-5***	**-12***	**-19***
COP AP	**10***	**19***	**27***
COP Excursion ML	-19	**-33***	**-37***
COP Excursion AP	0	-20	-9
COP Velocity ML	-12	-16	-11
COP Velocity AP	-10	-9	12

The effect of HHS experience for both tasks was similar. Regular HHS wearers generally had higher level of muscle activities in the thigh muscles RF, VM and VL, but lower activities in TA and MG, though the difference were found statistically significant in VL (p=0.011 <0.05) and MG (p=0.007 <0.05).

The mean COP value, maximum excursions and mean COP velocities in both ML and AP directions are significantly different when wearing shoes with different heel height (p<0.05). The post-hoc Bonferroni tests showed there were significant differences in the COP excursion in ML direction for 5cm, 8cm and 10cm when compared with 1cm.

Significant difference in the COP excursion in AP direction was found only between the heel height of 1 cm and 8 cm. For the COP velocity, there are significant differences between the heel height of 5 cm and 10 cm, and 8 cm and 10 cm in AP direction while there is no significant difference in the pairwise comparison in ML direction. Regular HHS wearers and non-regular HHS wearers showed no significant difference in the COP and the COP velocity. However, there is a significant lower maximum excursion in AP direction for regular HHS wearers. The mean and standard deviation of each measured variable collected from the two subject groups were plotted in figure 6-6 and 6-7. Significant difference (P<0.05) identified between the two subject groups were marked with an asterisk in the chart title.

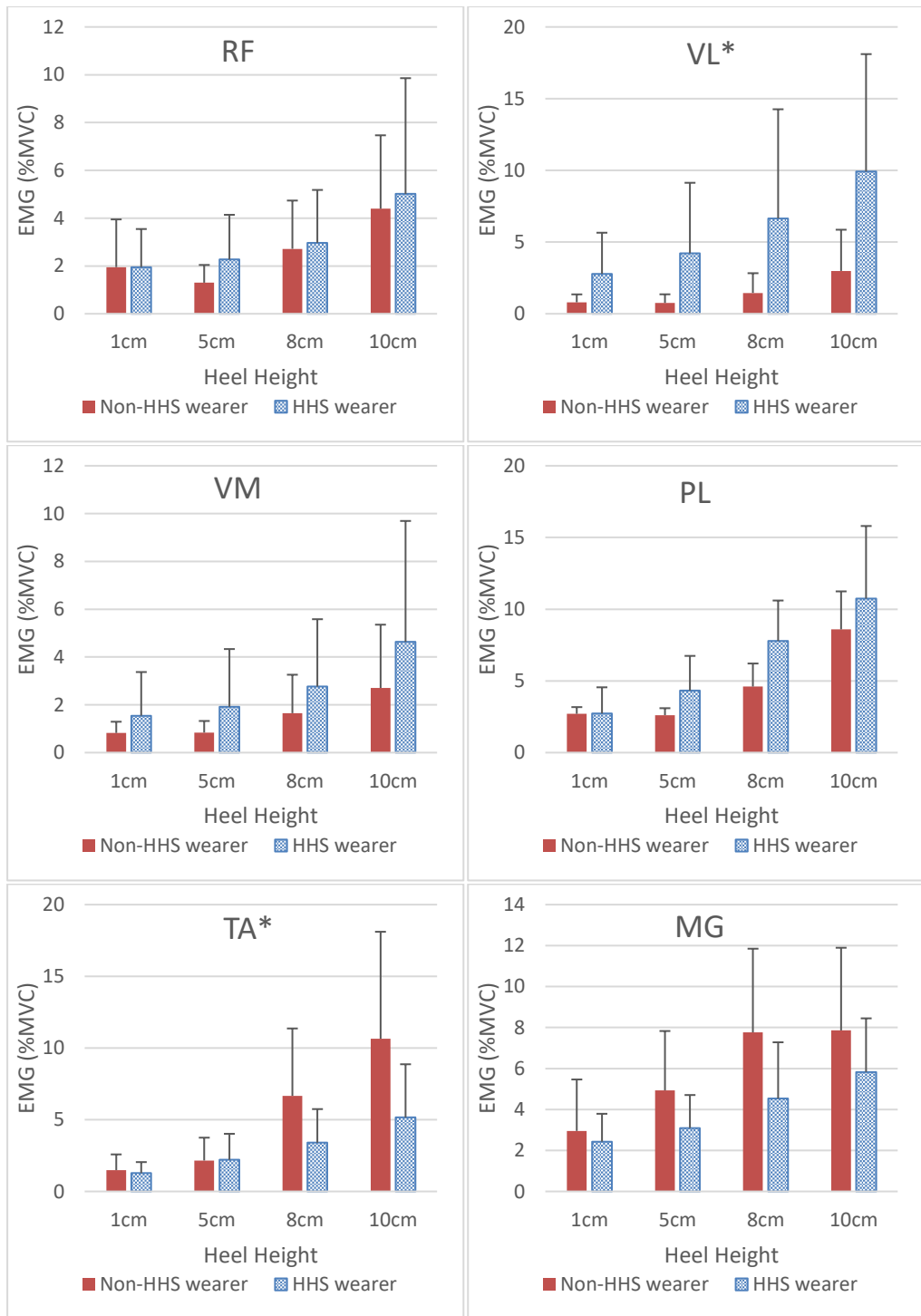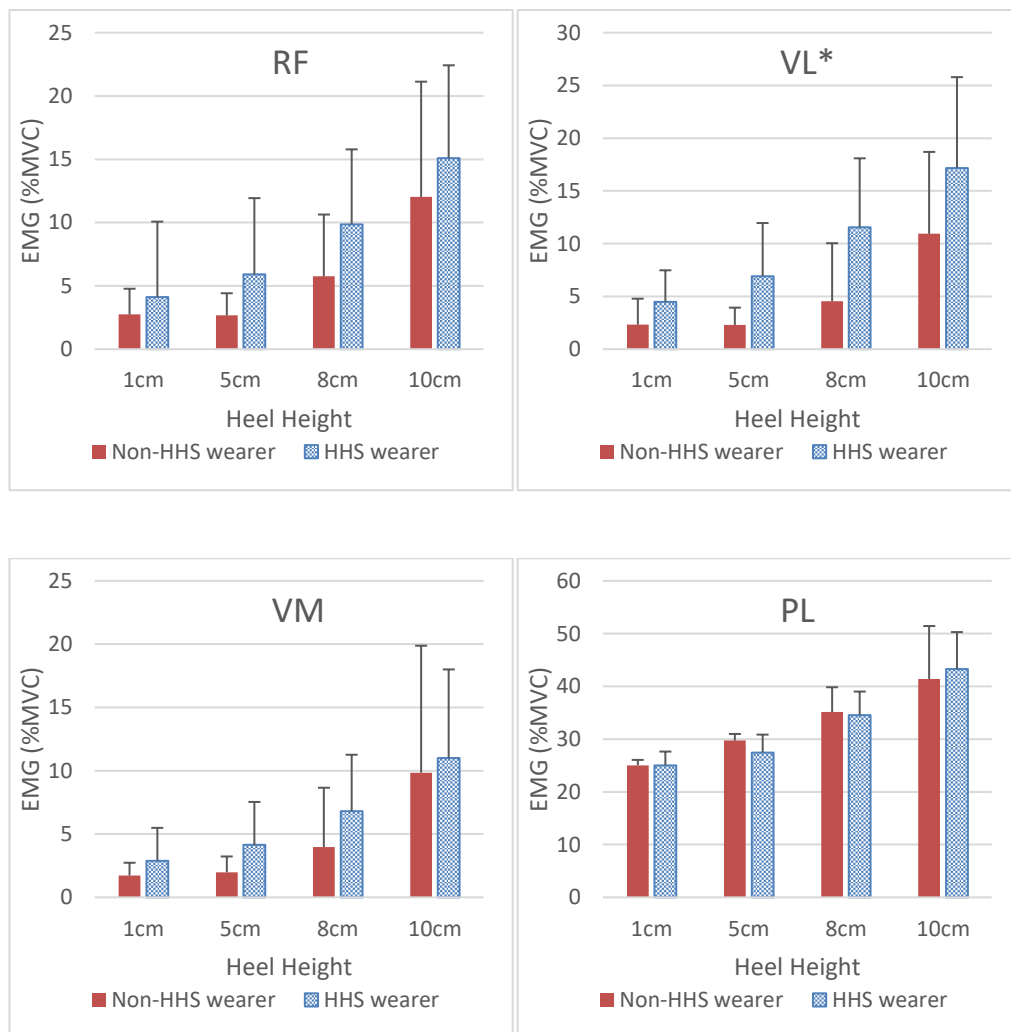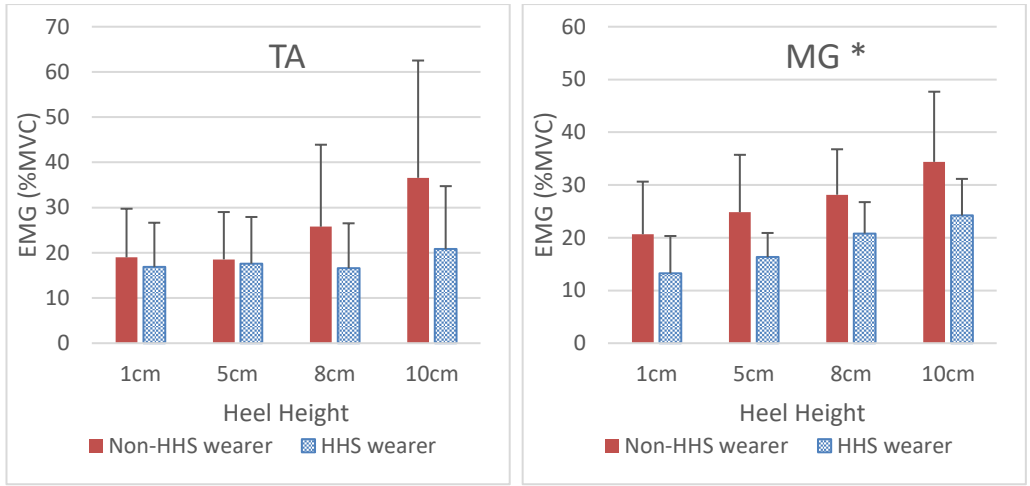**Figure 6-6. Mean and S. D. of the EMG (%MVC) of the six selected muscles in SLS. Variables with significant difference (P<0.05) between the two subject groups were marked with an asterisk**
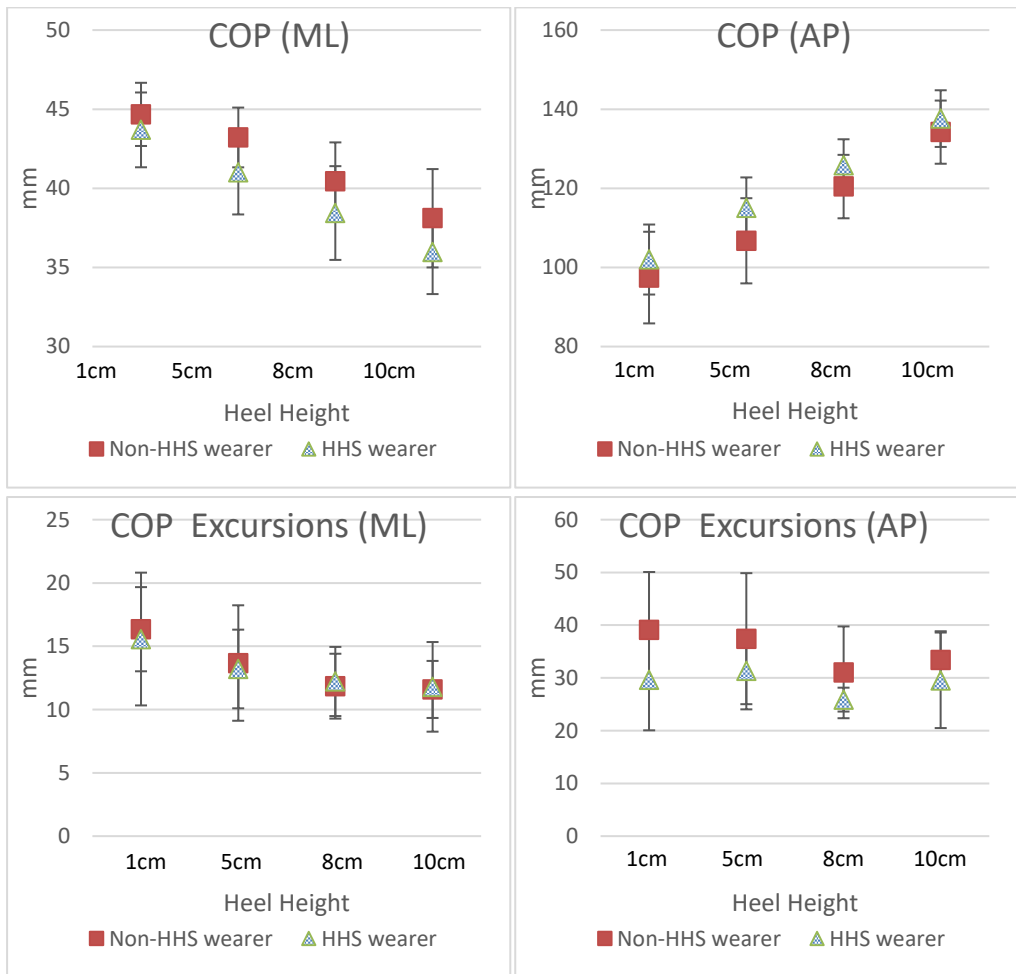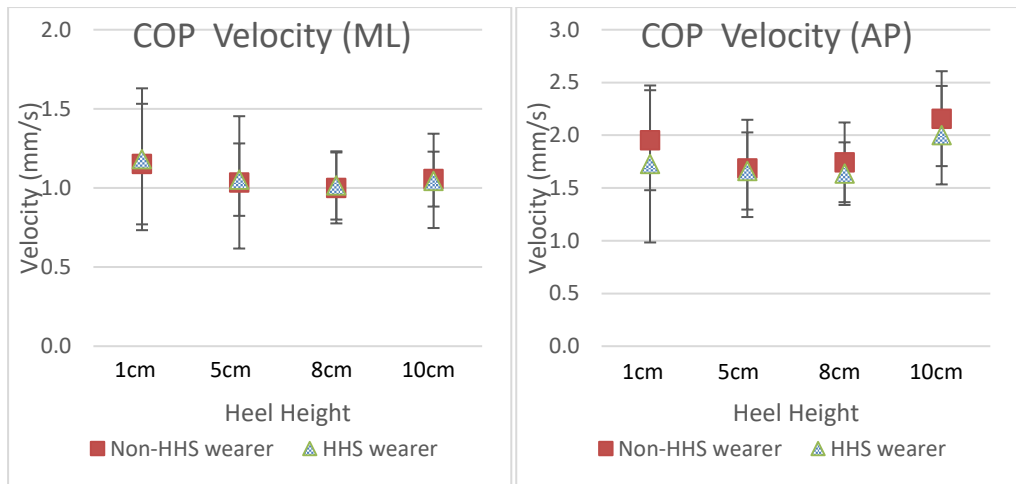
Figure 6-7. Mean and S.D. of the six COP-related variables in SLS

When comparing the data obtained in BS and SLS, it was found that the muscle activities in SLS are significantly higher for all selected muscles for all heel conditions (p <0.05). As shown in figure 6-8, the mean differences of the level of muscle activation between the two tasks were much greater for PL, TA and MG. The level of muscle activities in SLS could reach about four times of that of BS in high-heeled conditions. When the heel height increased to 10 cm, TA and MG achieved nearly 30% MVC and PL achieved nearly 40% while activity levels of RF, VL and VM were within 15% MVC.
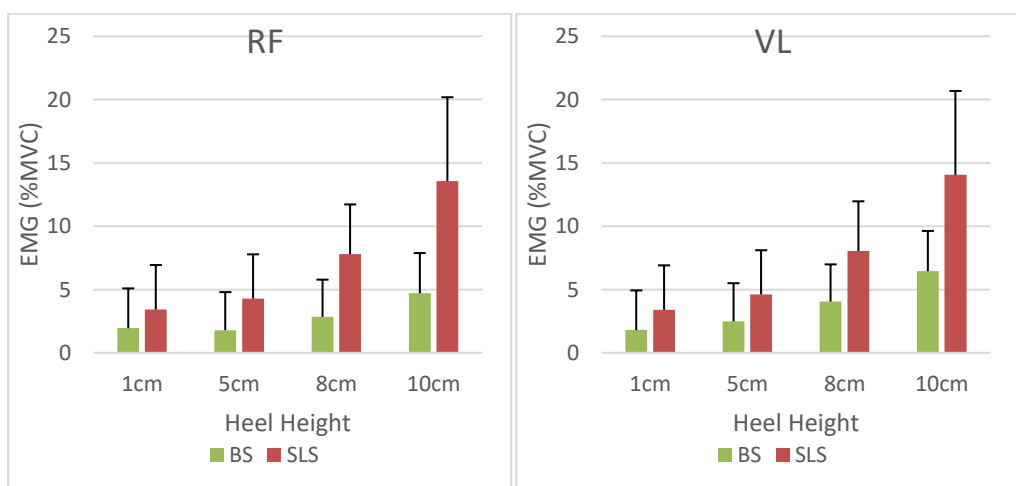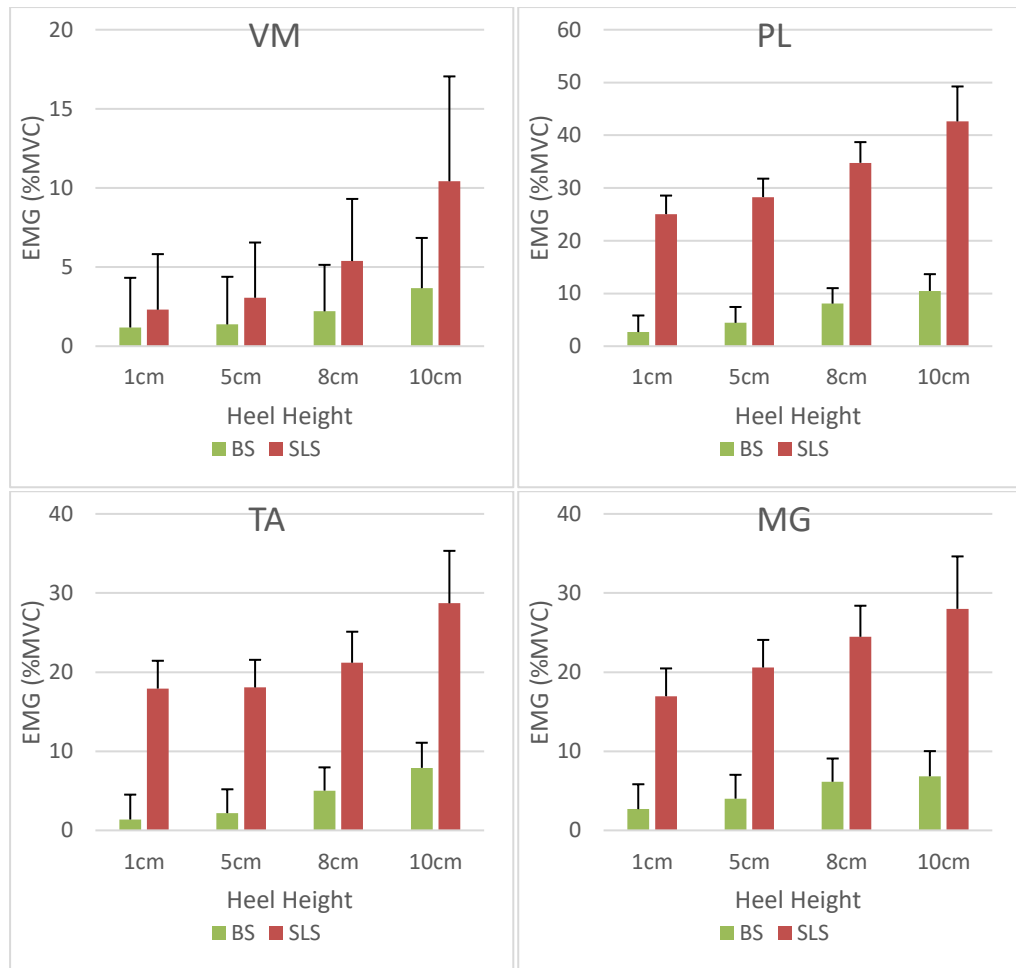
Figure 6-8. Mean and S.D. of the six selected muscles in BS and SLS

6.6. Discussion

In the present study, BS and SLS were used to assess the balance control ability and the muscle activities level when wearing shoes with different heel heights. These findings were largely consistent with many previous studies (Hapsari and Xiong, 2016, Mika et al., 2012; Cronin et al., 2012; Opila-Correia, 1990a) and supported our first hypothesis that with the increase of heel heights, the muscle activities of RF, VL, VM, PL, TA and MG increased, indicating more intense muscle contraction and increased co-activation around both the knee joint and ankle joint for better joint stiffness to maintain postural steadiness (Ebbeling et al., 1994).

However, the first hypothesis was partly fulfilled as the magnitude of body sway did not increase with heel height in SLS. In BS, the COP excursions in both directions increased with heel height, indicating the magnitude of body sway increased with heel height. However, the increase of heel height in SLS in the present study did not lead to an increase in maximum excursion in AP direction as described in Shimizu and Andrew (1999)'s study; the maximum excursion in ML direction even decreased with heel height, though not statistically significant. The decrease could be explained by the significant reduction in base of support (BOS) in the ML direction introduced by narrow heel base in heeled-conditions. To avoid falling, one has to keep his centre of gravity falling within the limits of BOS (Luximon et al., 2015; Chien et al., 2013). As the widths of heel base in the heeled-shoes were smaller than that of the flat-heeled shoes, the limit of COP oscillations allowed were smaller. Moreover, the use of HHS hinders the range of motion and eversion of the ankle joint (Mika et al. 2012; Son et al., 2008), which might affect the efficiency of using the ankle strategy to regulate the COP in postural control.

Although previous studies had shown positive correlations between magnitude of body sways in ML direction and TA activities and modulations during quiet standing in flat-heeled shoes (Sayenko et al., 2017; Lemos et al, 2015; O'Connell, 1958), no such correlations were found in HHS. As magnitude of COP oscillations in ML direction did not increase with heel height, the increase of muscular effort due to heel height might be spent on increasing joint stiffness instead of joint movements for regulating COP. As the COM is lifted and BOS is decreased in HHS, the standing posture is a more unstable equilibrium. Greater ankle and metatarsal joint torque is required to maintain the balance.

The second research question is about the muscular efforts of the ankle invertor and evertor in BS and SLS. In this study, PL is the prime foot evertor, TA is a major foot

dorsi-flexor and invertor, and MG is a major plantar flexor. While heel height being the main factor contributing instability in AP direction to the standing posture, the narrower BOS in SLS added instability to the standing equilibrium in the ML direction. As shown in figure 6-8, muscle activation levels of PL, TA and MG in SLS are 3 to 4 times of that of BS for all heel conditions, while RF, VL and VM activities only doubled in SLS, indicating much muscular effort were exerted around the ankle to bear the full body load as well as to increase the joint torque to counteract the greater moment of inertia of the COM fluctuations. The ankle strategy still dominates balance control in HHS. This finding was in accord with the observations made by Amiridis et al. (2003), in which young adults rely more on the ankle muscles (TA and MG) than thigh muscles in SLS. The second hypothesis was supported.

Another aim of this study is to understand whether the experience in wearing of HHS can train up lower limbs muscles to improve the postural steadiness in HHS in different heel height conditions. Though statistical significance was not reached, regular HHS wearers generally had smaller values in COP excursions and velocities in both directions during BS, as well as in COP excursion and velocity in AP direction during SLS. This could be regarded as an indicator of better postural steadiness. When comparing the two subject groups, regular HHS wearers showed relatively higher muscular effort from thigh muscles (RF, VL and VM) and lower muscular effort from lower leg muscles (TA and MG) during both BS and SLS. The findings did not quite agree with previous studies where experienced HHS wearers were found to exert significantly more muscular effort from MG (Hapsari and Xiong, 2016, Cronin et al., 2012), and less effort from VL and TA. This contradiction might be caused by the different tasks being performed in the study. While the study led by Cronin (2012) was on high-heeled gait, Hapsari and Xiong's EMG measurements were taken during the sensory

organization test programmed by NeuroCom's Balance Master System, where external perturbations were introduced.

Based on the findings of the RANOVA results, experienced HHS wearers seem to be able to make better use of the thigh muscles to compensate the demand of muscular effort of the lower leg to achieve better postural steadiness in high-heeled conditions. While the thigh muscles work with abdominals, paraspinals and hamstrings to cope with body sways in hip strategy, TA and MG are the prime movers for plantarflexion and dorsiflexion in ankle strategy. Lower muscle activation in the lower leg muscles but higher muscle activation in thigh muscles might indicate a shift from using ankle strategy to hip strategy in experienced HHS wearers.

There are several limitations inherent in the current study. First, the tasks provided for measuring static human balance were not very challenging. More dynamic and difficult tasks such as adding perturbations could be further investigated. Second, the sample size (N=12 for each subject group) is relatively small, which may limit the statistical power of this study. Finally, the definition of the regular HHS wearers might affect the effect of habitation. Regular HHS wearers of higher heels (8-10cm) might exhibit more obvious chronic adaptation.

6.7. Conclusion

The present study examined the effects of heel height and high-heeled experience on muscle activation of selected thigh and lower leg muscles and postural steadiness in both AP and ML directions during BS and SLS. The results showed that the muscle activity of selected extrinsic lower extremity muscles increases significantly with heel heights. Body sways in both directions increase with heel height in BS but decreases in ML direction for SLS. Regular HHS wearers could achieve better postural steadiness

during BS and SLS in HHS through better utilization of thigh muscles. PL, TA, and MG muscles that are associated to ankle movements exert significantly higher muscle activation in SLS than BS to improve ankle stiffness for greater protection from ankle sprain. These findings enhance our knowledge in the balance strategies adopted in HHS of various heel heights.

Chapter 7 – The New Insole Design and Foot-Insole Pressure Analysis through finite element modelling

7.1.   Introduction

With the advancement of computer technology, finite element analysis (FEA) has become one of the most common methods in simulation analysis. In this study, an FEA is carried out to investigate the effects of different insole design parameters such as thickness, material properties, and presence of certain insole features on plantar pressure reduction during standing in HHS. In this simulation, a 3D plantar-flexed foot model with simplified bones and tissues structures is developed. After validating the mechanical properties of the bones and tissues through experimental data, an FEA simulating the mechanical interactions between the foot model, the new insole, a shoe-sole of a HHS of 10cm heel and a rigid floor surface during balanced standing is carried out. The corresponding magnitude of the peak plantar pressure is predicted.

Eight insole design factors including insole thickness, arch cushion thickness, mid-foot cushion thickness, height of heel cup rim, insole stiffness, stiffness of pads for metatarsal and heel, cushion stiffness, were evaluated through FEA. In order to identify the optimal design that possesses the best pressure relief ability, 3 levels of values were examined for each design parameters. A set of 16 designs is generated with combinations of different levels of each design parameters through applying the techniques of fractional factorial design. FE simulations were carried out for each of these 16 designs. Through assessing the magnitude of the peak plantar pressures of these simulations, the mean effect of each level of the design factor on pressure relief could be computed. The optimal design on plantar relief would be the combination consisting the "best" level (greatest effect on plantar relieve) of each design factor.

7.2. The new insole design

Based on the results from the literature review and biomechanical study, several insole features were suggested:

1) Due to the limited space in the toe box, thickness of insole for the forefoot should not exceed 5 mm;

2) medial forefoot (MTHs 1-2) and heel are areas of peak pressures. Pads with softer material should be used to maximize effect of pressure relief. Harder and more durable materials can be used for rest of foot zones to provide adequate foot support and reduce deformation over time;

3) a cushion can be added in the medial arch region to serve as an arch support to increase the weight-bearing contact area for better pressure redistribution effect;

4) a cushion can be added between metatarsal heads and metatarsal shaft to provide better support to the arch;

5) the presence of a heel cup might enhance foot stability in the ML direction and provide better foot support at heel strike.

Based on the pressure distribution maps obtained in the plantar pressure experiments presented in Chapter 5, different plantar regions were identified. The geometries and locations of the MTH pad and heel pad were outlined such that they cover most of the high peak pressure areas resulted in the balanced standing and walking experiments when wearing 8 cm and 10 cm HHS. Similarly, the arch cushion and midfoot cushion were placed on areas of the lowest pressures in the same experiments. Figure 7-1 shows the insole design with all suggested features.
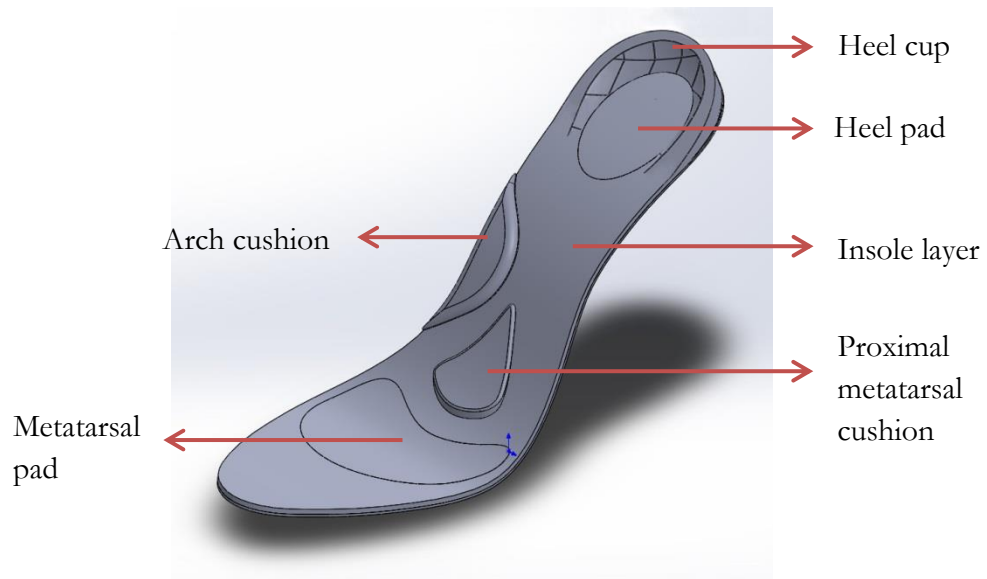
Figure 7-1. Possible features of the new insole design

7.3. Development of the Foot Model

The foot model was created from the 3D surface scans on a left foot of a female subject (height= 168cm, weight = 56kg, age = 22) by a handheld scanner, Artec Eva 3D scanner (Artec-Group, Luxembourg). Scanning was performed while subject was sitting on a chair with her left leg extended horizontally and supported by another chair at the lower leg. The subject was asked to maintain the plantar-flexed posture throughout the 2-minute scan. The plantar-flex angle was checked against with the 10cm heel platform (figure 4.19) at the beginning and at the end of the scanning process. Scan images were pre-processed with Artec Studio 10 Professional software where cleaning, smoothing, re-aligning and merging of scans were performed. The resulting model was then exported to Rapidform XOR3 to create the solid model for FEA. Figure 7-2 shows the resulting solid model of the scanned foot.
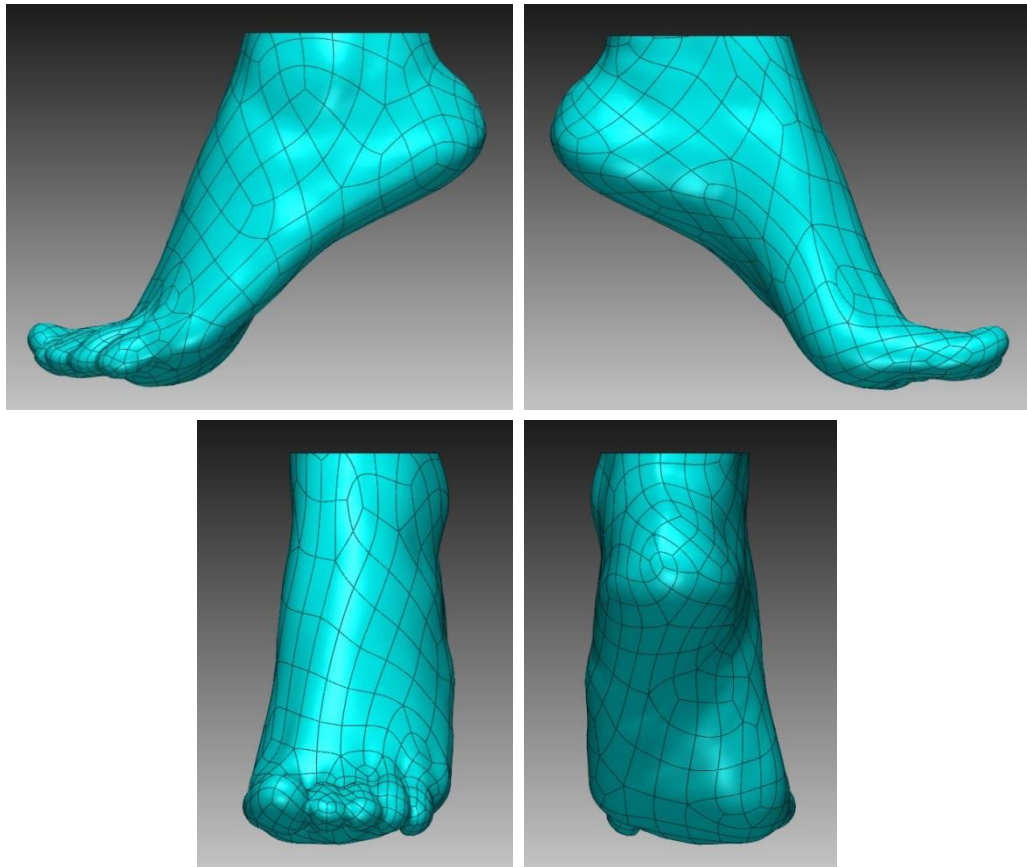
Figure 7-2. The plantar-flexed surface foot model obtained from 3D scanning.

A simplified model of the bone and ligament structures was inserted into the foot model (Figure 7-3). The raw bone structures were obtained online and were generated from CT scan data of a male adult. They were then rescaled and aligned with the scanned foot model in Rapidform® XOR3™. The bones were further grouped and merged leaving gaps only at the major joints, namely, the subtalar joint, transverse tarsal joint, and metatarsal-phalangeal joints, allowing proper foot movements in the simulation (Patil et al, 1993). The plantar fasciitis and ligaments that connect the foot bones were simplified as a solid volume filling up the gaps between the bones. The resulting bone structure consisted of eight bone and five ligament components.
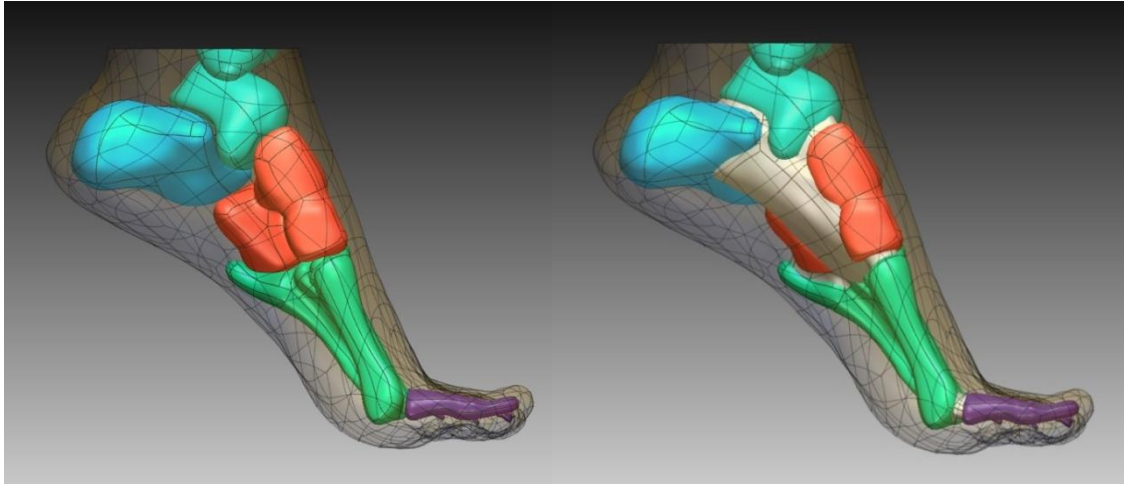
Figure 7-3. The simplified bone and ligament structure (medial view)

7.4. FE Model development

7.4.1. Assignment of material properties

All FE simulations were carried out in ABAQUS/CAE 6.14. After importing to ABAQUS the solid models of the insole, shoe-sole, and floor created from SOLIDWORKS and the solid foot model processed in RapidFrom XOR, they were assembled to form proper contact relationships. Material properties were then defined for each region according the reference from previous studies (Yu et al., 2008, Hsu et al., 2008, Cheung et al., 2008). In order to reduce the complexity of the FE model, all components were idealized as homogenous, isotropic and linearly elastic. The Young's Modulus (E) and Poisson's ratio (v) that describe the linearly elastic properties were defined for bones (E = 7,300 MPa, v = 0.3) ; ligaments (E = 100 MPa, v = 0.45); soft tissues (E = 0.15 MPa, v = 0.45) ; shoe sole of HHS (E = 1000 MPa, v = 0.42); heel of HHS (E = 10,000 MPa, v = 0.4); and ground (E = 1,000,000 MPa, v = 0.1). Mechanical properties of the insole were assigned according to the output of the 16 treatment combination generated through applying techniques of fractional factorial design.

7.4.2. Mesh Generation

Since tetrahedral elements (C3D10) are geometrically versatile to mesh a complex shape, they were chosen as the mesh elements for the bones, ligaments and soft tissues of the foot, as well as the insole and the shoe sole. All meshes were generated by the automatic meshing algorithm provided in ABAQUS. The foot model consisted of 305,831 elements; The insoles consisted of 8726 to 12,927 elements depending on the presence and thickness of various insole features; the shoe sole with a 10 cm heel consisted of 12,187 elements; the floor, which was a 216 mm x 86 mm horizontal rectangular plane of 5cm thickness, was meshed with 8-noded linear hexahedral elements (C3D8R) with a total of 27 elements. Figures 7-4 and 7-5 show the meshed models the foot, insole, shoe-sole and ground.
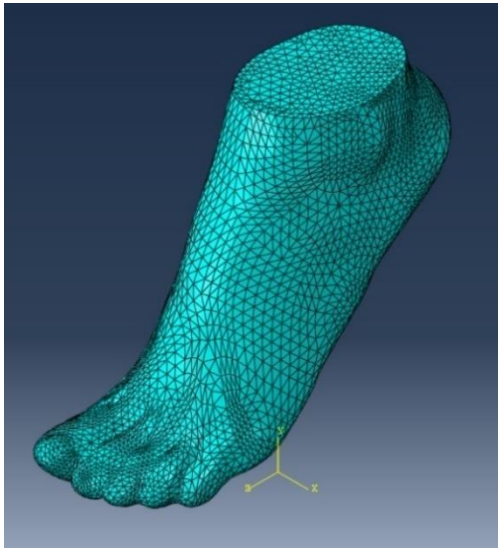
Figure 7-4. The meshed foot model.
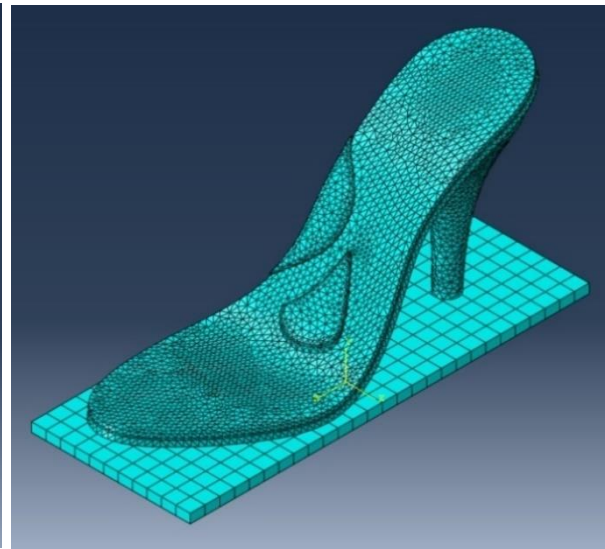
Figure 7-5. The meshed insole, shoe-sole and ground

7.4.3. Defining loads and boundary conditions of FEM

The FE model would be used to simulate balanced stance. The foot and shoe-insole models were initially aligned such that they would touch each other when one of them moves towards the other in the y-direction. The position of the uppermost surface of the foot model was constrained to translation or rotation in all direction (Figure 7-6). The floor was constrained to move only in positive y-direction (upward). An upward point force of half the subject's body weight (280N) was applied upward onto the floor according to the position of the mean COP (Figure 7-7) obtained from experimental data. A surface-to-surface interaction was defined between the whole plantar surface (the slave surface) (Figure 7-8) and the upper surface of the insole (the master surface) with a co-efficient of friction of 0.6 (Yu et al., 2008, Zhang and Mak, 1999). Elements bounded by these surfaces are known as contact elements, on which contact pressure would be computed during simulation. Tie constraints were established between shoe sole and ground surfaces to avoid sliding or separation.
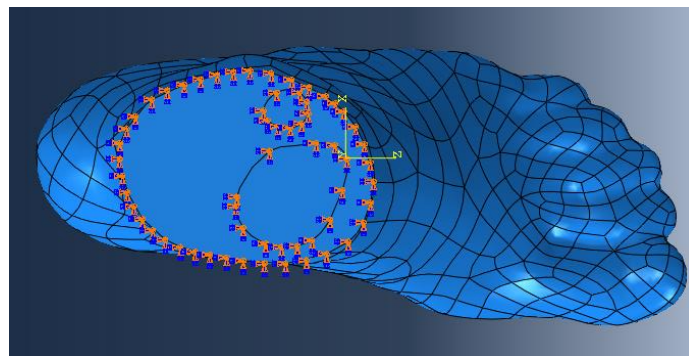
Figure 7-6. The nodes of the uppermost surface of the bone and foot was constrained to translation or rotation in all directions.
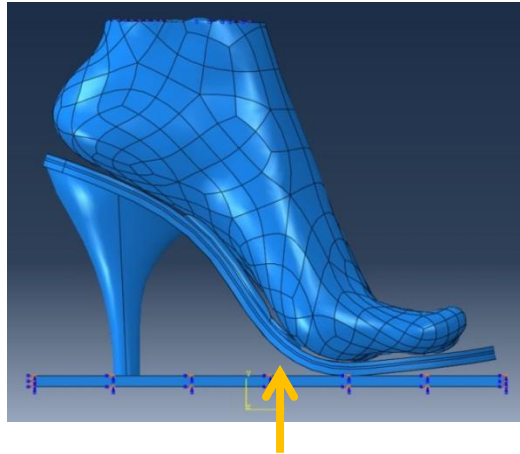
Figure 7-7. The ground support was constrained to move only in positive y (upward) direction. An upward point force of half the subject's body weight (280N) was applied upward at the COP according to Pedar measurement.
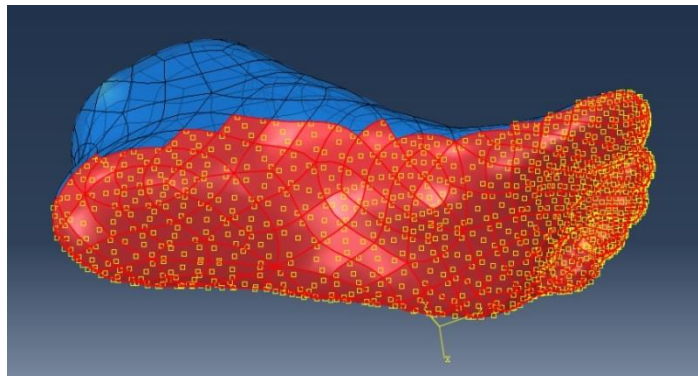
Figure 7-8. Contact elements defined across the whole plantar surface (surfaces highlighted in red.

7.4.4. FE model Validation

Model validation has to be carried out on FE foot model before it was used to evaluate the 16 design treatments. In this study, the accuracy and reliability of the foot model to quantify the plantar pressure were investigated through comparison with experimental plantar pressure measurements. Balanced standing on a pair of foot supports with 10 cm heel elevation (Figure 4-21) was simulated to validate the FE predictions.

The same subject who volunteered 3D foot scanning for the FE foot model reconstruction was asked to perform balanced standing on the foot supports, while

161

plantar measurements were taken with Pedar-X for three 30-second trials. The mean peak pressures at the forefoot and heel regions were computed to validate the FE simulation result. The Young's modulus and Poisson's ratio of the wooden foot support were defined as 15,000 MPa and 0.3 respectively. Figure 7-9 shows the FE model used in validation.
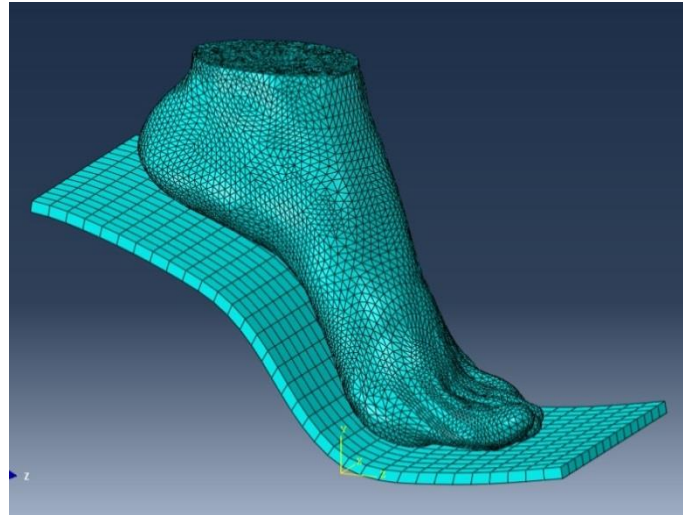
Figure 7-9. Validation of the FE foot model through simulating balanced standing on a 10 cm heel foot platform

7.5. Design optimization through fractional factorial design

In a design optimization process, an objective function that measures the performance of the design has to be determined. The aim of the FE simulations was to predict the plantar pressure reduction ability of an insole in high-heeled condition. Hence, the forefoot peak plantar pressure was defined as the objective function. The "optimal" design is the one that result the lowest forefoot peak plantar pressure. Different from previous FEM studies (Cheung and Zhang, 2008; Hsu et al., 2008; Franciosa at al., 2016) where flat-heel conditions were simulated, pressure measurements from midfoot and rearfoot were not included in the objective function.

In order to describe different design outputs and to evaluate their effect on plantar pressure relief, seven design factors governing the design output were defined. Factors F1 to F3 governed the thickness of insole, midfoot cushion and arch cushion respectively. Factor F4 described the height of rim of the heel cup. These four factors governed the geometries of the insole and its features. The remaining three factors, F5 to F8, described the stiffness of the insole, pads (MTH and heel) and proximal MTH cushion and arch pad respectively. Three levels of values were assigned for each design factor for the parametric analysis. Range of values covered between the first and third levels approximated the reasonable range of values of each design factor. The descriptions and levels of suggested values to be tested in FEA are given in Table 7-1.

Table 7-1. Design parameters and their levels for optimization

Factor ID	Design factors	Level 1	Level 2	Level 3
F1	Insole thickness (mm)	2	4	6
F2	Thickness of midfoot cushion (mm)	1	3	5
F3	Thickness of arch cushion (mm)	1	4	8
F4	Height of heel cup rim (mm)	1	5	9
F5	Insole stiffness (E, v)	0.5, 0.3	5, 0.3	10, 0.3
F6	Pad (for MTHs and heel) stiffness (E, v)	0.2, 0.3	2, 0.3	4, 0.3
F7	Cushion (for proximal MTH) stiffness (E, v)	0.2, 0.3	3, 0.3	5, 0.3
F8	Cushion (for medial arch) stiffness (E, v)	0.2, 0.3	3, 0.3	5, 0.3

Since a full factorial design would require a large number of simulation trials ($3^7 = 2187$) and each simulation might take several hours for model development and computation, a fractional factorial design approach was adopted in this FE studies to establish the "most effective" insole configuration for each FE simulation. A D-optimal array consisting 16 treatment combinations of the seven 3-level design factors (Table 7-2) was generated through a built-in Matlab function "rowexch" (Franciosa at al., 2016). The algorithm involves two main steps. First, a candidate set of all feasible treatments ($3^8 =$

6561) was generated. Next, the D-optimal design matrix is generated through iterative search algorithms. This is accomplished by changing an entire row of the design matrix with a row from a candidate set of all feasible treatments to increase the model determinant (that is, to minimize the covariance of the parameter estimates) at each iteration. There is randomness built into the selection of the initial design and into the choice of the incremental changes. As a result, a local D-optimal design might be resulted. To minimize the chance of getting a local D-optimal design, the rowexch algorithm was run 10 times with different initial design selection and the best D-optimal design matrix was chosen among the 10 trials.

The 16 treatments were generated such that the main effects of each design factor can be captured through minimizing the covariance of the factor estimates. Unlike traditional designs such as the Taguchi method (Cheung and Zhang, 2008, Dar et al., 2002), D-optimal designs do not require orthogonal design matrices. This further reduces the number of treatments but the correlations between parameter estimates are not accounted for.

Table 7-2. The 16 treatment combinations (T1 – T16) selected through D-Optimal design for the design factors (F1 – F8).

	F1	F2	F3	F4	F5	F6	F7	F8
T1	1	1	3	2	2	3	1	2
T2	1	1	3	3	1	2	3	1
T3	1	2	1	1	1	1	1	3
T4	1	3	1	3	2	1	2	2
T5	1	3	2	2	3	3	2	1
T6	2	1	1	3	3	2	1	1
T7	2	1	2	1	1	3	2	2
T8	2	2	2	1	2	2	3	3
T9	2	2	3	2	1	1	2	3
T10	2	3	1	2	1	2	3	2
T11	3	1	1	2	2	2	2	3
T12	3	1	2	2	3	1	3	2
T13	3	2	1	3	2	3	3	1
T14	3	2	2	3	1	2	1	2
T15	3	2	3	1	3	2	2	2
T16	3	3	3	1	2	1	1	1

The 16 insole designs were created in SOLIDWORKS® Premium 2015 CAD system and were imported to ABAQUS for FE model generation. Through FE simulation, the forefoot peak pressure would be predicted for each design treatment. The mean effects of each level of the design factors on the forefoot plantar pressure could be computed. For example, the mean response of insole stiffness (F5) at level 1 on forefoot peak plantar pressure would be the mean values over T1, T2, T6, T8, T9, T13. For each design factor, the level attaining the lowest mean forefoot peak pressure would be selected to form the "optimal" design. A confirmation FE experiment was then carried out on the resulting optimal design to demonstrate the validity of the results emerging from the mean response analysis (Hsu et al., 2008; Franciosa at al., 2016).

To determine the sensitivity of each design factor, an analysis of variance (ANOVA) was performed to compute the sum of squares related to each factor (Cheung and Zhang, 2008) with the following equation:

$$SS_j = \sum_{i=1}^{N_l}(R_i - R_m) \qquad \forall j = 1, ..., N_f$$

Where SS_j is the sum of squares of design factor j, N_l and N_f are the number of levels and number of factor respectively, R_i is the mean response of factor j at level i. R_m is the overall mean response of the entire 16 experimental treatments.

7.6. Results

7.6.1.1. FE Model Validation

From the Pedar measurement of the same subject who volunteered 3D foot scanning for the FE foot model reconstruction, the forefoot and rear foot peak pressures were 116.3 kPa and 89.7 kPa respectively whereas the FE predicted values were 132.5 kPa

and 109.3 KPa. The differences between experimental data and FE simulation were within acceptable range when compared with similar studies (Cheung and Zhang 2008; Hsu et al., 2008). Both of measured and predicted values showed high contact pressures at the first and second metatarsal heads and the central heel region, thus confirming the reliability of the FE model. Figure 7-10 shows the coloured contour maps of the contact pressure from Pedar measurements and FE simulation.

-

(a)

(b)

Peak forefoot contact pressure

= 132.5 kPa

Peak rearfoot contact pressure

= 109.3 kPa

Peak forefoot contact pressure

= 116.3 kPa

Peak rearfoot contact pressure

= 89.7 kPa
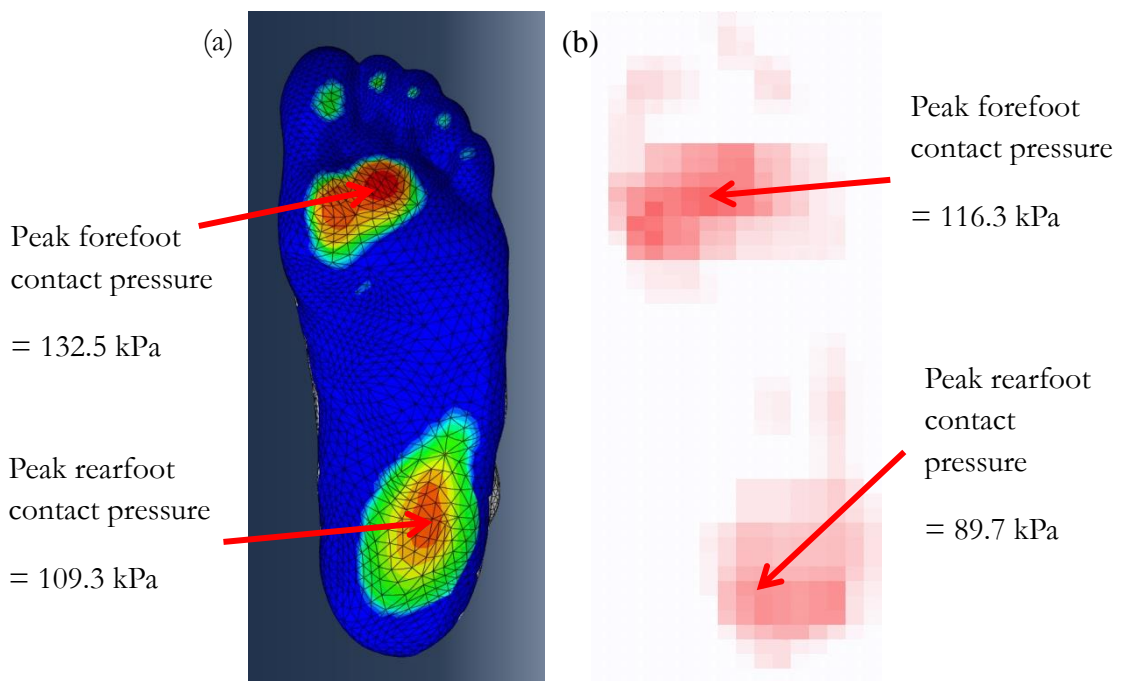
Figure 7-10. Plantar pressure distribution maps of (a) the FE simulation result and (b) the Pedar measurements for model validation

7.6.2. Design Optimization

The result of the FE simulations corresponding to the 16 design treatments are presented in Table 7-3. The highest and lowest predicted peak forefoot pressures were resulted in T1 (113.2 kPa) and T16 (95 kPa) respectively. The location of the peak

forefoot pressure was found underneath the region between the first and second metatarsal head.

Table 7-3. FE predicted peak forefoot pressures of the 16 design treatments

Design Treatments	Peak forefoot pressure (kPa)
T1	113.2
T2	109.2
T3	106.6
T4	107.3
T5	112.9
T6	105.1
T7	106.3
T8	105.7
T9	99.6
T10	103.3
T11	103.7
T12	98
T13	102.5
T14	98.4
T15	100.1
T16	95

The mean response of each level of the eight design factors are plotted in figure 7-11. Among the eight design factors, the insole thickness (F1) and the stiffness of the pads (F6) were found to be the most critical factors in forefoot plantar pressure reduction. The use of thicker insole and softer materials for the pads at MTH and heel could result a larger pressure reduction. The optimal thickness of midfoot cushion (F2) was found to be 3mm (Level 2). Increasing or decreasing this value would result in an increase in predicted peak plantar pressure. The optimal height of heel cup rim was found to be 9mm (level 3). The presence of heel cup, however, did not always improve the performance in plantar pressure reduction. A heel cup of a rim height at 5mm (level 2) did not perform better than the 1mm (level 1). Mean responses of the remaining factors, namely, arch cushion thickness (F3), insole stiffness (F5), stiffness of cushion at

proximal MTH (F7) and medial arch (F8) were not obvious. The sensitivity of each design factor on pressure reduction can be further examined through ANOVA.
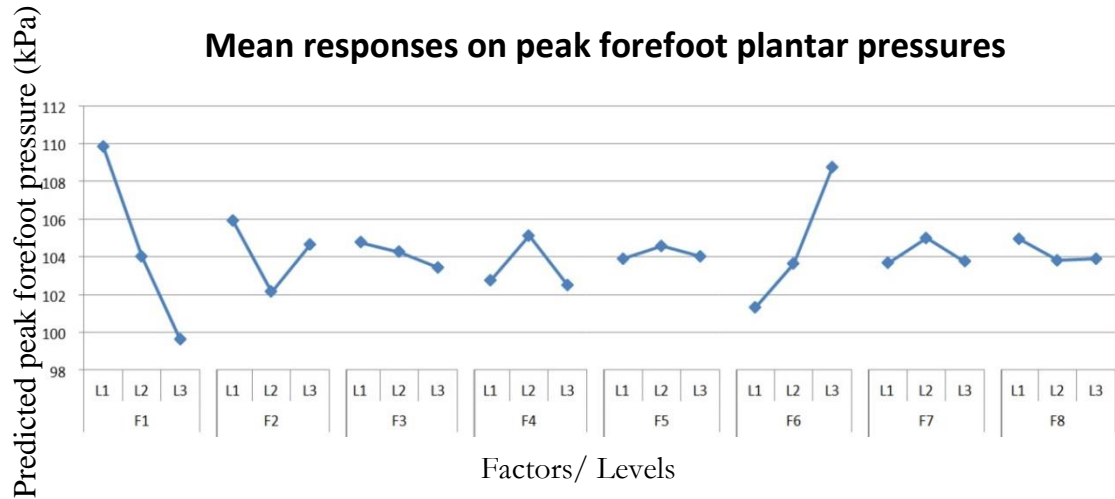
Figure 7-11. Mean responses of all levels of the design factors on peak forefoot pressures

The level that obtained the lowest predicted peak pressure in each factor was selected for the optimal design. The optimal design combination for F1 to F8 was therefore 3-2-3-3-1-1-1-2. An FE simulation was then carried out to evaluate its performance on forefoot plantar pressure reduction. The predicted peak forefoot pressure is 93.8 kPa, which is lower than any of the values resulting from the 16 treatments (please refer to Table 7-3). When compared with the predicted forefoot peak pressure (132.5kPa) during balanced standing on wooden supports without insole, the optimal design could reduce the forefoot pressure by 21.4%.

The ANOVA result presented in Table 7-4 described the sensitivity of each factor on forefoot pressure reduction. Insole thickness (F1) was identified as the most important factor ($SS = 52.9$) in forefoot plantar pressure reduction in high-heeled condition. Stiffness of the pads (F6) was found to be the 2nd most important factor ($SS = 29.2$). Thickness of arch cushion (F2) and height of rim of heel cup (F4) had minor effects

$(SS_{F2} = 10.3, SS_{F4} = 5.8)$ on plantar pressure reduction. The sensitivity of proximal MTH cushion thickness (F3), insole stiffness (F5), stiffness of cushion at proximal MTH (F7) and medial arch (F8) were negligible (SS < 1.1).

Table 7-4. ANOVA of the predicted forefoot peak pressure for the eight design factors

Factor ID	Factor	Sum of squares (SS) (kPa^2)
F1	Insole thickness (mm)	52.9
F2	Thickness of arch cushion	10.3
F3	Thickness of midfoot cushion	0.9
F4	Height of heel cup rim	5.8
F5	Insole stiffness	0.3
F6	Pad (for MTHs and heel) stiffness	29.2
F7	Proximal metatarsal cushion stiffness	1.1
F8	Arch cushion stiffness	0.8

7.7. Discussion

In this study, the pressure relieving performance of the new insole design with different structural and material configurations were evaluated using FE simulations. The optimal design could reduce forefoot pressure by 21.4%. This value was comparable to previous studies in which the peak plantar pressures were found to be reduced by 15.2% to 16.8% when 6.3mm flat insoles were used (Lemmon et al., 1997, Goske et al., 2006), and by 35.6% to 37.5% when full conformity insoles or total contact insoles where used (Chen et al., 2003; Goske et al., 2006).

The ANOVA result showed that for an insole to be used in HHS, the thickness and stiffness to the insole underneath the MTH area were the most critical factors determining its pressure relieving capability. This observation is generally in accord with previous FEM studies (Cheung and Zhang, 2008, Lemmon et al., 1997) in which an inverse relationship was identified between insole thickness and peak plantar pressure, as well as experimental studies (Luximon et al., 2014) in which the softer insole

materials were found to be able to reduce plantar pressure effectively. The presence of arch support, which had been identified as an important factor in plantar pressure reduction in many previous studies (Cheung and Zhang, 2008; Hsu et al., 2008), was not recognized as an important factor in high-heeled condition according to the FE simulation results of the present study. This might be explained by the orientation of the arch when standing in HHS. As the heel elevates, the foot is plantar-flexed and the foot arch is inclined, the body load transferred to the foot from the tibia do not reach the ground at the heel, but is further transferred to the MTH region through the inclined metatarsal shaft. Since the metatarsal shaft is inclined and no longer horizontal to the ground surface, the amount of body load (which acts vertically downward) that acts upon the shoe sole at the mid-foot region is reduced. Hence even though the arch support might increase the contact area in the midfoot region, the pressure reduction effect is not significant. The same explanation might also apply to the effectiveness of the heel cup in pressure reduction. Hence, the most effective strategy in reducing peak forefoot pressures in HHS would be to use thicker and softer materials underneath the medial MTH region. Increasing the pressure contact area by adding additional features such as arch support, and cushion at proximal MTH and heel cup to enhance the conformity of the insole is a less effective approach.

According to the FE simulation results, softer materials with Young's modulus < 2 MPa were suggested to be used in the MTH region to maximize the insole's pressure reliving capability; whilst the choice of materials in other areas is of less importance. The insole thickness, being identified as the most critical factor in determining its pressure relieving ability, is a bit more complicated when a recommended value is required. Although the FE simulations illustrated best pressure relieving capability for an insole of 6 mm thickness, it has to be noticed that the upper construction of the HHS was not included

in the simulations. In real situations, extra space might not be present in HHS to accommodate a 6 mm insole, especially when most HHS adopts "slim" designs. If the insole is too thick to be used in HHS, increased forefoot pressures (including plantar and in-shoe pressures) might be resulted. Indeed, previous studies found that the effect of insole thickness in pressure reduction become less obvious when the thickness exceed 6mm (Cheung and Zhang, 2008). Therefore, the optimal range of insole thickness would be 4mm to 6mm, according to the FE simulation result.

There were several imitations in this study. Apart from the simplifications of the structural and material properties of the bony and soft tissue structures in the FE computation, there are several assumptions that would affect the results. Firstly, the upper construction of the HHS was not included in the simulation. The foot-shoe interfacial forces, which might be particularly significant regarding the tight toe box environment in HHS, were not simulated. Secondly, only balanced standing was analysed in this study. The different foot-sole loading conditions introduced during certain gait instances such as heel strike and push off would provide a more complete picture to evaluate the effect of different insole features on pressure relief, thus worth further investigations. Lastly, in this design optimization approach, the design factors were "categorized" into 3 levels, while the design factors are actually continuous variables. The "optimal" value (level) resulted in this study might be different from the real optimal values which would lie close to the value assigned to the optimal level. Other optimization methods (such as the surface response method) can be used to search for the real optimal values.

7.8. Conclusion

Designing a new product might involve many design variables. This present study combined the use of D-Optimal design and FEM to identify the "best" combination of

design factors of an insole design that possess the best capability in forefoot pressure reduction for a specific user. The validation experiment proved the pressure relieving performance of the resulted "optimal" design and proved this method is an effective optimization approach to reduce the experimental costs in the product design stage.

The design requirements for insoles to be used in HHS were found to be different from those of insole to be used in flat-heeled condition. Insole thickness was identified as the most critical design factor, followed by the stiffness of materials to be used at the metatarsal regions. In general, softer (Young's modulus < 2 MPa) and thicker materials (4mm to 6mm) could effectively reduce peak pressures at medial metatarsal region. The effects of other insole features such as the arch support, heel cup and cushion at proximal MTH regions on forefoot pressure reduction were negligible.

Chapter 8 – Conclusion and Future Work Recommendations

8.1. Conclusions

The primary goal of this research was to design, with reference to experimental and numerical analysis, an insole with different mechanical stress-strain properties in different foot regions that could lower peak plantar pressure whilst provide adequate foot support to maintain foot stability.

The project objectives, which are discussed in detail in Section 1.3 of Chapter 1 of the study, have been realized and the achievements of the research are summarized as follows:

1. In order to identify specific high plantar pressure regions and determine the functional requirements of the insole for different foot plantar regions, a thorough evaluation on plantar pressure distribution, foot stability, and activities of selected lower extremity muscles during the use of HHSs was carried out. Twenty young female subjects participated in the study. Four heel height conditions (1cm, 5cm, 8 cm and 10 cm) covering the most common heel range were tested. Muscles activities of rectus femoris (RF), vastus lateralis (VL), vastus medialis (VM), peroneous longus (PL), tibialis anterior (TA) and medial gastrocnemius (MG) were found to increase with heel height in both balanced stance and single-leg stance, suggesting that extra efforts were required to maintain body balance in HHS. From the pressure measurements taken from the Pedar®-X insole measuring system, the plantar pressure distribution during quiet standing and normal walking were found to change significantly in HHS in comparison to flat-heeled shoes. During quiet standing, the toes and metatarsal region was found to bear nearly 60% of the body weight at 10 cm heels, which was almost a double when compared to the flat-heeled condition. The peak and mean plantar pressures in the medial and centre metatarsal

regions were found to increase significantly (>100% increase) in high-heeled conditions. When walking in 10 cm high-heeled shoes, the pressure contact area decreased significantly in the mid and rear-foot. These findings suggested that highly pressure relieving materials are necessary to cushion the forefoot area, while an arch cushion and a heel cup could help increasing the contact area in the rearfoot and thus maximize the pressure redistribution ability of the new insoles.

Through the examination of trajectories of centre of pressure (COP), the use of HHS was found to worsen foot stability in quiet standing as the variations of COP in both antero-posterior (AP) and medio-lateral (ML) directions increased with heel height. The adverse effects starts to accentuate when heel height reaches 8cm and become even worse at 10cm. High heel experience, however, appears to help maintaining one's postural control in high heeled conditions. The foot stability analysis also presented a method to quantify and analyse walking stability. By constructing a mean curve of the centre of pressure in ML direction (COPx) during the stance phase, the pattern of COPx progression, the intra-subject COPx variability among strides, and thus the walking stability could be determined.

2. A 3D foot and ankle imaging system was developed to study female foot anthropometry in heel-elevated postures. The high resolution scans acquired by the system allowed fine details to be recorded. The short capture time (within 1 second) minimized measurement errors introduced by unintentional body sways. After validating the accuracy and reliability of the system, foot anthropometric data of fifty young female subjects were collected by using the system. To the best of my knowledge, this foot anthropometric study was the first to focus on forefoot measurements with different heel heights. The shape characteristics of the forefoot, as illustrated by the various length, width and height measurements, were shown to change with different heel elevations. The most obvious observation is a wider toe

174

spread in the horizontal plane, indicating that slight compensations might be required in the toe box design when fabricating shoes of different heel heights, especially in the metatarsal-phalangeal joint regions of the fourth and fifth toes and the distal interphalangeal region of the hallux and second toes. The anthropometric data depicted how the foot morphology changes with increasing heel elevations and provided a scientific basis for the geometric design parameters of the new insole.

3. Based on the results from the biomechanical study, several insole features were suggested: (1) medial forefoot (MTHs 1-3) and heel are areas of peak pressures. Pads with softer material can be used for greatest effect of pressure relief. Harder and more durable materials can be used for rest of foot zones to provide adequate foot support and reduce deformation over time; (2) Cushions can be added in the arch and midfoot to increase the weight -bearing contact area for better pressure redistribution effect; (3) the presence of a heel cup might enhance foot stability in the ML direction.

4. The effects of different insole design parameters (insole geometries, material properties) on plantar pressure relief were analysed through FEM. Eight design factors including insole thickness, thickness of cushions at midfoot and arch, height of rim of heel cup, insole stiffness, stiffness of pads for MTH and heel, and stiffness of cushions at midfoot and arch presence of arch were evaluated. Three levels were assigned for each factor. Through applying the techniques of fractional factorial design, a set of 16 designs was generated with combinations of different levels of each design parameters. The sensitivity of each design parameter on pressure relief was evaluated.

5. Results of the FEA showed that thicker and softer materials (Young's modulus < 2 MPa) to be used underneath the MTH region could effectively reduce the forefoot peak pressures at medial metatarsal region. The optimal range of insole thickness is

4mm to 6mm. Effects of the heel cup and arch support were of less importance. The mean effects of the remaining design factors, namely, thickness of midfoot cushion, insole stiffness, midfoot and medial arch cushion stiffness on plantar pressure reduction were negligible.

The research enhanced our knowledge on female foot morphology in heel-elevated postures and provided useful information for the selection of suitable materials for insoles to be used in HHS. Having demonstrated satisfactory repeatability and accuracy, the newly developed 3D imaging system could be adopted in other anthropometric studies. The simulation model provided numerical solutions to evaluate the effects of different insole parameters on the pressure distribution in high-heeled condition, optimising the effectiveness of the new insole design. The output of the study could extend to the development of other customized insoles and inserts.

8.2. Limitations of the study

Some of the limitations of this study that limit the generalization of the results are listed as follows:

1. Although it is suggested in the literature that the height of heels being frequently worn by regular HHS wearers might have impacts on the degree of chronic adaptation, to recruit regular HHS wearers who wear HHS (> 8cm heel) frequently is difficult.
2. Steppage gait was found in some of non-regular HHS wearers in 10cm heel condition, making it difficult to differentiate different stages of the stance phase base on the variations of plantar measurements at different plantar regions as suggested in literatures.

3. Due to the limitations of the instrumentation, EMG and plantar measurements were not synchronized. Synchronized COP measurements and EMG signal would allow better understanding of the use of leg muscles on balance control in AP and ML directions.

8.3. Recommendations for Future Work

A few recommendations for future work based on the established research findings are provided as follows:

1. Geometries of the plantar in plantar-flexed position and weight-bearing condition were not measured in this study. As a better understanding of the plantar shape in heel-elevated position could improve the footbed design of HHS, further research work is required.

2. 3D motion analysis might be carried out in accordance with COP and muscle activities measurements to examine the balance control strategies adopted in high-heeled condition.

3. FE models that simulate different loading conditions at different stages of the stance phase such as heel strike and push off can be developed to predict the effects of the design parameters on plantar pressure relief during gait.

4. FE simulations with specific insole materials as well as their structure (such as honeycomb, nodule designs) can be carried out to predict their performance on plantar pressure reduction in high-heeled conditions.

5. Upper part of the HHS can be added to the FE model to evaluate the interfacial stresses on forefoot within the toe-box.

References

Adrian, M. J., and Karpovich, P. V. (1966). Foot instability during walking in shoes with high heels. *Research Quarterly. American Association for Health, Physical Education and Recreation*, *37*(2), 168-175.

Abu-Bader, S. (2010). Advanced and multivariate statistical methods for social science research with a complete SPSS guide. Chicago, Ill.: Lyceum Books.

American Podiatric Medical Association. Public Opinion Research on Foot Health and Care (2014) https://www.apma.org/files/APMA2014TodaysPodiatristSurveyAllFindin gs.pdf

Antunes, P., Dias, G., Coelho, A., Rebelo, F., and Pereira, T. (2008). Hyperelastic modelling of cork-polyurethane gel composites: non-linear FEA implementation in 3D foot model. *Material Science Forum*, 4. 700-705.

Bae, Y. H., Ko, M., Park, Y. S., and Lee, S. M. (2015). Effect of revised high-heeled shoes on foot pressure and static balance during standing. *Journal of physical therapy science*, *27*(4), 1129-1131.

Barani, Z., Haghpanahi, M., and Katoozian, H. (2005). Three dimensional stress analysis of diabetic insole: a finite element approach. *Technology and Health Care-European Society for Engineering and Medicine*, *13*(3), 185-192.

Barisch-Fritz, B., Schmeltzpfenning, T., Plank, C., and Grau, S. (2014). Foot deformation during walking: differences between static and dynamic 3D foot morphology in developing feet. *Ergonomics*, *57*(6), 921-933.

Barnicot, N. A., and Hardy, R. H. (1955). The position of the hallux in West Africans. *J. Anat.*, 89: 355-361, 1955

Beauchet, O., Annweiler, C., Lecordroch, Y., Allali, G., Dubost, V., Herrmann, F. R., and Kressig, R. W. (2009). Walking speed-related changes in stride time variability: effects of decreased speed. *Journal of neuroengineering and rehabilitation*, *6*(1), 32.

Bendix, T. S., Sørensen, S., and Klausen, K. (1984). Lumbar Curve, Trunk Muscles, and Line of Gravity with Different Heel Heights. *Spine*, 9(2), 223.

Blanchette, M. G., Brault, J. R., and Powers, C. M. (2011). The influence of heel height on utilized coefficient of friction during walking. *Gait and posture*, *34*(1), 107-110.

Branthwaite, H., Chockalingam, N., and Greenhalgh, A. (2013). The effect of shoe toe box shape and volume on forefoot interdigital and plantar pressures in healthy females. *Journal of foot and ankle research*, *6*(1), 28.

Braune, W., and Fischer, O. (1987). *The human gait*. Berlin ; New York: Springer-Verlag.

Brodsky, J., Pollo, F., Cheleuitte, D., and Baum, B. (2007). Physical properties, durability, and energy-dissipation function of dual-density orthotic materials used in insoles for diabetic patients. *Foot and Ankle International*, 28(8): 880-889.

Campbell, G., Newell, E., and McLure, M. (1982). Compression testing of foamed plastics and rubbers for use as orthotic shoe insoles. *Prosthetics and Orthotics International*, 6(1): 48-52.

Carlson, J., Coulter, J., and Duclos, T. (1990). *Patent No. 4,923,057.* US.

Carroll M, Annabell M E, Rome K. (2011). Reliability of capturing foot parameters using digital scanning and the neutral suspension casting technique. *Journal of Foot and Ankle Research* 2011, 4:9

Che, H., Nigg, B. M., and De Koning, J. (1994). Relationship between plantar pressure distribution under the foot and insole comfort. *Clinical Biomechanics*, *9*(6), 335-341.

Chen, G. X. (2005). *The Last Design*, China Light Industry Press, Beijing. (In Chinese)

Chen MJL, Chen CPC, Lew HL, Hsieh WC, Yang WP, and Tang SFT. (2003). Measurement of forefoot varus angle by laser technology in people with flexible forefoot. *Am J Phys Med Rehabil, 2003;83:842-846.*

Chen, W. M., Lee, S. J., and Lee, P. V. S. (2014). The in vivo plantar soft tissue mechanical property under the metatarsal head: implications of tissues' joint-angle dependent response in foot finite element modeling. *Journal of the mechanical behavior of biomedical materials*, *40*, 264-274.

Chen, W. P., Ju, C. W., and Tang, F. T. (2003). Effects of total contact insoles on the plantar stress redistribution: a finite element analysis. *Clinical Biomechanics*, *18*(6), S17-S24.

Chien, H. L., Lu, T. W., and Liu, M. W. (2013). Control of the motion of the body's center of mass in relation to the center of pressure during high-heeled gait. *Gait and posture*, *38*(3), 391-396.

Chu, T. M., Reddy, N. P., and Padovan, J. (1995). Three-dimensional finite element stress analysis of the polypropylene, ankle-foot orthosis: static analysis. *Medical engineering and physics*, 17(5), 372-379.

Cheung, J., and Zhang, M. (2005). A 3-Dimensional finite element model of the human foot and ankle for insole design. Arch Phys Med Rehabil, 86. 353-358.

Cheung, J., and Zhang, M. (2008). Parametric design of pressure-relieving foot orthosis using statistics-based finite element method. *Medical Engineering Physics*, 30(3):269-277.

Cho, W., & Choi, H. (2005). Center of pressure (COP) during the Postural Balance Control of High-Heeled Woman. *Conference Proceedings: Annual International Conference of the IEEE Engineering in Medicine and Biology Society. IEEE Engineering in Medicine and Biology Society. Annual Conference*, 3, 2761-4.

Cobey, J. C., and Sella, E. (1981). Standardizing methods of measurement of foot shape by including the effects of subtalar rotation. *Foot and Ankle*, 2(1), 30-36.

Cong, Y., Cheung, J. T. M., Leung, A. K., and Zhang, M. (2011). Effect of heel height on in-shoe localized triaxial stresses. *Journal of Biomechanics*, 44(12), 2267-2272.

Corner, B. D., and Hu, A. (1998, March). Effect of sway on image fidelity in whole-body digitizing. In *Three-Dimensional Image Capture and Applications* (Vol. 3313, pp. 90-100). International Society for Optics and Photonics.

Corrigan J. P., Moore D. P., Stephens M. M. (1993) Effect of heel height on forefoot loading. *Foot and Ankle International* 1993; 14:148–152.

Coughlin, M. J. (1995). Women's shoe wear and foot disorders. *Western Journal of Medicine*, 163(6), 569.

Cowley, E. E., Chevalier, T. L., and Chockalingam, N. (2009). The effect of heel height on gait and posture: a review of the literature. *Journal of the American Podiatric Medical Association*, 99(6), 512-518.

Crabtree, P., Dhokia, V., Ansell, M. and Newman, S. (2008). Design and manufacturing of customized orthotic for sporting application. *The Engineering of Sport 7* (1 ed., pp. 309-317). Paris: Springer Paris.

Crabtree, P., Dhokia, V.G., Newman, S.T. and Ansell, M.P. (2009). Manufacturing methodology for personalised symptom-specific sports insoles. *Robotic and Computer-Integrated Manufacturing*, 25(6), 972-979.

Creaby, M. W., May, K., and Bennell, K. L. (2011). Insole effects on impact loading during walking. *Ergonomics*, 665-671.

Cronin, N. J., Barrett, R. S., and Carty, C. P. (2012). Long-term use of high-heeled shoes alters the neuromechanics of human walking. *Journal of Applied Physiology*, 112(6), 1054-1058.

Cronin, N. J. (2014). The effects of high heeled shoes on female gait: a review. *Journal of Electromyography and Kinesiology*, 24(2), 258-263.

Csapo, R., Maganaris, C. N., Seynnes, O. R., and Narici, M. V. (2010). On muscle, tendon and high heels. *The Journal of Experimental Biology*, *213*(15), 2582-2588.

Dahlberg, G., and Lander, E. (1950). Size and form of the foot in men. *Human Heredity*, *1*(2), 115-162.

Dar, F. H., Meakin, J. R., and Aspden, R. M. (2002). Statistical methods in finite element analysis. *Journal of Biomechanics*, *35*(9), 1155-1161.

de Lateur, B. J., Giaconi, R. M., Questad, K. F., Ko, M., and Lehmann, J. (1991). FOOTWEAR AND POSTURE: Compensatory Strategies for Heel Height. *American Journal of Physical Medicine and Rehabilitation*, 70(5), 246-254.

de Oliveira Pezzan, P. A., João, S. M. A., Ribeiro, A. P., and Manfio, E. F. (2011). Postural assessment of lumbar lordosis and pelvic alignment angles in adolescent users and nonusers of high-heeled shoes. *Journal of Manipulative and Physiological Therapeutics*, *34*(9), 614-621.

do Nascimento, N. I. C., Saraiva, T. S., da Cruz Jr, A. T. V., da Silva Souza, G., and Callegari, B. (2014). Barefoot and high-heeled gait: changes in muscles activation patterns. *Health*, *6*(16), 2190-2196.

Ebbeling, C. J., Hamill, J., and Crussemeyer, J. A. (1994). Lower extremity mechanics and energy cost of walking in high-heeled shoes. *Journal of Orthopaedic and Sports Physical Therapy*, *19*(4), 190-196.

Erdemir, A., Saucerman, J. J., Lemmon, D., Loppnow, B., Turso, B., Ulbrecht, J. S., and Cavanagh, P. R. (2005). Local plantar pressure relief in therapeutic footwear: design guidelines from finite element models. *Journal of Biomechanics*, *38*(9), 1798-1806.

Esenyel, M., Walsh, K., Walden, J. G., and Gitter, A. (2003). Kinetics of high-heeled gait. *Journal of the American Podiatric Medical Association*, *93*(1), 27-32.

Foster, A., Blanchette, M. G., Chou, Y. C., and Powers, C. M. (2012). The influence of heel height on frontal plane ankle biomechanics: implications for lateral ankle sprains. *Foot and Ankle International*, *33*(1), 64-69.

Franciosa, P., Gerbino, S., Lanzotti, A., and Silvestri, L. (2013). Improving comfort of shoe sole through experiments based on CAD-FEM modeling. *Medical Engineering Physics*, 35, 36-46.

Freedman, A., Huntington, E. C., Davis, G. C., Magee, R. B., Milstead, V. M., and Kirkpatrick, C. M. (1946). Foot dimensions of soldiers (Third Partial Report Project No. T-13). *Armored Medical Research Laboratory, Fort Knox, Kentucky*.

Frey, C. (2000). Foot health and shoewear for women. *Clinical Orthopaedics and Related Research*, *372*, 32-44.

Frey, C., Thompson, F., Smith, J., Sanders, M., and Horstman, H. (1993). American Orthopaedic Foot and Ankle Society women's shoe survey. *Foot and Ankle*, *14*(2), 78-81.

Gefen, A., Megido-Ravid, M., Itzchak, Y., and Arcan, M. (2002). Analysis of muscular fatigue and foot stability during high-heeled gait. *Gait Posture*, 15. 56-63.

Gerber, S. B., Costa, R. V., Grecco, L. A. C., Pasini, H., Corrêa, J. C. F., Lucareli, P. R. G., ... and Oliveira, C. S. (2012). Interference of high-heel shoes in static balance among young women. *Gait and Posture*, *36*, S58-S59.

Ghassemi, A., Mossayebi, A. R., Jamshidi, N., Naemi, R., and Karimi, M. T. (2015). Manufacturing and finite element assessment of a novel pressure reducing insole for Diabetic Neuropathic patients. *Australasian physical and engineering sciences in medicine*, *38*(1), 63-70.

Goonetilleke, R. (1999). Footwear Cushioning: Relating Objective and Subjective Measurements. *Human Factors: The Journal of Human Factors and Ergonomics Society*, 41(2), 241-256.

Goonetilleke, R. (2012). *Human Factors and Ergonomics: The Science of Footwear*. Baton Rouge: CRC Press.

Goske, S., Erdemir, A., Petre, M., Budhabhatti, S., and Cavanagh. P. R. (2006). Reduction of plantar heel pressures: Insole design using finite element analysis. *Journal of Biomechanics*, 39(13), 2363-2370.

Guéguen, N. (2015). High heels increase women's attractiveness. *Archives of Sexual Behavior*, 44(8), 2227-2235.

Guldemond, N.A., Leffers, P., Sanders, A.P., Emmen, H., Schaper, N.C. and Walenkamp, G.H.I.M. (2006). Casting methods and plantar pressure- effects of custom-made foot orthoses on dynamic plantar pressure distribution. *Journal of the American Podiatric Medical Association*, 96(1), 9-18.

Guo, L. Y., Lin, C. F., Yang, C. H., Hou, Y. Y., Liu, H. L., Wu, W. L., and Lin, H. T. (2012). Effect on plantar pressure distribution with wearing different base size of high-heel shoes during walking and slow running. *Journal of Mechanics in Medicine and Biology*, *12*(01), 1250018.

Guskiewicz, K. M., and Perrin, D. H. (1996). Research and clinical applications of assessing balance. *Journal of Sport Rehabilitation*, *5*(1), 45-63.

Han, T. R., Paik, N. J., and Im, M. S. (1999). Quantification of the path of center of pressure (COP) using an F-scan in-shoe transducer. *Gait and Posture*, *10*(3), 248-254.

Hapsari, V. D., and Xiong, S. (2016). Effects of high heeled shoes wearing experience and heel height on human standing balance and functional mobility. *Ergonomics*, *59*(2), 249-264.

Hawke L. F., Burns J., J. A .Radford, and du Toit V. (2008) Custom-made foot orthotics for the treatment of foot pain. *Cochrane Database Syst Rev*, 2008;16:CD006801.

Hawes, M. R., and Sovak, D. (1994). Quantitative morphology of the human foot in a North American population. *Ergonomics*, *37*(7), 1213-1226.

Hawes, M. R., Sovak, D., Miyashita, M., Kang, S. J., Yoshihuku, Y., and Tanaka, S. (1994). Ethnic differences in forefoot shape and the determination of shoe comfort. *Ergonomics*, 37(1), 187-196.

Heikkilä, J. and Silvén, O (1997). A Four-step Camera Calibration Procedure with Implicit Image Correction. *IEEE Computer Society Conference on Computer Vision and Pattern Recognition* (CVPR'97), San Juan, Puerto Rico, p. 1106-1112.

Hermens, H., Commission of the European Communities. Biomedical Health Research Programme, and SENIAM project. (1999*). European recommendations for surface electromyography: Results of the SENIAM project (2nd ed*.). The Netherlands: Roessingh Research and Development.

Hong, W. H., Lee, Y. H., Lin, Y. H., Tang, S. F., and Chen, H. C. (2013). Effect of shoe heel height and total-contact insert on muscle loading and foot stability while walking. *Foot and Ankle International*, *34*(2), 273-281.

Hong, Y., Wang, L., Xu, D., and Li, J. (2011). Gender differences in foot shape: A study of Chinese young adults. *Sports Biomechanics*, 10(2), 85-97.

Hoogvliet, P., van Duyl, W. A., de Bakker, J. V., Mulder, P. G., and Stam, H. J. (1997). A model for the relation between the displacement of the ankle and the center of pressure in the frontal plane, during one-leg stance. *Gait and Posture*, *6*(1), 39-49.

Hotter Shoes. 2010. Online Research Report. "Hotter Shoes Survey Reveals Women Fall for Killer Heels." Accessed 22 Feb 2018. http://www.prnewswire.com/news-releases/hotter-shoes-survey-reveals-women-fall-for-killer-heels-107499643.html

Houston, V. L., Luo, G., Mason, C. P., Mussman, M., Garbarini, M., and Beattie, A. C. (2006). Changes in male foot shape and size with weightbearing. *Journal of the American Podiatric Medical Association*, *96*(4), 330-343.

Hsu, Y., Gung, Y., Shih, S., Feng, C., Wei, S., Yu, C., and Chen, C. (2008). Using an optimization approach to design an insole for lowering plantar fascia stress — a finite element study. *Annals of Biomedical Engineering*, 36. 1345-1352.

Hyun, S. H., Kim, Y. P., and Ryew, C. C. (2016). Effect on the parameters of the high-heel shoe and transfer time of ground reaction force during level walking. *Journal of Exercise Rehabilitation*, 12(5), 451.

JezerĹĄek, M., and MoĹžina, J. (2009). High-speed measurement of foot shape based on multiple-laser-plane triangulation. *Optical Engineering*, *48*(11), 113604-113604.

Jordan, C., Payton, C., and Bartlett, R. (1997). Perceived comfort and pressure distribution in casual footwear. *Clinical Biomechanics (Bristol, Avon)*, *12*(3), S5-S5.

Kang, H. G., and Dingwell, J. B. (2006). A direct comparison of local dynamic stability during unperturbed standing and walking. *Experimental Brain Research*, *172*(1), 35.

Kerrigan, D., Todd, M., and Riley, P. (1998). Knee osteoarthritis and HHS. *The Lancet*, 351. 1355-1401.

Kim, Y., Lim, J., and Yoon, B. (2013). Changes in Ankle Range of Motion and Muscle Strength in Habitual Wearers of High-Heeled Shoes. *Foot and Ankle International*, 34(3), 414-419.

Kim, K., Chen, Y. J., Tu, H. T., Peng, H. T., and Song, C. Y. (2017). Effect of fore-medially pitted high-heeled shoes modification on foot pressure during standing and walking. *Footwear Science*, *9*(sup1), S84-S86.

Ko, P. H., Hsiao, T. Y., Kang, J. H., Wang, T. G., Shau, Y. W., and Wang, C. L. (2009). Relationship between plantar pressure and soft tissue strain under metatarsal heads with different heel heights. *Foot and Ankle International*, *30*(11), 1111-1116.

Konrad, P. (2006). The abc of emg (version 1.4). *A practical introduction to kinesiological electromyography*, *1*, 30-35.

Kouchi, M., and Tsutsumi, E. (2000). 3D foot shape and shoe heel height. *Anthological Science*, 108(4): 331-343.

Krauss I., Grau S., Mauch M., Maiwald C., and Horsemann T. (2008). Sex-related differences in foot shape. *Ergonomics*, 2008;51:1693-1709.

Lam, S. F., and Hodgson, A. R. (1958). A comparison of foot forms among the non-shoe and shoe-wearing Chinese population. *JBJS*, *40*(5), 1058-1062.

Lam, YN, Yick, KL, Ng, SP, Leung, DM, and Yeung, KL. (2014). Plantar pressure distribution and perceived comfort with elevated heel heights during standing and walking. PolyU IRA, 722-728.

Le Clair, K., and Riach, C. (1996). Postural stability measures: what to measure and for how long. *Clinical Biomechanics*, *11*(3), 176-178.

Lee, C. M., Jeong, E. H., and Freivalds, A. (2001). Biomechanical effects of wearing high-heeled shoes. *International Journal of Industrial Ergonomics*, *28*(6), 321-326.

Lee, K., and Hong, W. (2005). Effects of shoe inserts and heel height on foot pressure, impact force, and perceived comfort during walking. *Applied Ergonomics*, 36, 355-362.

Lee, Y. C., Lin, G., and Wang, M. J. J. (2014). Comparing 3D foot scanning with conventional measurement methods. *Journal of Foot and Ankle Research*, *7*(1), 44.

Lemmon, D., Shiang, T. Y., Hashmi, A., Ulbrecht, J. S., and Cavanagh, P. R. (1997). The effect of insoles in therapeutic footwear—a finite element approach. *Journal of Biomechanics*, *30*(6), 615-620.

Levine, D., Richards, J., and Whittle, M. (2012). *Whittle's gait analysis* (5th ed.). Edinburgh ; New York: Churchill Livingstone/Elsevier.

Lewis, G., Tan, T., and Shiue, Y. (1991). Characterization of the performance of shoe insert materials. *Journal of the American Podiatric Medical Association*, 81(8): 418-424.

Li, Y., and Dai, X. (2006). *Biomechanical Engineering of Textiels and Clothing.* CRC Press, Woodhead Publishing.

Liederbach, M. (2014). Ankle sprain rate differences between dancers and athletes: Shoe heel height effects on landing biomechanics. *Medicine and Science in Sports and Exercise*, 46(5), 416-416.

Linder, M., and Saltzman, C. L. (1998). A history of medical scientists on high heels. *International Journal of Health Services*, *28*(2), 201-225.

Lord, S., and Bashford, G. M. (1996). Shoe Characteristics and Balance in Older Women. *Journal of the American Geriatrics Society*, 44(4), 429-433.

Luo, G., Houston, V. L., Mussman, M., Garbarini, M., Beattie, A. C., and Thongpop, C. (2009). Comparison of male and female foot shape. *Journal of the American Podiatric Medical Association*, 99(5), 383-390.

Luximon, A. and Goonetilleke, R. (2004). Foot shape modelling. *Human Factors*, 46:304-315.

Luximon, A., Goonetilleke, R., Tsui K.(2010). Foot landmarking for footwear customization. *Ergonomics*, 2003, VOL. 46, NO. 4, 364 ± 383

Luximon, A., and Luximon, Y. (2013). Shoe-last design templates. In Luximon, A.. *Handbook of Footwear Design and Manufacture* (pp. 217-235). Woodhead Publishing Ltd.

Luximon, Y., Yu, J., and Zhang, M. (2014). A Comparison of Metatarsal Pads on Pressure Redistribution in High Heeled Shoes. *Research Journal of Textile and Apparel*, 18(2), 40-48.

Luximon, Y., Cong, Y., Luximon, A., and Zhang, M. (2015). Effects of heel base size, walking speed, and slope angle on center of pressure trajectory and plantar pressure when wearing high-heeled shoes. *Human Movement Science*, *41*, 307-319.

Mandato, M. G., and Nester, E. (1999). The effects of increasing heel height on forefoot peak pressure. *Journal of the American Podiatric Medical Association*,*89*(2), 75-80.

Manna, I., Pradhan, D., Ghosh, S., Kumar Kar, S., and Dhara, P. (2001). A comparative study of foot dimension between adult male and female and evaluation of foot hazards due to using of footwear. *Journal of Physiological Anthropology and Applied Human Science*, *20*(4), 241-246.

Mauch M., Grau S., Krauss I., Maiwald C. and Horstmann T. (2008). Foot morphology of normal, underweight and overweight children. *International Journal of Obesity* (2008) 32, 1068–1075

Mauch M., Grau S., Krauss I., Maiwald C., and Horsemann T. (2009). A new approach to children's footwear based on foot type classification. *Ergonomics*, 2009;52:999-1008.

McBride, I., Wyss, U., Cooke, T., Murphy, L., Phillips, J., and Onley, S. (1991). First matatarsophangeal joint reaction forces during high-heel gait. *Foot and Ankle*, 11(5) 282-288.

Menz, H., and Lord, S. (1999). Footwear and postural stability in older people. *Journal of the American Podiatric Medical Association*, 89(7), 346-57.

Menz, H. B., and Morris, M. E. (2005). Footwear characteristics and foot problems in older people. *Gerontology*, *51*(5), 346-351.

Mika, A., Oleksy, Ł., Mika, P., Marchewka, A., and Clark, B. C. (2012a). The influence of heel height on lower extremity kinematics and leg muscle activity during gait in young and middle-aged women. *Gait and Posture*, *35*(4), 677-680.

Mika, A., Oleksy, L., Mika, P., Marchewka, A., and Clark, B. C. (2012b). The effect of walking in high-and low-heeled shoes on erector spinae activity and pelvis kinematics during gait. *American Journal of Physical Medicine and Rehabilitation*, *91*(5), 425-434.

Mittlemeier, T. W. F., and Morlock, M. (1993, February). Pressure distribution measurements in gait analysis: dependency on measurement frequency. In *39th annual meeting of the Orthopaedic Research Society*.

Neumann, D. (2010). *Kinesiology of the musculoskeletal system: Foundations for rehabilitation* (2nd ed.). St. Louis, Mo.: Mosby/Elsevier.

Nyska, M., McCabe, C., Linge, K., and Klenerman, L. (1996). Plantar Foot Pressures During Treadmill Walking with High-Heel and Low-Heel Shoes. *Foot and Ankle International*, 17(11), 662-666.

Opila-Correia, K. A. (1990). Kinematics of high-heeled gait. *Archives of Physical Medicine and Rehabilitation*, *71*(5), 304-309.

Opila-Correia, K. A. (1990b). Kinematics of high-heeled gait with consideration for age and experience of wearers. *Archives of Physical Medicine and Rehabilitation*, *71*(11), 905-909.

Opila, K. A., Wagner, S. S., Schiowitz, S., and Chen, J. (1988). Postural alignment in barefoot and high-heeled stance. *Spine*, *13*(5), 542-547.

Orlin, M. N., and McPoil, T. G. (2000). Plantar pressure assessment. *Physical Therapy*, *80*(4), 399-409.

Owings, T. M., and Botek, G. (2012). *Human Factors and Ergonomics : The Science of Footwear.* (pp.291-307) Baton Rouge: CRC Press.

O'Connell, A. L. (1958). Electromyographic study of certain leg muscles during movements of the free foot and during standing. *American Journal of Physical Medicine and Rehabilitation*, *37*(6), 289-301.

Patil, K. M., Braak, L. H., and Huson, A. (1993). Stresses in a simplified two dimensional model of a normal foot: A preliminary analysis. *Mechanics Research Communications*, *20*(1), 1-7.

Paton, J., Jones, R., Stenhouse, E., and Bruce, G. (2007). The physical characteristics of materials used in the manufacture of orthoses for patients with diabetes. *Foot and Ankle International*, 28(10): 1057-1063.

Payne C. (2007) Cost Benefit comparison of plaster casts and optical scans of the foot for the manufacture of footorthoses. *Aust J Podiat Med*, 2007; 41(2):29-31.

Peng, X., and Cao, J. (2002). A dual homogenization and finite element approach for material characterization of textile composites. *Composites Part B: Engineering*, *33*(1), 45-56.

Perry, J., and Burnfield, J. (2010). *Gait analysis : Normal and pathological function* (2nd ed.). Thorofare, NJ: SLACK.

Pfeiffer M, Kotz R, Ledl T, Hauser G, Sluga M (2006). Prevalence of flat foot in preschool-aged children. *Pediatrics* 2006, 118:634-639.

Prieto, T. E., Myklebust, J. B., Hoffmann, R. G., Lovett, E. G., and Myklebust, B. M. (1996). Measures of postural steadiness: differences between healthy young and elderly adults. *IEEE Transactions on Biomedical Engineering*, *43*(9), 956-966.

Psikuta, A., Frackiewicz-Kaczmarek, J., Mert, E., Bueno, M. A., & Rossi, R. M. (2015). Validation of a novel 3D scanning method for determination of the air gap in clothing. *Measurement*, *67*, 61-70.

Qiu, T. X., Teo, E. C., Yan, Y. B., and Lei, W. (2011). Finite element modeling of a 3D coupled foot–boot model. *Medical Engineering and Physics*, *33*(10), 1228-1233.

Rao, K. R., and Yip, P. (2014). Discrete cosine transform: algorithms, advantages, applications. *Academic press*.

Robinson, J. R., Frederick, E. G., and Cooper, L. B. (1984). Running participation and foot dimensions. *Medicine and Science in Sports and Exercise, 16*(2), 200.

Rossi WA (1983). The high incidence of mismated feet in the population. *Foot and Ankle* 1983 Sep-Oct; 4(2):105-12.

Ruhe, A., Fejer, R., and Walker, B. (2010). The test–retest reliability of centre of pressure measures in bipedal static task conditions–a systematic review of the literature. *Gait and Posture*, *32*(4), 436-445.

Saghazadeh, M., Kitano, N., and Okura, T. (2015). Gender differences of foot characteristics in older Japanese adults using a 3D foot scanner. *Journal of Foot and Ankle Research*, *8*(1), 29.

Sarikhani, A., Motalebizadeh, A., Asiaei, S., and Kamali Doost Azad, B. (2016). Studying maximum plantar stress per insole design using foot CT-Scan images of hyperelastic soft tissues. *Applied Bionics and Biomechanics*, *2016*.

Schmeltzpfenning, T., Plank, C., Krauss, I., Aswendt, P., and Grau, S. (2009). Dynamic foot scanning: A new approach for measurement of the human foot shape while walking.

Schwartz, R. P., Heath, A. L., Morgan, D. W., and Towns, R. C. (1964). A quantitative analysis of recorded variables in the walking pattern of" normal" adults. *JBJS*, *46*(2), 324-334.

Shimizu M., and Andrew, P. D. (1999). Effect of Heel Height on the Foot in Unilateral Standing. *Journal of Physical Therapy Science*, 11(2), 95-100.

Silvino, N., Evanski, P.M., and Waugh, T.R. (1980). The Harris and Beath foot printing mat: diagnostic validity and clinical use. *Clinical Orthopaedics and Related Research*, 151, 265–269.

Simonsen, E. B., Svendsen, M. B., Nørreslet, A., Baldvinsson, H. K., Heilskov-Hansen, T., Larsen, P. K., ... and Henriksen, M. (2012). Walking on high heels changes muscle activity and the dynamics of human walking significantly. *Journal of Applied Biomechanics*, *28*(1), 20-28.

Smith, E. O., and Helms, W. S. (1999). Natural selection and high heels. *Foot and Ankle International*, *20*(1), 55-57.

Snow, R. E., Williams, K. R., Holmes G (1992) The effects of wearing high-heeled shoes on pedal pressure in women. *Foot and Ankle* 1992; 13:85-92

Snow, R. E., and Williams, K. R. (1994). High heeled shoes: their effect on center of mass position, posture, three-dimensional kinematics, rearfoot motion, and ground reaction forces. *Archives of Physical Medicine and Rehabilitation*, *75*(5), 568-576.

Lee, S., Wang, L., and Li, J. X. (2016). Effect of Asymmetrical Load Carrying on Joint Kinetics of the Lower Extremity During Walking in High-Heeled Shoes in Young Women. *Journal of the American Podiatric Medical Association*, *106*(4), 257-264.

Speksnijder CM, R. Munckhof, S. Moonen, G. Walenkamp (2005). The higher the heel the higher the forefoot-pressure in ten healthy women.*The Foot,* 15.17-21.

Stefanyshyn, D. J., Nigg, B. M., Fisher, V., O Flynn, B., and Liu, W. (2000). The influence of high heeled shoes on kinematics, kinetics, and muscle EMG of normal female gait. *Journal of Applied Biomechanics*, *16*(3), 309-319.

Thompson, F. M., and Coughlin, M. J. (1994). The high price of high-fashion footwear. *J Bone Joint Surg Am*, *76*, 1586-1593.

Tong, J., and Ng, E. (2010). Preliminary investigation on the reduction of plantar loading pressure with different insole materials. *The Foot*, 20. 1-6.

Voloshin, A., and Loy, D. (1994). Biomechanical evaluation and management of the shock waves resulting from the high-heel gait: I — temporal domain study. *Gait and Posture*, 2(2), 117-122.

Wang, C. S. (2010). An analysis and evaluation of fitness for shoe lasts and human feet. *Computers in Industry*, *61*(6), 532-540.

White, R. M. (1982). *Comparative anthropometry of the foot* (No. NATICK/IPL-230). Army natick research and development labs ma individual protection lab.

Whittle, M. W. (2014). *Gait analysis: an introduction*. Butterworth-Heinemann.

Winter, D.A. (1995), Human balance and posture control during standing and walking. *Gait and Posture*, vol. 3 (4) December 1995, 193-214

Witana C. P., Feng J. and Goonetilleke R. S. (2004) Dimensional differences for evaluating the quality of footwear fit, *Ergonomics*, 47:12, 1301-1317

Witana, C. P., Goonetilleke, R. S., Au, E. Y. L., Xiong, S., and Lu, X. (2009). Footbed shapes for enhanced footwear comfort. *Ergonomics*, *52*(5), 617-628.

Wunderlich, R. E., and Cavanagh, P. R. (2001). Gender differences in adult foot shape: implications for shoe design. *Medicine and Science in Sports and Exercise*, *33*(4), 605-611.

Yorkston, E. A., Nunes, J. C., and Matta, S. (2010). The malleable brand: The role of implicit theories in evaluating brand extensions. *Journal of Marketing*, *74*(1), 80-93.

Yu, J., Cheung, J., Zhang, Y., Leung, A., and Zhang, M. (2008). Development of a finite element model of female foot for high-heeled shoe design. *Clinical Biomechanics*, 23, Suppl 1, 31-38.

Yu, J. (2009). *Development of a computational foot model for biomechanical evaluation of high-heeled shoe designs* (Doctoral dissertation, The Hong Kong Polytechnic University).

Yu, J., Cheung, J. T. M., Wong, D. W. C., Cong, Y., and Zhang, M. (2013). Biomechanical simulation of high-heeled shoe donning and walking. *Journal of Biomechanics*, *46*(12), 2067-2074.

Abu-Faraj Ziad, G.F. Harris, A.H. Chang and M.J. Shereff. (1996). Evaluation of a rehabilitative pedorthic: plantar pressure alterations with scaphoid pad application, *IEEE Transactions on Rehabilitation Engineering* 4(4).